ANTI-CANCER EFFICACY OF SELENIUM NANOPARTICLES DECORATED BY POLYSACCHARIDE-PROTEIN COMPLEX ISOLATED FROM *PLEUROTUS TUBER-REGIUM*: CELLULAR UPTAKE AND ANTI-TUMOR MECHANISMS ON HCT 116 COLORECTAL CANCER CELLS

LIU ZUMEI

M.Phil

The Hong Kong Polytechnic University

2017

The Hong Kong Polytechnic University

Department of Applied Biology and Chemical Technology

Anti-cancer efficacy of selenium nanoparticles decorated by polysaccharide-protein complex isolated from *Pleurotus tuber-regium*: Cellular uptake and anti-tumor mechanisms on HCT 116 colorectal cancer cells

LIU Zumei

A thesis submitted in partial fulfillment of the requirements for the degree of Master of Philosophy

May 2016

CERTIFICATE OF ORIGINALITY

I hereby declare that this thesis is my own work and that, to the best of my knowledge and belief, it reproduces no material previously published or written, nor material that has been accepted for the award of any other degree or diploma, except where due acknowledgement has been made in the text.

LIU Zumei

Abstract

Colorectal cancer (CRC) is one of the major causes of cancer morbidity and mortality in the world, yet current choices for adjuvant therapy are limited due to the suboptimal response rate. Selenium (Se) is an essential trace element to human health. Recently, selenium nanoparticles (SeNP) have become the new research topic, since they were found to possess remarkable anti-cancer efficacy and low toxicity. Although apoptosis induction was found to be the critical cellular event of SeNP-induced anti-tumor activity *in vitro*, their cell inhibition mechanisms are not fully understood at cellular and molecular levels at present. Besides, for further development of SeNP into a novel anti-tumor agent, information on their cellular uptake behavior is crucial. However, related information is currently very limited.

By using a water soluble polysaccharide-protein complex (PSP) isolated from the mushroom *Pleurotus tuber-regium* (Fr.) Singer, our lab has successfully prepared a highly stable SeNP (PTR-SeNP) under a simple redox system. PTR-SeNP was found to significantly inhibit the growth of human breast carcinoma MCF-7 cells (IC_{50} = 3.7 μM) as well as possess higher stability and lower toxicity towards

normal cells.

In order to gain a better understanding on the anti-cancer efficacy of PTR-SeNP on CRC, in this project, the *in vitro* anti-proliferative effect was firstly determined with six human colorectal cancer cell lines (SW1116, SW620, COLO205, HT-29, HCT-15 and HCT 116). Apart from cellular uptake behavior, different cell inhibition mechanisms such as apoptosis, cell cycle arrest and autophagy were then further investigated in the most susceptible human colorectal cancer cell line.

Among the panel of six different human colorectal cancer cell lines, PTR-SeNP exhibited the highest dose- and time-dependent anti-proliferation effect on the HCT 116 cells with an IC_{50} value of 4.0 μM. Besides, PTR-SeNP were found to induce dose- and time-dependent apoptosis in the HCT 116 cells (significant increase in phosphatidylserine translocation, DNA fragmentation and sub-G1 population), via a caspase-3 independent pathway. In addition, PTR-SeNP markedly induced G2/M cell cycle arrest after 48 h treatment by down-regulating Cyclin D1 and Cyclin D3 at 12 h, CDK2 and CDK4 at 24 h, and cdc2/CDK1 at 48 h. Considering the role of Cyclin D1 in regulating cell cycle progression and cell proliferation, Cyclin D1 may serve as the primary molecular target of PTR-SeNP

induced G2/M cell cycle arrest.

Further investigation on autophagy also discovered that PTR-SeNP could induce initiation and completion of autophagic flux in the HCT 116 cells as evidenced by the presence of autophagosomes in EGFP-LC3 plasmid transfected cells, as well as time-dependent increase of autophagy initiators, such as Beclin 1 (peaked at 24 h), LC-3 II (peaked at 24 h) and p62/SQSTM1 (peaked at 12 h) after Western Blot analysis.

Last but not least, PTR-SeNP were found to colocalize with both Golgi apparatus and lysosomes in the HCT 116 cells after cellular internalization as early as 2 and 5 min, respectively. It is the first study to discover that SeNPs could colocalize with Golgi apparatus, suggesting the involvement of caveolae-mediated endocytosis.

We anticipated that findings of this study would provide significant insights into the development of PTR-SeNP as novel anti-tumor agent for treating CRC.

Acknowledgements

There are many people that have given me tremendous support in various aspects, without whom this thesis won't be possible to be accomplished. I am really grateful for this unique experience of scientific learning and life maturation.

First, I would like to thank my Board of Committee members: Professor M.S. Wong, Dr. Edmund Li, and Dr. H.Y. Chung, for their time and valuable suggestions to help me improve my research and thesis.

I would like to thank my supervisor, Dr. Wong Ka-hing, for his patience, supervision and guidance in the course of my study. He has been a source of encouragement and motivation and to whom I am truly indebted.

I would also love to thank the many people of the scientific community who have given me tremendous help. I would like to thank all the former and present members of this research group and the collaborators and their students, including but not limited to: Dr. CHEN Tian Feng, Dr. WU Xiao Qian , Dr. Karen Y.J. GU, Dr. Stephen C.F. Kim, Dr. Amber J.C. Chiou, Dr. Ben C.B. Ko, Dr. Vincent W.K. Keng, Dr. Chen Sheng, Ms. ZHANG Huan, Dr. Iris L.K. Wong, Mr. LIN Da Chuan, Mr. LI Ruichao, Dr. GUO Jiubiao, Dr. WONG Chi-fai, Ms. Zhou Liping, Dr. Zhang Rui, Ms.

Amy P.H. Chiu, Ms. Lilian H.W. Lo, and Ms. Cindy X.X. Li.

In addition, I would like to thank the technicians of the Department of Applied Biology and Chemical Technology for their prompt and reliable technical assistance; and the staff at Pao Yue-Kong Library of Hong Kong Polytechnic University for their kind support.

Last but not the least, I would like to thank my parents, for their trust and support emotionally and financially throughout the long journey of life learning and progression.

Table of Contents

List of Figures

List of Table

Abbreviations

3-MA	3-Methyladenine
5-FU	5-fluorouracil
AIF	Apoptosis inducing factor
APC	Adenomatous polyposis coil
ATG	Autophagy related gene
Atg	Autophagy related protein
AVd	Degradative autophagic vacuoles
AVi	Initial autophagic vacuoles
BH	Bcl-2 homology
CAD	Caspase-activated Dnase
CDK	Cyclin-dependent protein kinases
CIE	Clathrin-independent endocytosis
CIMP	CpG island methylation
CIN	Chromosomal instability
CKI	CDK inhibitors
CME	Clathrin-mediated endocytosis

CPZ	Chloropromazine
CRC	Colorectal cancer
DAPI	4',6-diamidino-2-phenylindole
EE	Early endosome
EGF	Epidermal growth factor
EGFP	Enhanced green fluorescent protein
EGFR	Epidermal growth factor receptor
ENDOG	Endonuclease G
EPR effect	Enhanced permeability and retention effect
EP tube	Eppendorf microcentrifuge tube
ER	Endoplasmic reticulum
ERK	Extracellular signal - regulated kinase
FA	Folinic acid
FAP	Familial adenomatous polyposis
FITC	Fluorescein
FITC-A	Fluorescein signal – Area
FITC-W	Fluorescein signal – Width
FOLFOX	Chemotherapy regime of Folinic acid, Fluorouracil and Oxaliplatin

FOLFIRI	Chemotherapy regime of Folinic acid, Fluorouracil and Irinotecan
FSC/SSC	Forward scatter/Side scatter
GFP	Green fluorescent protein
HNPCC	Hereditary nonpolyposis colon cancer
HTRA2	High temperature requirement protein A2
ICP-OES	Inductively coupled plasma optical emission spectrometry
LC3	Microtubule-associated protein 1A/1B-light chain 3
MAPK	Mitogen-activated protein kinases
MSI	Microsatellite instability
mTOR	Mammalian target of rapamycin
MTT	3-(4,5-Dimethylthiazol-2-yl)-2,5-diphenyltetrazolium bromide
NaN_3	Sodium azide
NCCD	Nomenclature Committee on Cell Death
NP	Nanoparticle
PARP-1	Poly(ADP-ribose)polymerase-1
PAS	Pre-autophagosomal structure
PCD	Programmed cell death
PE	Phosphatidylethanolamine

PI (staining)	Propidium iodide
PI3K	Phosphoinositide 3-kinase
PS	Phosphatidylserine
PSP	Polysaccharide-protein complex
PTR	Pleurotus tuber-regium, or its polysaccharide-protein complex
ROS	Reactive oxygen species
Se	Selenium
Sec	Selenocysteine
SEER	Surveillance, Epidemiology and End Results system
Se-met	Selenomethionine
SeNP	Selenium Nanoparticle
Tf	Transferrin
TGN	Trans-Golgi network
TNF	Tumor necrosis factor
TRAIL	TNF related apoptosis inducing ligand
UBA domain	Ubiquitin-binding domain
VEGF	Vascular endothelial growth factor

Chapter 1 - Literature Review

1.1 Colorectal cancer

1.1.1 Prevalence

As a major cause of morbidity and mortality, cancer is a public health problem, causing 14 million new cases and 8.2 million cancer-related deaths worldwide in 2012 (World Health Organization 2014). Colorectal cancer (CRC) is the term referring to the cancer happening in colon or rectum, which are parts of the large intestine joining the small intestine and the anus. In 2012, CRC is the third leading cause of cancer in man and second leading cause in woman, which also claimed 700,000 deaths worldwide, ranking the fourth among all cancer-related deaths (World Health Organization 2014).

Since colorectal cancer is largely linked to Western life-style, obesity and diet, developed countries have higher prevalence. In the United States in 2016, CRC is estimated to be the third cause of new cancer cases and deaths in both genders (Siegel et al. 2016). It is estimated that around 5 % of the US population will develop CRC in their life time (Jemal et al. 2008).

As estimated by the Chinese National Cancer Center (Chen et al. 2016), CRC caused 376,300 new cases and 191,000 deaths in China in 2015, ranking the fifth

among all cancers. Also, urban dwellers were found to have twice the incidence and morbidity rate than rural residents (263,200 vs. 113,200 new cases, 126,600 vs. 64,500 deaths). As China is now modernizing quickly and transiting to an aging society, incidence and morbidity rate of CRC are expected to rise significantly in the coming years.

Hong Kong could offer an excellent perspective of what China is facing. Its population has similar genetic pool and it went through economic boom in 1960s which caused a dramatic change in the lifestyle and diet; the life expectancy also extended more than 10 years in both genders from 1971 to 2014 (Hong Kong Department of Health 2015a). These factors collectively tripled the colorectal patient hospitalization (1993 – 2013), and tripled incidence rate and death rate (1981 – 2013) (2015b). According to Hong Kong Cancer Registry, CRC is the second leading cause of cancer in both genders in 2013 (Hong Kong Cancer Registry 2015). In fact, this increase in morbidity rate has been observed among all the Four Asian Tigers (National Registry of Disease Office (NRDO) 2014; Shin et al. 2012; Su et al. 2012).

Although the mortality rate could be mitigated by early screening (Siegel et al. 2016) and conscious behavioral intervention, the picture remains dire for China in the upcoming decade, considering its large population. It is imperative to

understand its etiology and find effective method of prevention and cure for colorectal cancer.

1.1.2 Risk factors

Gene and Age

Only about 5 - 10% of all patients are predisposed genetically (Lynch and de la Chapelle 2003; Siegel and Jemal 2014). The two major genetic syndromes are familial adenomatous polyposis (FAP) and hereditary nonpolyposis colon cancer (HNPCC), also called Lynch syndrome (Lynch and de la Chapelle 1999; Lynch and de la Chapelle 2003; Murff et al. 2007). Around 90% of all CRC cases are sporadic colorectal cancer (World Health Organization 2014), and age is a predominant risk factors: most patients are diagnosed after mid-60s (Chan and Giovannucci 2010).

Dietary habit

Many dietary components are effective preventative or causative agents for CRC (Corpet and Tache 2002; Kuppusamy et al. 2014; Rajamanickam and Agarwal 2008). High consumption of red meat or processed meat would significantly increase the risk (Norat et al. 2005), while high intake of dietary fiber or daily vegetable consumption would reduce it (Aune et al. 2011; Howe et al. 1992). Besides, vitamin D, folic acid, Vitamin B6, garlic, fish oil and omega-3 fatty acids

have weak links to CRC (Chan and Giovannucci 2010; Connelly-Frost et al. 2009; Hou et al. 2013; Touvier et al. 2011).

Selenium shows inverse correlation with colorectal cancer in most cases (Bjelakovic et al. 2004; Clark et al. 1993; Reid et al. 2006), although some small scale trials could not establish the connection (Dennert et al. 2011; Vekariya et al. 2012).

Life style and obesity

A sedentary life style is strongly associated with increased risk of CRC (Boyle et al. 2012; Secretan et al. 2009). In addition, newly acquired active life style can also lower the risk of CRC (Siegel and Jemal 2014). Obesity, especially abdominal obesity, is a risk factor of CRC regardless of life style (Larsson and Wolk 2007).

Use of substances and medication

Exposure to tobacco and heavy alcohol use are strongly linked to CRC risk (Ferrari et al. 2007; Secretan et al. 2009; Zisman et al. 2006). Medications such as long-term use of aspirin (Rothwell et al. 2010) and postmenopausal use of hormones (Lin and Giovannucci 2010) have proven link towards reducing risk of CRC, although the latter could increase the risk of breast and endometrial cancer.

Gender and race

Women and older patients are more susceptible to tumors in proximal colon,

while men and younger patients more susceptible to distal colon (Iacopetta 2002; Matanoski et al. 2006; Nawa et al. 2008). In addition, CRC have different incident and mortality rates between different ethnic groups (Siegel et al. 2016).

Medical history

CRC survivors have a greater risk of developing further polyps and tumor, as in field cancerization theory (Damania et al. 2012). Patients with chronic inflammatory bowel disease, such as ulcerative colitis and Crohn's disease is also more susceptible to CRC.

1.1.3 Screening

Since the onset of colorectal cancer can take decades, screening for early stage colorectal cancer from age 50 onward is recommended for general population. There has been a steady decline in CRC-related death rates since the wide spread implementation of early screening (Neugut and Lebwohl 2009).

There are several CRC screening options (Levin et al. 2008). Each have their advantages and limitations in patient compliancy, sensitivity and specificity. These include annual fecal tests [guaiac-based fecal occult blood test (gFOBT), fecal immunochemical test (FIT) and stool DNA test (sDNA)] and structural examinations [such as flexible sigmoid0oscopy (FSIG), double-contrast barium

enema (DCBE), colonoscopy, and computed tomography colonogaphy (CTC)].

1.1.4 Staging and prognosis

95% of the colorectal cancer is adenocarcinoma, which originates from epithelial glandular cell on the colorectal mucosa that's responsible for mucus secretion (Fleming et al. 2012). Colorectal cancer can be divided into 3 types: (i) microsatellite instability (MSI phenotype); (ii) chromosomal instability (CIN phenotype) caused by mutations in *APC* and other genes that activate Wnt pathway; and (iii) epigenetic CpG island methylation (CIMP phenotype) (World Health Organization 2014). These causes induce adenoma or polyp development, and 10% of these polyps will further develop into malignant cancer (Siegel and Jemal 2014). The cancer progresses to penetrate the inner lining of the intestine, spread to nearby lymph node and local tissues, and further metastasize to remote

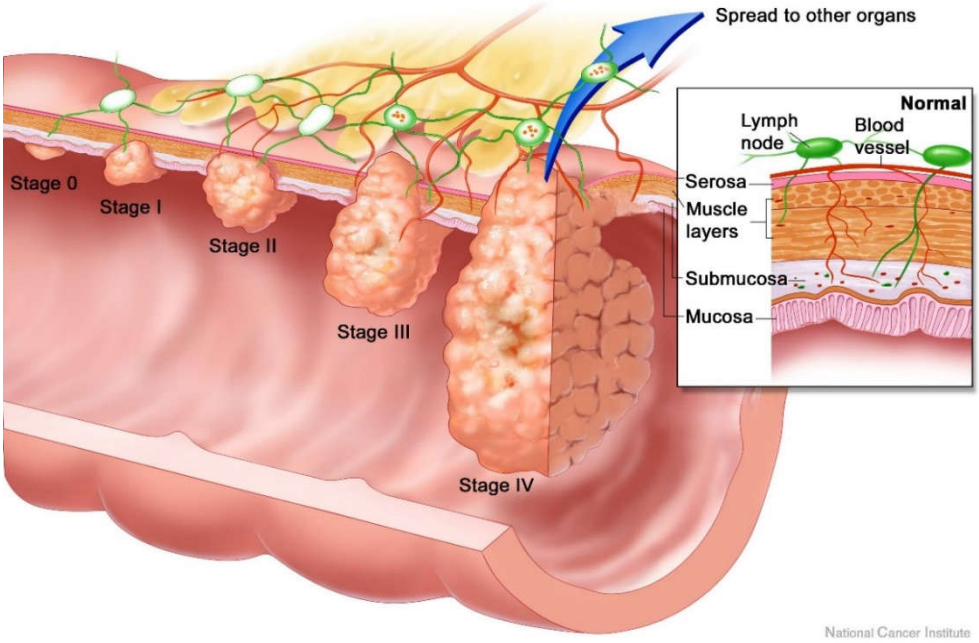

Figure 1: The four stages of colorectal cancer according to TNM standard. Cited from (Siegel and Jemal 2014).

tissues via lymphatic system or vascular system **(Figure 1)**. Liver is the most common site of metastases; other tissues include lung, peritoneum, and bones (Wolpin and Mayer 2008).

The most common staging systems are TNM system and SEER system. TNM system describes the degree of primary tumor invasion (**T**), regional lymph nodes invasion (**N**) and distant metastasis (**M**) in a quantitative way (Fleming et al. 2012), and is thus more convenient for clinical purposes (Wolpin and Mayer 2008). SEER system uses a more qualitative description, and is more suitable for statistical analysis (Siegel and Jemal 2014).

The TNM staging (American Joint Committee on Cancer 2013) corresponds largely with CRC prognosis. In stage I, the cancer is limited to the inside wall of the colon, and removal of the cancer by surgery is sufficient in most cases. Five-year survival rate is more than 90%. In stage II, the cancer has invaded the muscular wall, but not sentinel lymph nodes. Surgery is the standard treatment, while the benefit of chemotherapy is minimal with strong side effects. Five-year survival rate of stage II is 70 - 85%. In stage III, the cancer has spread to lymph nodes and/or penetrated the colon wall. Chemotherapy is necessary after surgery and radiation therapy may be needed. The five-year survival rate is 25 – 80%. At stage IV, the colorectal cancer has metastasized to other organs and the five-year survival rate is less than 10%. Treatment includes surgery, chemotherapy combined with monoclonal antibody, and radiation (O'Connell et al. 2004).

1.1.5 Treatment

While surgery is the first resort to resectable colorectal cancer (Wanebo et al. 2012), post-operative adjuvant chemotherapy is beneficial to the patient's survival among selected stage II and all stage III patients (Carrato 2008). The first-line therapy has evolved from 5-fluorouacil (5-FU) alone to combination of 5-FU/leucovorin regime, and targeted therapies in metastatic CRC.

5-fluorouracil is a pyrimidine analog that inhibits thymidylate synthase irreversibly, and incorporates its metabolite into DNA and RNA, resulting in DNA damage and apoptosis (Longley et al. 2003). It is used for systematic treatment of multiple cancers, and bolus or infusional fluorouracil has been used in the treatment of CRC for more than four decades. Folinic acid (FA), also called leucovorin, helps to stabilize the interaction between 5-FU and its target enzyme. The 5-FU/FA regime improves the response rate from 10 - 15% (Davies and Goldberg 2011; Longley et al. 2003) to 20%, and the median survival from 5 months to 11 months (Wolpin and Mayer 2008). Combining 5-FU/FA with platinum compounds oxaliplatin (FOLFOX) and rinotecan (FOLFIRI) have been found to improve both response rate and survival duration (35% to 53%, 14 to 18 months) (Berger et al. 2005; Compton and Greene 2004).

On top of these, metastatic CRC can be treated with targeted therapy, namely monoclonal antibodies. The two major types of targeted therapy include: (I) anti-angiogenesis by inhibiting vascular endothelial growth factor (VEGF) and (II) anti-proliferation by inhibiting epidermal growth factor receptor (EGFR). Some proven anti-VEGF and anti-EGFR antibodies include bevacizumab, cetuximab and panitumumab (Carrato 2008; Chee and Sinicrope 2010).

VEGF is a soluble signal protein secreted excessively by cancers that can

stimulate the growth of blood vessel and facilitate metastasis. Clinical trials have shown that bevacizumab could improve the reponse rate on other regimes (FOLFIRI from 35 to 45%, FOLFOX from 9 to 23%) (Méplan et al. 2010; van Houdt et al. 2010).

EGFR is a transmembrane glycoprotein receptor that inhibits apoptosis and induces cell proliferation and angiogenesis. Activation of EGF pathway would regulate Cyclin D1 expression and modulate cell proliferation via RAS/RAF/MAPK axis. Anti-EGFR therapy could result in an additional ~10% response rate when combined with other regimes (Bellinger et al. 2009; Scaltriti and Baselga 2006) .

In short, the current first-line therapy of CRC, 5-FU/FA combined with either oxaliplatin or irinotecan could improve both response rate and survival duration, while the monoclonal antibodies could help to inhibit metastasis and angiogenesis. Nevertheless, the five-year survival rate and the response rate to therapy is sub-optimal. Thus, there is a pressing need to develop better therapies for CRC.

1.2 Selenium and its different chemical forms

1.2.1 Physiological role of selenium

Selenium (Se) is an element with the atomic number of 34. It is in the same

group as oxygen, sulfur and tellurium in the periodic table, and has a wide range of biological, medical (Khiralla and El-Deeb 2015; Wang et al. 2015) and electronic (Chaudhary and Mehta 2014) applications. The toxicity of Se at high dosage is discovered first in history, and later Schwarz and Foltz found that Se is an essential micronutrient at lower dosage in 1957.

In normal human physiology, Se functions in the form of selenoproteins. Insufficient Se intake and defective selenoprotein synthesis lead to skin, muscular, cardiovascular, neurological and immunological diseases (Broome et al. 2004; Brown and Arthur 2001; Navarro-Alarcon and Cabrera-Vique 2008; Thomson 2004).

Seleno amino acids

Se can replace sulfur in amino acids due to their atomic similarity, and selenomethionine (Se-met), selenocysteine (Sec or Se-cys) and selenocystine are major forms of seleno amino acids in Se uptake and selenoprotein synthesis (Navarro-Alarcon and Cabrera-Vique 2008; Rahmanto and Davies 2012).

Diet is the major source of Se exposure (~80%), and the chemical form of Se affects its bio-availability (Navarro-Alarcon and Cabrera-Vique 2008). The main dietary source of Se is wheat and meats in the form of L - selenomethionine (L - Se-met), synthesized by plants from selenite and selenate and well absorbed by

human (Schrauzer 2000). Absorbed Se-met is either reserved in selenoproteins in place of methionine, or converted to selenocysteine for further metabolism.

For selenocysteine (Sec), the 21st amino acid (Berry et al. 2001), Se is incorporated into cysteine by covalent bond. Sec is the seleno amino acid that forms major functioning selenoproteins. Most of the 25 currently identified selenoproteins contains only one Sec, except for Selenoprotein P (SELP or SEPP), which contains Sec-rich domain and can serve as Se transporter and reservoir in the blood plasma (Burk and Hill 2009; Burk and Hill 2015).

Sec forms the active site of redox centers in many selenoproteins (Li et al. 2014). The biological functions of selenoproteins that have been reported so far include: selenoprotein transcription regulation (SELH) and biosynthesis (SPS2), phospholipid synthesis (SELI), ER stress regulation (SELN, SELS), protein folding on ER membrane (SELM, Sep15) and thyroid hormone activation (DIO) (Brown and Arthur 2001; Huang et al. 2012).

Selenoproteins and CRC

The early discovery of a link between serum Se level/Se supplementation and the incidence of adenoma or colorectal cancer (Duffield-Lillico et al. 2002), has aroused a lot of follow-up investigations. However, numerous studies showed contradicting results (Glade 1999; Nelson et al. 1995; Wallace et al. 2003) on the

relationship between Se level and CRC prevention. A meta-analysis of 55 epidemiological studies also reported that due to limitations of the experimental setting (such as scale, chemical forms of Se supplement and participant ethnicity), further investigation is required to draw a solid conclusion (Dennert et al. 2011).

Nevertheless, substantial evidences have been accumulated to support the inverse correlation between Se level and precancerous polyps (Fernandez-Banares et al. 2002; Jacobs et al. 2004; Peters et al. 2006; Russo et al. 1997). In different mouse models, Se supplementation was found to significantly reduce the polyps induced by carcinogens (Hu et al. 2008; Peters et al. 2006) or mutations in selenoprotein genes (Irons et al. 2006).

In colon cells, Se deficiency was found to reduce the mRNA expression of Gpx1, Selh, Selw and Selm, affecting downstream oxidative stress and ER stress (Huang et al. 2012). Besides, genetic polymorphisms of selenoproteins (GPX1, GPX4, Sep15, SELS, SELP and TXNRD2) have been previously reported to increase susceptibility to CRC (Bermano et al. 2007; Méplan and Hesketh 2012; Méplan et al. 2010; Tsuji et al. 2015). Thus, these findings are consistent with the roles of selenoproteins in oxidative stress, ER stress and inflammatory response modulation, which may directly affect those risk factors of CRC such as inflammatory bowel disease. In addition, Se supplementation has been found to

decrease DNA methylation level in colon mucosa, which may also help to check the epigenetic initiator and CIMP phenotype of CRC (Zeng et al. 2011).

1.2.2 Selenium nanoparticles

Se compounds such as methylselenocysteine (MeSeCys) have been found to possess strong anti-cancer efficacy, via mechanisms such as ROS generation, apoptosis, and cell cycle arrest (Sanmartín et al. 2012). However, their toxic dose to normal cells are quite low, making their therapeutic window rather narrow.

Since selenium nanoparticles (SeNP) were found to exhibit relatively low toxicity when compared with other Se compounds or elemental Se (Sanmartín et al. 2012; Wang et al. 2015), it has become a hot research topic in recent years. In general, SeNP were synthesized by chemical reduction of soluble ions of Se, such as selenate ($SeO4^{2-}$) and selenite ($SeO3^{2-}$), by “bottom-up” approach. In the process, newly reduced atoms or molecules form nuclei and particles continue to grow in size via constant condensation. Possessing a wide range of health prompting properties such as anti-bacterial (Chudobova et al. 2014; Khiralla and El-Deeb 2015), anti-fungal (Shakibaie et al. 2015), and anti-cancer effects (Mary et al. 2016; Yu et al. 2012), SeNP have been recently reported to be used in medical device coating (Ramos et al. 2012; Wang et al. 2015), as well as food

supplement (Kheradmand et al. 2014), and anti-cancer agent.

Concerning their anti-cancer efficacy, in addition to safety, SeNP tend to accumulate at the cancer tissues, due to their enhanced permeability and retention effect (EPR effect) via the cancer vasculature (Bertrand et al. 2014). Besides, surface modification of SeNP with water soluble polymers or small molecules, such as polysaccharides (Yang et al. 2012; Zhang et al. 2004; Zhang et al. 2010), PEG (Mary et al. 2016), amino acids (Feng et al. 2014), and ATP (Zhang et al. 2013), could also increase their cellular uptake efficiency, reduce opsonization of plasma proteins as well as reduce their clearance by macrophages as previously reported (Fröhlich 2012; Verma et al. 2008).

Various forms of SeNP have been extensively investigated in lung (Mary et al. 2016), liver (Xia et al. 2015), prostate (Kong et al. 2011), skin (Liu et al. 2012) and breast cancers (Vekariya et al. 2012). And previous studies reported that SeNP generated ROS, reduced mitochondria membrane potential, activated caspases and induced apoptosis. Synergistic anti-cancer effect using SeNP as drug carrier by conjugating anti-cancer drug such as 5-FU have also been reported in literature (Liu et al. 2012). Some recent studies found that sodium selenite induced apoptotic deaths in colorectal cancer cell lines (Fang et al. 2010; Yang et al. 2016), possibly via endogenous SeNP generated after selenite internalization (Bao et al.

2015)]. However, the anti-cancer efficacy of SeNPs on CRC was not well-studied so far, which leaves a knowledge gap to be studied.

1.3 Mechanisms of cell deaths: apoptosis, cell cycle arrest and autophagy

1.3.1 Apoptosis

When cells suffer acute and overwhelming external damage such as infection and trauma, cells will undertake unregulated cell death called necrosis. Necrotic cells go through organelle swelling, rupture of plasma membrane and cell lysis, which triggers inflammation.

Apoptosis is another cell death process and literally means “dropping off” in Greek (Wong 2011). Unlike necrosis, apoptosis is a highly regulated programmed cell death (PCD) process that is important in physiological development and pathological progression.

Apoptosis is also referred to as type I programmed cell death. It may be triggered externally or internally, either by death receptors on the cell surface such as Fas receptor (FasR) and TNF (Tumor Necrosis Factor) receptor superfamily, or by mitochondrial signaling **(Figure 2)**.

The morphological hallmarks of apoptosis include chromatin condensation, and nuclear condensation and fragmentation. The plasma membrane remains complete throughout the early phase, and in the later phase ruffles on the membrane (blebbing) is formed and membrane integrity is lost. The DNA

fragments are wrapped and secreted with the membrane blebbing as apoptotic bodies. The apoptotic bodies are mostly taken up by neighboring cells without triggering inflammatory response, or undergo necrosis-like degradation (Galluzzi et al. 2012).

The major biological changes in cell undergoing apoptosis include DNA fragmentation, phosphatidylserine (PS) translocation from the inner to the outer membrane, and caspase activation. However, it is noteworthy that any single one of these criteria should not be used to define apoptosis, since apoptosis can occur without DNA fragmentation or caspase activation (Galluzzi et al. 2012). PS translocation can be observed in other processes as well.

Apoptosis is traditionally thought to be caspase-dependent, but now caspase-independent apoptosis is also well recognized (Galluzzi et al. 2012). Although apoptosis can be induced by calpains, cathepsins and other proteases (Bröker et al. 2005), caspases are still important players in the process.

Caspase derives the name as cysteine-aspartic acid protease (caspase). There are two different types of caspases: the initiator and the effector. Upon activation by different apoptotic pathways, the initiators (caspase -2, -8, -9, and -10) cleave the inactive pro-form of effector caspases (caspase -3, -6, and -7). The

activated effector caspases forms enzymatic cascade and rapidly carry out the cell death functions.

Of the three effector caspases, caspase -6 functions by activating the other two (Wolf et al. 1999), and compared to caspase -7, caspase -3 is the major and well-studied caspase. The pro-form of caspase -3 can be cleaved into two units. Then the activated caspase -3 will cleave poly(ADP-ribose)polymerase-1 (PARP-1), an enzyme in DNA repair and transcriptional regulation (Los et al. 2002). Besides, activated caspase -3 will release caspase-activated DNase (CAD), which promotes DNA fragmentation by inhibiting its inhibitors (Wolf et al. 1999).

The two well identified apoptotic pathways are intrinsic mitochondrial pathway and extrinsic death receptor pathway, involving caspases and other apoptosis-inducing molecules **(Figure 2)**.

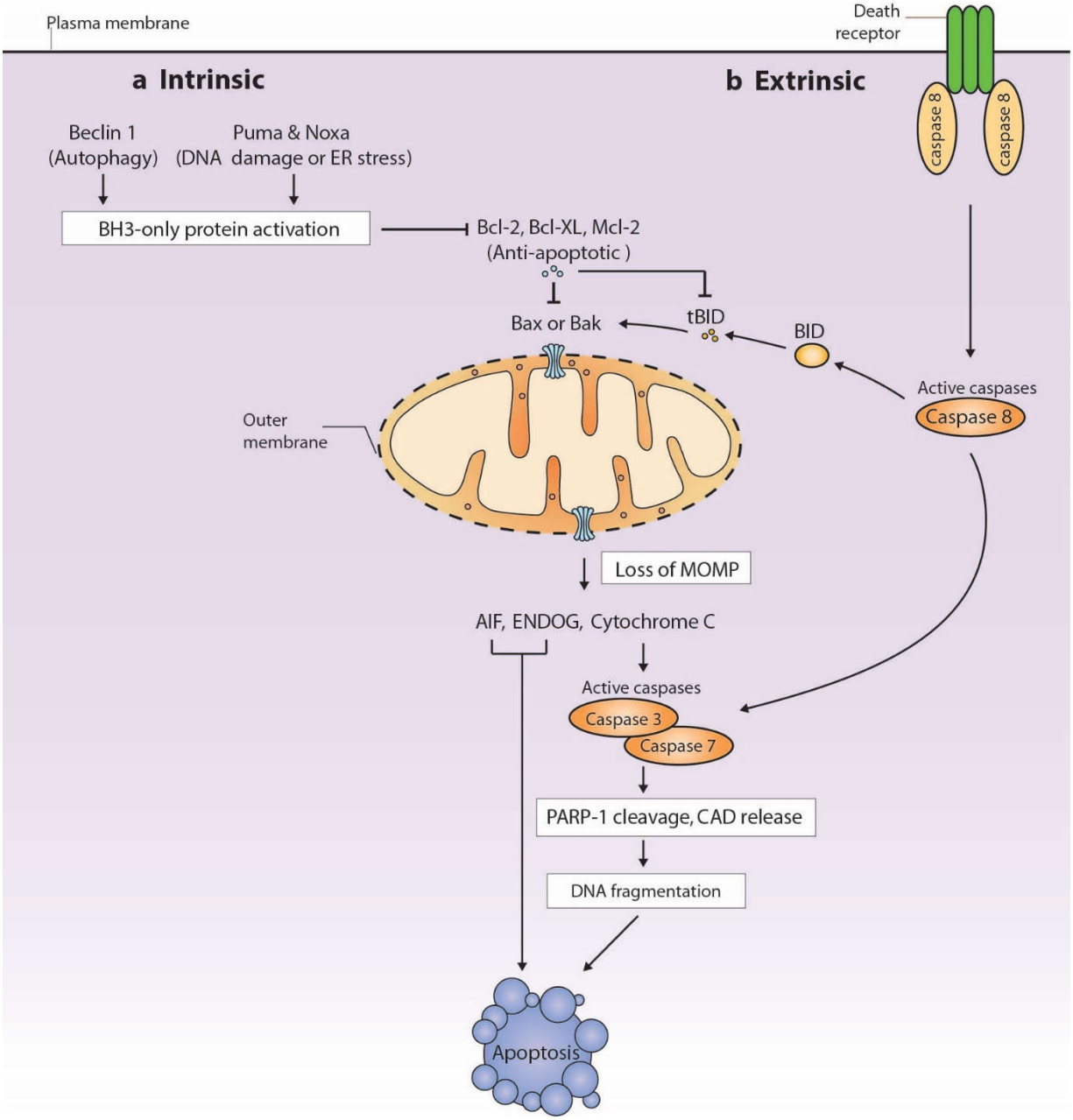

Figure 2: Intrinsic and extrinsic pathway of apoptosis.

Adapted from (Tait and Green 2010).

Mitochondrial apoptotic pathway

According to NCCD committee (Galluzzi et al. 2012), mitochondrial apoptotic pathway, also called the intrinsic pathway, occurs with the generalized and irreversible loss of mitochondrial outer membrane permeabilization (MOMP), ATP synthesis arrest by respiratory chain inhibition, as well as release of mitochondrial contents.

Mitochondrial apoptotic pathway is regulated by the Bcl-2 family proteins on the outer membrane of mitochondria. Bcl-2 family proteins contain at least one of the four Bcl-2 homology (BH) domains (BH1, BH2, BH3 and BH4) (Kelekar and Thompson 1998). They are either pro-apoptotic or anti-apoptotic, and are subdivided into three classes accordingly:

Class I consists of anti-apoptotic proteins such as Bcl-2, Bcl-xL, Bcl-W and Mcl-1. Class II consists of multidomain pro-apoptotic proteins Bax and Bak, which can form channels allowing selective passage of ions and loss of MOMP, leading to activation of apoptosis. Under normal conditions, pro-apoptotic Bax and Bak (class II) are regulated by Class I anti-apoptotic proteins, and the pore-forming activity is kept at bay. Class III are pro-apoptotic molecules that has only BH3 domains, such as Bid, Bik, Bim and Bad. Without the inhibition of Class I anti-poptotic proteins, Class III BH3-only proteins will initiate the Bax/Bak to form channels on mitochondria membrane. This leads to mitochondrial swelling and

outer membrane rupture, releasing of mitochondrial content (such as cytochrome C), loss of MOMP and consequent signaling cascades and apoptosis (Rello-Varona et al. 2015) **(Figure 2)**.

Most Bcl-2 family members have transmembrane sections. Only regulator Bad and Bid exist diffusively in cytoplasm (Kelekar and Thompson 1998; Perfettini et al. 2002).

The consequent apoptosis induced by the MOMP change can be caspase-independent also (Selznick et al. 2000). The content released from mitochondria include cytochrome C, apoptosis inducing factor (AIF), Endonuclease G (ENDOG) and high temperature requirement protein A2 (HTRA2). Once released from the mitochondria, cytochrome C forms apoptosome with other adaptor proteins that triggers caspase -9 / caspase -3 cascade. On the other hand, AIF and ENDOG relocate to nucleus and mediate caspase-independent DNA fragmentation that prevails upon caspase inhibition (Bröker et al. 2005; Cande et al. 2004; Chipuk and Green 2005; Constantinou et al. 2009; Cregan et al. 2002). As a serine protease, HTRA2 may also enhance caspase-independent apoptosis by cleaving a range of molecules (Galluzzi et al. 2012).

The mitochondria-dependent apoptosis is a converging point where apoptosis interacts with multiple signaling pathways and respond to various

signals, such as DNA damage and cytoplasmic homeostasis. It is because BH3-only proteins also exist in other pathways. For example, PUMA and Noxa are p53 mediated sensors in respond to DNA damage and ER stress (Michalak et al. 2008; Schuler et al. 2003); while Beclin 1 is an important molecule in the initiation of autophagy, which will be covered later **(Figure 2)**.

Death receptor-mediated apoptotic pathway

The second pathway is death receptor-mediated pathway, or extrinsic apoptotic pathway. As mentioned previously, death ligands such as cytokines activates the death receptors such as Fas and TRAIL on the cell surface, and caspase -8 is activated. Caspase -8 induces apoptosis by either direct caspase -3 activation, or BH3-only protein Bid truncation. Full length Bid is located in cytosol. After truncated by caspase -8, tBid will relocate into mitochondria and regulate mitochondrial apoptotic pathway (Li et al. 1998) **(Figure 2)**.

1.3.2 Cell cycle arrest

When cells go through apoptosis, cell cycle arrest is generally observed simultaneously as a process that ensure DNA repair. Cell cycle is the series of recurrent steps every cell goes through to grow, copy their DNA content, and

ventually divide into daughter cells. It is essential in development and differentiation from embryos to adults.

Cell cycle is divided into four phases according to DNA and cellular content, namely G1, S, G2 and M phase, while G0 phase is a quiescent stage outside of the cell cycle. The cell after division is in G1 phase, in which it has only one copy of chromosomes, and synthesizes mRNA and proteins for later mitosis. Then the cell goes into S phase to duplicate its DNA. Successful completion of S phase leads to G2 phase, in which the cell has two copies of chromosomes and further synthesizes proteins for mitosis. M phase is the final stage, in which the cell divides its content and DNA into two daughter cells (Malumbres and Barbacid 2009).

In the "classical" cell cycle model **(Figure 3)**, progression from one phase into the next is tightly controlled by cell-cycle checkpoints. The function of the cell-cycle checkpoints is to slow down or arrest the cell cycle in response to DNA damage repair or growth factor availability (Abraham 2001). The cell-cycle checkpoints include core cell-cycle machinery and surveillance pathways, such as DNA damage check point and spindle-assembly checkpoint (Malumbres and Barbacid 2009). Cyclin-dependent protein Kinases (CDKs) are responsible for cell cycle progression, whose activity and substrate specificity are regulated by

specific cyclins and inhibited by CDK inhibitors (CKIs) (Xie et al. 2008). CDK misregulation would lead to unscheduled proliferation and genomic instability (Malumbres and Barbacid 2009). Therefore, developing cancer therapy via blocking cell cycle progression has always been a research interest of scientists.

In G1 phase, Cyclin Ds and Cyclin E bind to CDK4/CDK6 and CDK2 respectively. These CDK-Cyclin complexes then enables the transcription of necessary genes for later cell cycle phases, by phosphorylate and inactivate pocket protein Rb that sequester E2F family transcription factors. In G2 phase, Cyclin A binds with CDK2 and activates the transcriptional activity of FoxM1, which regulates a large array of G2/M genes. In G2 phase, Cyclin A binds with CDK1 or its homolog cdc2 to promote G2/M progression, which may be associated with the RNA polymerase II based transcription (Lim and Kaldis 2013). Besides, Cyclin B/CDK1 complex is activated by Cdc25 and triggers mitosis. Signals of DNA damage can be transducted by ATR/chk1 or ATM/chk2 pathways to deactivate Cdc25 via phophorylation, which induces G2 arrest (Abraham 2001). Thus, G2 arrest is regarded as the checkpoint against DNA damage **(Figure 3)**.

There are two families of CDK inhibitors (CKIs): INK4 family (p16INK4a, p15INK4b, p18INK4c, p19INK4d) which inhibits CDK4/CDK6, and the CIP/KIP family (p21CIP1/WAF1, p27KIP1, p57KIP2) that is able to inhibit all CDKs. The INK4

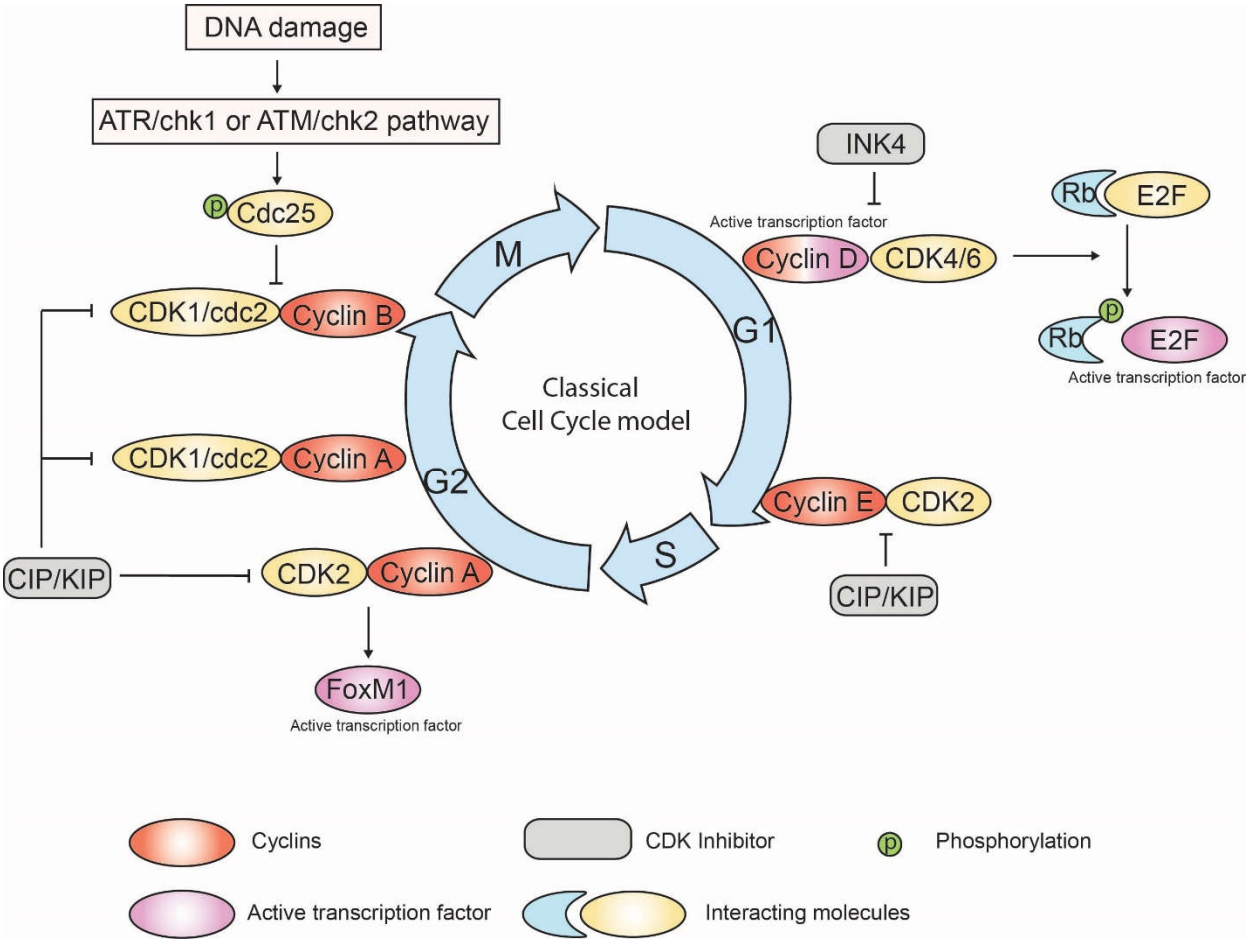

family binds to CDKs and inhibits its association with Cyclin Ds, while the CIP/KIP family can form inhibitory binding with the CDK/Cyclin D complexes (Lim and Kaldis 2013; Roussel 1999).

Figure 3: Demonstration of the molecular interactions in classical cell cycle model.

Cyclin Ds has three subtypes, Cyclin D1, D2 and D3. Their functions and sites of expression are not always overlapping. Cyclin D1 is the only expressed cyclins in retina (Lim and Kaldis 2013), and has been found to be the major Cyclin Ds in tumorigenesis with elevated expression.

Other than the CDK-dependent functions in cell cycle promotion, Cyclin D1 also has many CDK-independent functions. Cyclin D1 can bind to DNA repair proteins and be recruited to DNA damage sites via BRCA2 to enhance DNA damage repair (Jirawatnotai et al. 2011). In contrast, it can also enhance the DNA damage response and apoptosis as previously reported (Li et al. 2010b). More importantly, Cyclin D1 was found to be associated with multiple transcriptional factors in multiple pathways, regulating numerous cell functions (Lim and Kaldis 2013), such as promoting cell migration (Li et al. 2006). In addition, Cyclin D1 could also regulate nuclear hormone receptors, such as activating estrogen-receptor α and inhibiting androgen receptor, thereby modulating their downstream effect on cell proliferation (Fu et al. 2004).

It's worth noting that the classical model may not fully cover every aspects of cell cycle regulation **(Figure 4)**. For example, Xie et al. (Xie et al. 2008) have discovered that mice model lacking individual Cyclin Ds, Cyclin E, CDK4, CDK6 or CDK2 could still be viable, suggesting other alternative regulators for Cyclin Ds and

E might be present in normal physiological processes. Besides, previous studies (Berglund 2008) have also found that silencing CyclinD1 in MDA-MB-435 cancer cells could increase migratory capacity, and Cyclin D1 was over-expressed in tumors, contributing cell proliferation and migration. Interestingly, these findings postulate that malignant cells may require more Cyclin Ds than normal cells, indicating a new angle of cancer therapy.

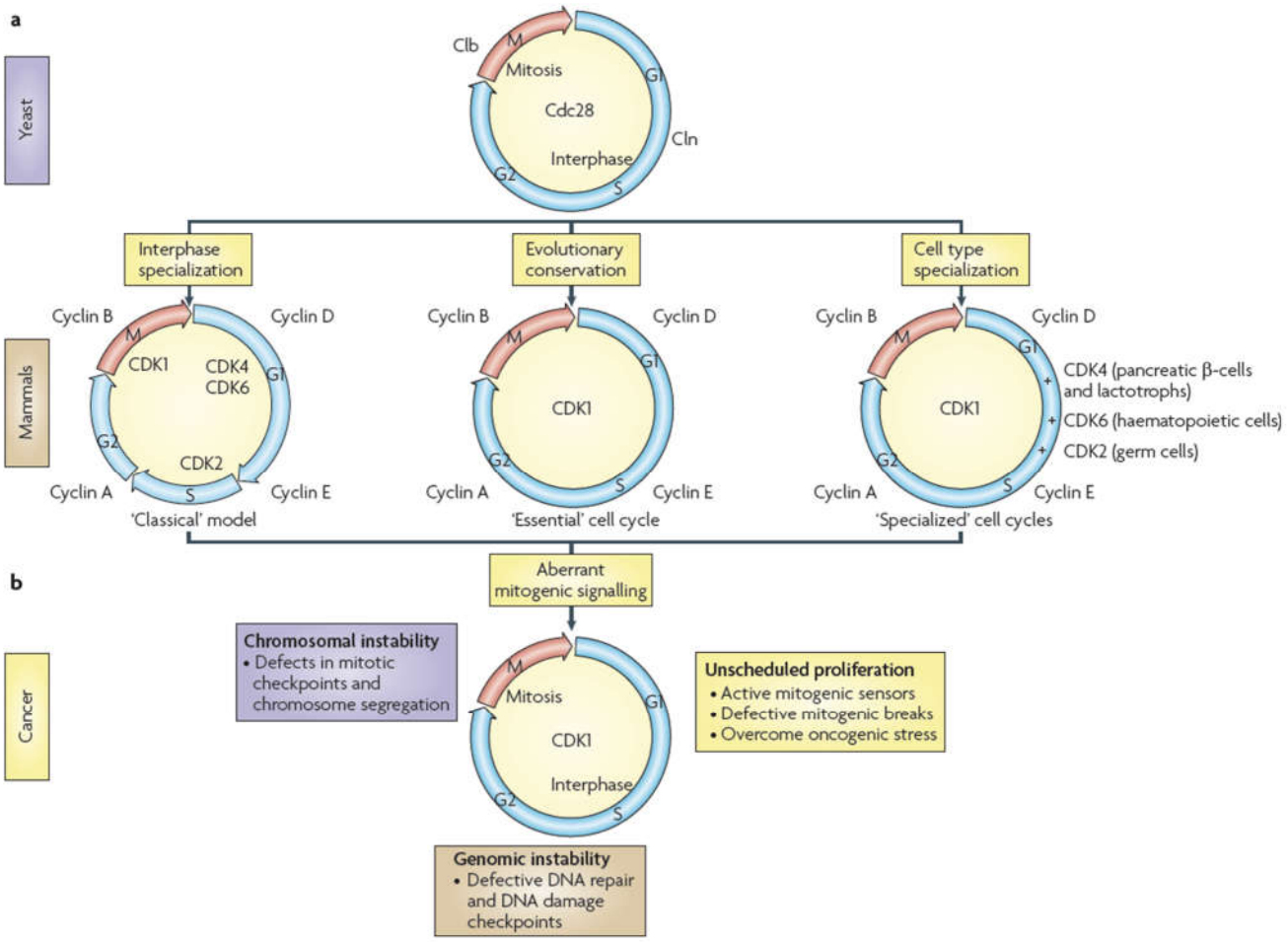

Figure 4: Comparison of the *Saccharomyces cerevisiae* cell cycle with the mammalian cell cycle, highlighting the major defects implicated in human cancer.

a The *S. cerevisiae* cell cycle and three models of the mammalian cell cycle. In the 'classical model' based on biochemical evidence, each of the main events that take place during interphase (G1, S and G2) is driven by CDKs bound to specific cyclins. The 'essential' cell cycle is based on genetic evidence indicating that CDK1 is sufficient to drive proliferation of all cell types up to mid gestation as well as during adult liver regeneration. The 'specialized' cell cycles are based on the unique requirements of specialized cell types for specific CDKs. **b** Unscheduled cell proliferation is induced by aberrant mitogenic signalling or decrease in the threshold for mitogenic signalling. This unregulated cell cycle provokes DNA replication stress, increased mutation rate and ultimately genomic instability. During mitosis, defects within the spindle assembly checkpoint induce deregulation of CDK1 activity that may result in abnormal chromosome segregation. All these defects converge in deregulation of CDK activity, eventually leading to tumour development. Cited from (Malumbres and Barbacid 2009).

1.3.3 Autophagy

1.3.3.1 Classification of autophagy

Autophagy is derived from Greek, which means “eating of self”. It is closely linked to lysosomal degradation; after the discovery of lysosome under electron microscope, autophagy is observed in 1960s and later described as “autophagy” or “pre-lysosome” (Castro-Obregon 2010; Essner and Novikoff 1961).

Autophagy is regulated by highly conserved genes and proteins in yeast as well as in plants, worms and mammals, signifying its evolutionary importance. In recent years there were increasing research studies concerning the relationship between autophagy and disease progression. Dysregulated autophagy is found to be highly related to many neurodegenerative diseases and muscular disorders (Polajnar and Žerovnik 2014), such as Huntington disease (Martin et al. 2015), Alzheimer’s disease (Wolfe et al. 2013), Parkinson’s disease (Xiao et al. 2015), heart failure (Linton et al. 2015) and amyotrophic lateral sclerosis (ALS) (Yang and Klionsky 2010). Increased levels of autophagy is also associated with longevity, such as extending the median life span of mice by 17.2% (Pyo et al. 2013). Nevertheless, the relationship between autophagy and cancer remains ambivalent. Mutation or deletion of autophagic genes such as *BECLIN1* and *ATG5* was found to increase protein aggregates, ROS, DNA damage and induce cancer

cell death; on the other hand, it may also increase cancer incidence (Ma et al. 2016).

Under normal situation, autophagy exists as a housekeeping process via self-degradation, and also serves as an important source of energy supply (Kuma and Mizushima 2010). Autophagy enables the cells to remove misfolded proteins or damaged organelles, such as mitochondria and endoplasmic reticulum. The lysosome-autophagy system is an important part of cellular homeostasis maintenance, along with ubiquitin-proteasome system: the former system removes long-lived proteins and maintains amino acid supply, while the latter removes short-lived, defective proteins (Li et al. 2011).

Under stressed conditions, such as energy deprivation or DNA damage, autophagy plays a dual role. It serves as a pro-survival mechanism to maintain metabolite supply and organelle recycle for cell survival. For example, Atg5 deficient neonatal mice were reported to have a shorter survival time and lower plasma amino acid concentration than normal mice (Kuma et al. 2004). On the other hand, autophagy would switch to promote cell death if the accumulated cell damage exceeds certain threshold. This autophagic cell death is also known as type II programmed cell death (PCD) (Tsujimoto and Shimizu 2005).

Generally speaking, there are three main types of autophagy: macro-

autophagy, micro-autophagy and chaperone-mediated autophagy**.** All of them lead to the translocation of proteins with lysosomes and proteolysis. In macro-autophagy, double membranes are formed in cytosol to sequester the cytosolic components in vesicle called autophagosome, which then fuses with lysosome to form autolysosome (Glick et al. 2010). In micro-autophagy, lysosomal membrane invaginates and uptakes the cytosolic components directly (Li et al. 2011). Both macro- and micro-autophagy can be non-selective or selective [e.g. towards mitochondria (mitophagy) and peroxisome (pexophagy)], although the mechanism of selectivity has not been fully understood. In chaperone-mediated autophagy, chaperone heat shock cognate 70 (hsc70) recognizes five-amino-acid motifs on the target proteins and translocate them into lysosome (Cuervo and Wong 2014). This helps to remove proteins selectively and plays a role in regulating various pathways.

Since macro-autophagy has been more extensively studied and have a wider implication in cancer therapy, we will focus on macro-autophagy hereafter, and referred to it as “autophagy”.

1.3.3.2 The stages of autophagy

The progression of autophagy (macroautophagy) can be divided into five steps **(Figure 5)**: (I) nucleation (phagophore formation), (II) elongation (double

membrane extension), (III) closure (autophagosome formation), (IV) maturation (autolysosome formation) and (V) degradation (protein breakdown) (Kang et al. 2011).

In eukaryotic cells, double membranes named “phagophores” are nucleated in cytosol at the initial stage, which may originate from mitochondria outer membrane, endoplasmic reticulum or plasma membrane (Lynch-Day and Klionsky 2010). Then the phagophore further elongates and forms vesicle called autophagosome, sequestering the selective or non-selective cargo in the process. Next, autophagosome matures by fusing the outer membrane with lysosome forming autolysosome, and its contents and inner membrane are degraded by lower pH and lysosomal hydrolases (Glick et al. 2010). The endosome can also fuse with autophagosome before fusing with lysosome, which is called amphisome (Mauvezin et al. 2015). The pH of autolysosome is maintained by V-ATPase proton pump, which is dependent on ATP. The low pH is crucial for the proteolysis via cathepsin and acid hydrolases (Castro-Obregon 2010). The

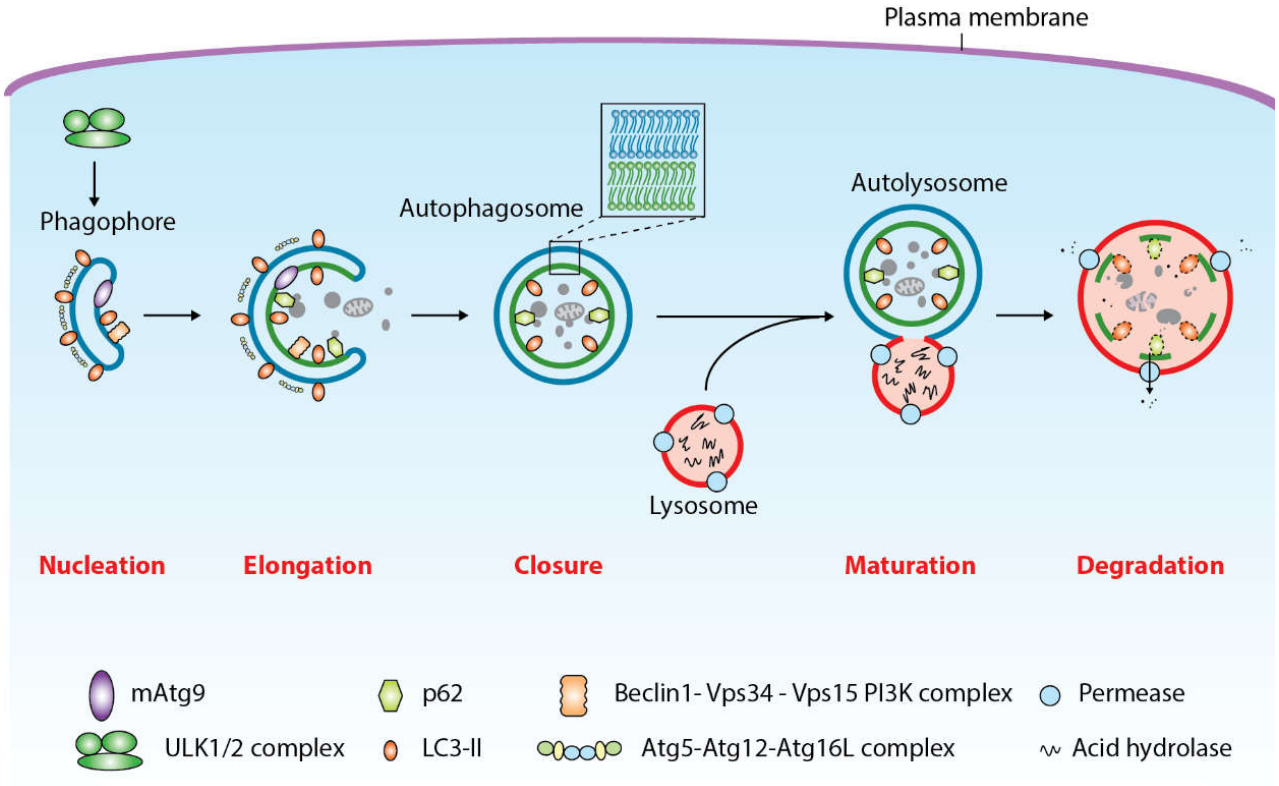

Figure 5: The stages of autophagy in mammalian cells.

From nucleation to degradation, adapted from (Yang and Klionsky 2010).

enzymes break down the inner membrane of autolysosomes and the cargo, and the molecules are released by permease into cytosol for metabolite recycle.

In autophagy, there are intricate interplays between molecules. Many discoveries of the pathway molecules are originated from yeast study. In yeast, there are 38 autophagy-related proteins (Atg), regulated by autophagy-related genes (*ATG*) essential for autophagosome formation.

Molecular interaction in autophagosome formation

In yeast, the major machinery of autophagosome formation includes: (1) Atg1-Atg13/Atg17-Atg29-Atg31 kinase complex, (2) PI3K(III) complex I Atg6-Vps34-Vps15, and (3) two ubiquitin-like protein systems, namely Atg5-Atg12-Atg16 and Atg8. Upon starvation and TORC1 kinase inhibition, Atg13 is dephosphorylated and have stronger affinity to Atg1 and Atg17. Then Atg13 binds to Atg1 and forms Atg1-Atg13 complex, followed by recruitment of Atg17-Atg29-Atg31 complex, forming a scaffold of pre-autophagosomal structure (PAS) (Xie and Klionsky 2007). PAS provides a platform for further protein recruitment (Atg9, Atg6-Vps34-Vps15, Atg2-Atg18 and Atg5-Atg12-Atg16) (Ohsumi 2014). Atg8 is an ubiquitin-like protein, which is essential for membrane elongation. After lipidated to form Atg8-PE by Atg8 conjugation system (including Atg7, Atg3 and Atg5-Atg12 complex), Atg8-PE is further recruited by Atg5-Atg12-Atg16 to PAS, resulting in the elongation of PAS and formation of autophagosome.

In eukaryotic systems, some Atg proteins like Atg5-Atg12 remain conserved, while other exist as homologues, such as ULK1/2 (Atg1 mammalian homolog), Beclin 1 (Atg6 homolog), microtubule-associated protein light chain 3 (namely LC3, Atg8 homolog), P150 (Vps15 homolog) and Atg16L (Atg16 homolog). Besides, the term phagophore is used in place of PAS, although autophagy is initiated in a

similar way **(Figure 5)**.

In mammalian cell, upon sensing stress by the mammalian target of rapamycin complex 1 (mTORC1), ULK1/2 signals the initiation of autophagy. ULK and the class III PI3K complex (Atg6/Beclin 1-Vps34-Vps15) helps to form the phagophore with Atg13 and Atg14L1 (Gottlieb et al. 2015). Of the PI3K complex, Vps34 is the unique class III PI3-Kinase that transforms PI (phosphatidylinositol) to PI3P (phosphatidyl inositol triphosphate), which is essential for membrane extension and Atg recruitment. This catalytic ability of Vps34 is promoted by Beclin 1 interaction (Glick et al. 2010), while the activity of Beclin 1 is in turn regulated by various molecules.

Next, Atg5-Atg12-Atg16L complex is recruited to phagophore, which is thought to induce curvature through asymmetric recruitment of LC3-II (Glick et al. 2010). LC3-II is formed by cleaving LC3 on the C-terminus by Atg4 (LC3-I), then activated and conjugated to PE by Atg7 and Atg3. LC3-II is recruited to the outer and inner surface of autophagosome for membrane elongation. The LC3-II on the outer membrane is released by Atg4 once autolysosome is formed, while the LC3-II on the inner membrane remains throughout the process (Gottlieb et al. 2015). This makes the truncated LC3-II a marker for both phagophore formation and autophagic degradation.

P62

In the process of autophagosome formation, proteins, organelles and cytosol are not only engulfed non-selectively, but also bind and transported selectively by adaptor proteins such as p62/SQSTM1 and NBR1 (Lynch-Day and Klionsky 2010) **(Figure 6)**. Evidences have suggested that p62 is an essential part of autophagy. P62 is an adaptor molecule that contains multiple domains: (1) PB1 and ZZ (Zinc finger) domains that interact with molecules in pathways such as NFκB and ERK (extracellular signal-regulated kinases) (Puissant et al. 2012); (2) UBA domain (ubiquitin-binding domain) that mediates the recognition of ubiquitinated proteins (Klionsky et al. 2014); and (3) LIR (LC3-interacting region) domains that bound to LC3 on phagosomal membrane directly (Pankiv et al. 2007; Puissant et al. 2012). Thus, p62 is able to act as cargo carrier that targets misfoled, ubiquinated protein aggregates and damaged organelles, further carrying them to autophagic degradation (Moscat and Diaz-Meco 2009);(Bjørkøy et al. 2005; Kirkin et al.). Besides, p62 was also found to bind to non-ubiquitinated protein aggregates, facilitating non-selective protein degradation via PB1 domain (Watanabe and Tanaka 2011).

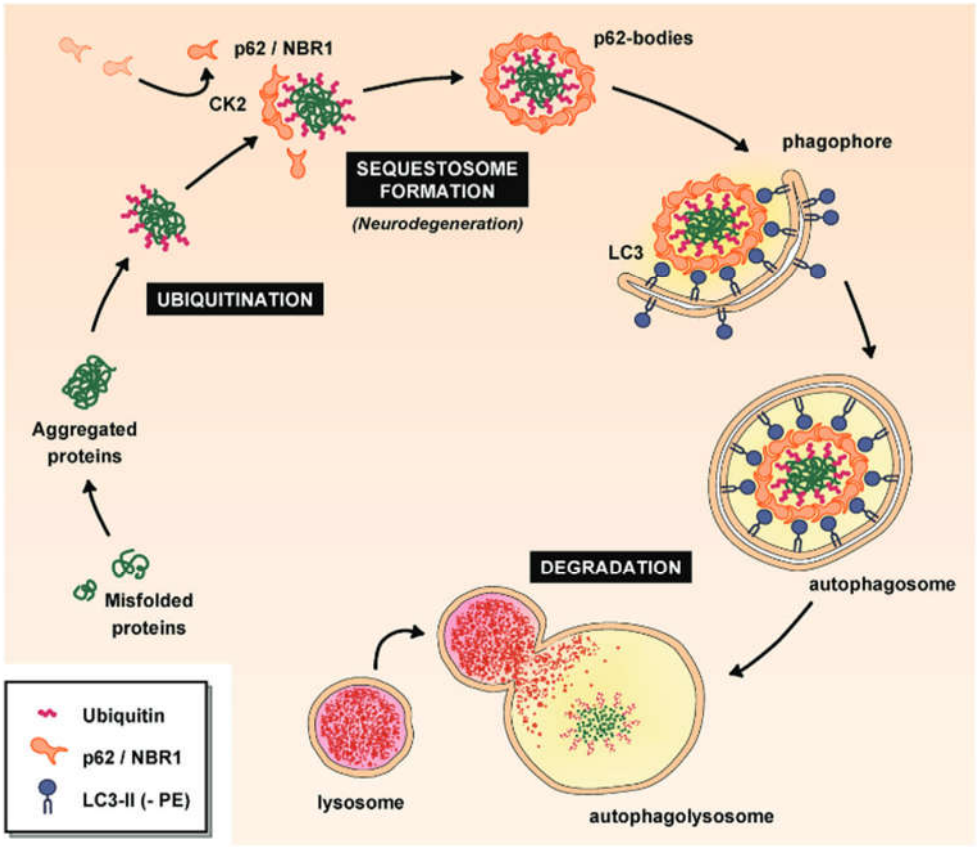

Figure 6: p62 involves in the selective degradation of ubiquitinated proteins.

Cited from (Puissant et al. 2012).

1.3.3.3 Molecular detection and quantification of Autophagy

Atg8-PE and its mammalian homolog LC3-II have been used as indicators of autophagy initiation in yeast and mammalian cells for a long time.

Given that Atg8-PE/LC3-II is truncated from its pro-form at C-terminus by Atg4 at the initiation stage, this molecular event is used to measure Atg4 activity and autophagy initiation. Modified Atg8/LC3 has GFP or phospholipase A2 linked on the C-terminus, and the truncation is shown by loss of fluorescence or fluorogenic assay. Besides, measuring the protein levels of Atg8-PE/LC3-II and their ratios with the pro-forms by Western blot is also a widely used method. Furthermore, the formation of LC3 containing vesicles could be visualized by GFP-Atg8/LC3 transgenic cells or animals as puncta, via immunofluorescence or fluorescence (Klionsky et al. 2012).

Other methods to identify autophagy also include: morphological detection of the lysosomal size expansion and autophagic structures using TEM and fluorescence probes, detecting other Atg protein levels (such as Atg1/ULK, Atg6/Beclin 1) with Western blot, immunochemistry and/or TEM (Gottlieb et al. 2015).

1.3.3.4 Autophagic cell death

Autophagy has remained an elusive subject of study regarding cell death mechanism until recent years. Autophagic structure was found by TEM in dying cells and it was found to contribute to cell death. For example, RNAi of Atg7 and Beclin 1 suppressed cell death in $bax^{-/-}$, $bak^{-/-}$ cells or cells inhibited by caspase inhibitor (Pattingre et al. 2005). Thus, autophagic cell death was listed as one of the programmed cell death mechanisms (type II programmed cell death) (Clarke 1990).

However, there were often ambiguity and arguments regarding the role of autophagy in cell death: whether it plays a causative role or is just one of the simultaneous processes that is trying to rescue the cell from cell death. This is complicated by the various alternative autophagy mechanism, since non-canonical autophagy or autophagic cell death in developmental stage are different from the autophagy under nutrition deprivation (Lindqvist et al. 2015). This should be taken into consideration when evaluating previous studies on the causative role of autophagy in cell death.

In 2012, the Nomenclature Committee on Cell Death (NCCD) has renewed its recommendation on the classification of “autophagic cell death”, in order to

promote the understanding and communication of the scientific community. This recommendation replaced the 2009 definition from morphological-based perspective to molecular and functional based evaluation. Autophagic cell death should "… be suppressed by the inhibition of the autophagic pathway by chemicals" and "… [it] may be advisable to interrogate possible cases of autophagic cell death by knocking down at least two distinct essential autophagic proteins" (Galluzzi et al. 2012).

One of the current opinion is that, autophagy can induce cell death that's completed via other cell death mechanisms, such as apoptosis and necroptosis (programmed necrosis) (Nikoletopoulou et al. 2013; Su et al. 2013). One explanation is that prolonged starvation leads to elevated Bcl-2 phosphorylation, which not only releases Beclin 1 to induce autophagy, but also release the pro-apoptotic Bax/Bak from Bcl-2, activating apoptotic cell death (Wei et al. 2008). The relationship between Beclin 1 and Bcl-2 will be explained in detail later.

Another possibility is that autophagy by itself can complete the process of cell death, which is called autosis. Liu et al. (Liu and Levine 2015) recently found that Tat-Beclin 1 acted as an autophagy-inducer which induced time- and dose-dependent cell death, without overlapping apoptosis or necroptosis. In accordance with NCCD criteria, this autophagic cell death exhibited unique

morphological changes: loss of outer nuclear membrane, ER depletion and increased substrate adherence. This process was inhibited only by Na^+, K^+- ATPase inhibitor. Taking into account the function of Na^+, K^+- ATPase and the connection of nuclear membrane to ER, the authors postulated that under physiological conditions, ER membrane was used selectively for autophagosome formation, and when ER was depleted, the outer nuclear membrane was exploited and triggered autophagic cell death. Further investigation is expected to understand the role of autosis in various processes.

So far, the understanding and research on autophagic cell death is mostly to be unfolded. As our understanding grows, past literatures regarding autophagic cell death should be reviewed with a grain of salt.

1.3.3.5 Interactions between autophagy and apoptosis

Since autophagy is an essential physiological pathway with dual roles in cell survival and cell death, there should be a delicate balance between it and other functions. It was found that autophagy is intertwined with secretion, endocytosis, cell cycle arrest, and other cell death pathways, such as apoptosis and necrosis (Lindqvist et al. 2015). The mechanism of mutual regulation involves a complicated web of interactions, and investigations are still under way to understand it. The known regulatory conjunctures between autophagy and

apoptosis include Bcl-2:Beclin 1 interaction, caspase induced Beclin 1 cleavage, calpain mediated Atg5 cleavage and such (Moscat and Diaz-Meco 2009; Su et al. 2013).

Beclin 1 is the most studied modulator between apoptosis and autophagy. As it associates with class III PI3Kinase to promote the formation of phagophore, its modulation by other cofactors signify the interactions among different pathways. Beclin 1 can be positively regulated by Atg14L, UVRAG, Ambra1 and negatively regulated by Rubicon (Fu et al. 2013; Kang et al. 2011).

Also, as a BH3 family member, Beclin 1 could be associated and sequestered by anti-apoptotic Bcl-2/Bcl-xL, losing its activity (Descloux et al. 2015). Another homolog of Bcl-2, Mcl-1 was also found to be inhibitory (Descloux et al. 2015).

Pattingre et al. found that defective Bcl-2 cannot bind Beclin 1 or inhibit autophagy, and mutant *BECLIN 1* was more potent in autophagy induction (Pattingre et al. 2005). Kang et al. reported that the Bcl-2:Beclin 1 interaction can be inhibited by Bcl-2 and Beclin 1 phosphorylation and Beclin 1 ubiquitination (Kang et al. 2011). Other BH3-only proteins such as Bax, Bim, Nip3, Noxa and Puma can also interact with Bcl-2 and dislodge Bcl-2:Beclin 1 interaction (Descloux et al. 2015), while Beclin 1 can in turn release pro-apoptotic Bax/Bak from Bcl-2 and induce apoptosis (Sun et al. 2010) **(Figure 7)**.

Furthermore, caspases have ambivalent effects on autophagy induction and inhibition. Beclin 1 has been found to be cleaved by caspase -3, -7 or -8 and failed to induce autophagy (Djavaheri-Mergny et al. 2010); the subsequent C-terminal fragment of Beclin 1 was found to localize to mitochondria and induce mitochondrial apoptosis. In contrast, caspase -3 could cleave Atg4D, which in turn cleaved Atg8/LC3 and increased autophagic activity (Djavaheri-Mergny et al. 2010).

Besides, autophagy has been found to reciprocally degrade active caspase -8 (Hou et al. 2010) and downregulate proapoptotic Bad and Bim, inhibiting apoptosis (Zhou et al. 2014).

Autophagic molecules could promote apoptosis under certain conditions. It was reported (Galluzzi et al. 2012) that some Atg proteins (such as Atg5 and Atg6) could be converted to pro-death proteins when cleaved proteolytically. For example, calpain-cleaved Atg5 fragment aggregated Bcl-xL and induced intrinsic apoptosis. Atg5 could also regulate caspase 8-dependent apoptosis (Lindqvist et al. 2015). To sum up, the relationship between autophagy and other cellular processes awaits further investigation.

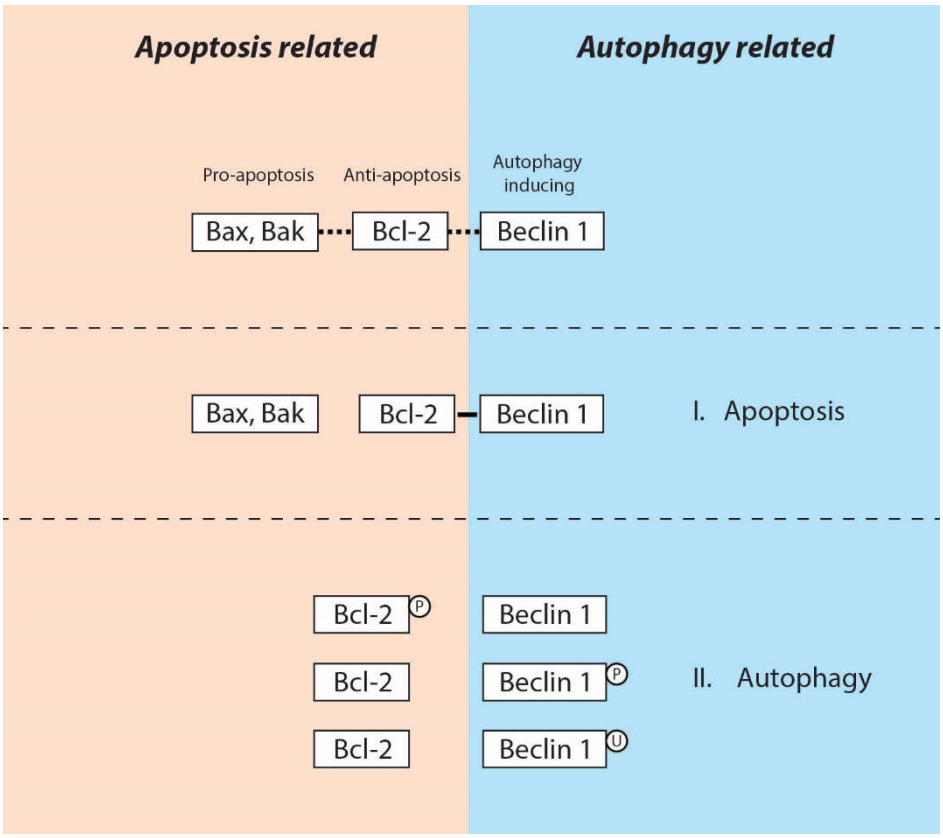

Figure 7: The interaction between Bcl-2 and Beclin 1

Bcl-2 can bind with Beclin 1 or Bax/bak, inhibiting autophagy or apoptosis, respectively. When Bcl-2 bind with Beclin 1, Bax/bak will be released, leading to apoptosis, while autophagy induced by Beclin 1 will be inhibited. Phosphorylation of Bcl-2, Beclin 1 or ubiquitination of Beclin 1 can dislodge Bcl-2:Beclin 1 interaction, leading to autophagy.

1.4 Cellular uptake behavior

1.4.1 Active cellular uptake

There are many routes for cells to actively engulf or uptake extra-cellular

molecules, which are essential to sustain metabolism, sample extracellular environment, elicit immune response and regulate cell surface components. In the past few decades, the understanding of cellular uptake behavior has been expanded by new technologies. There is no “fixed” classification on cellular uptake processes, but current understandings based on the receptors could categorize the processes into three major types **(Figure 8)**:

1.4.1.1 Phagocytosis

Phagocytosis exists mostly in immune cells such as macrophages, monocytes, and neutrophils (dos Santos et al. 2011), facilitating rapid immune response to engulf cell debris and apoptotic cells as well as tackle pathogen infections. In specialized cells such as macrophages, phagocytosis is carried out for uptaking external materials less than 1 μM within an hour (Kuhn et al. 2014), whereas in non-specialized cells such as epithelial cells and fibroblasts, the process takes much longer time, if ever exists. Phagocytosis also needs receptors for

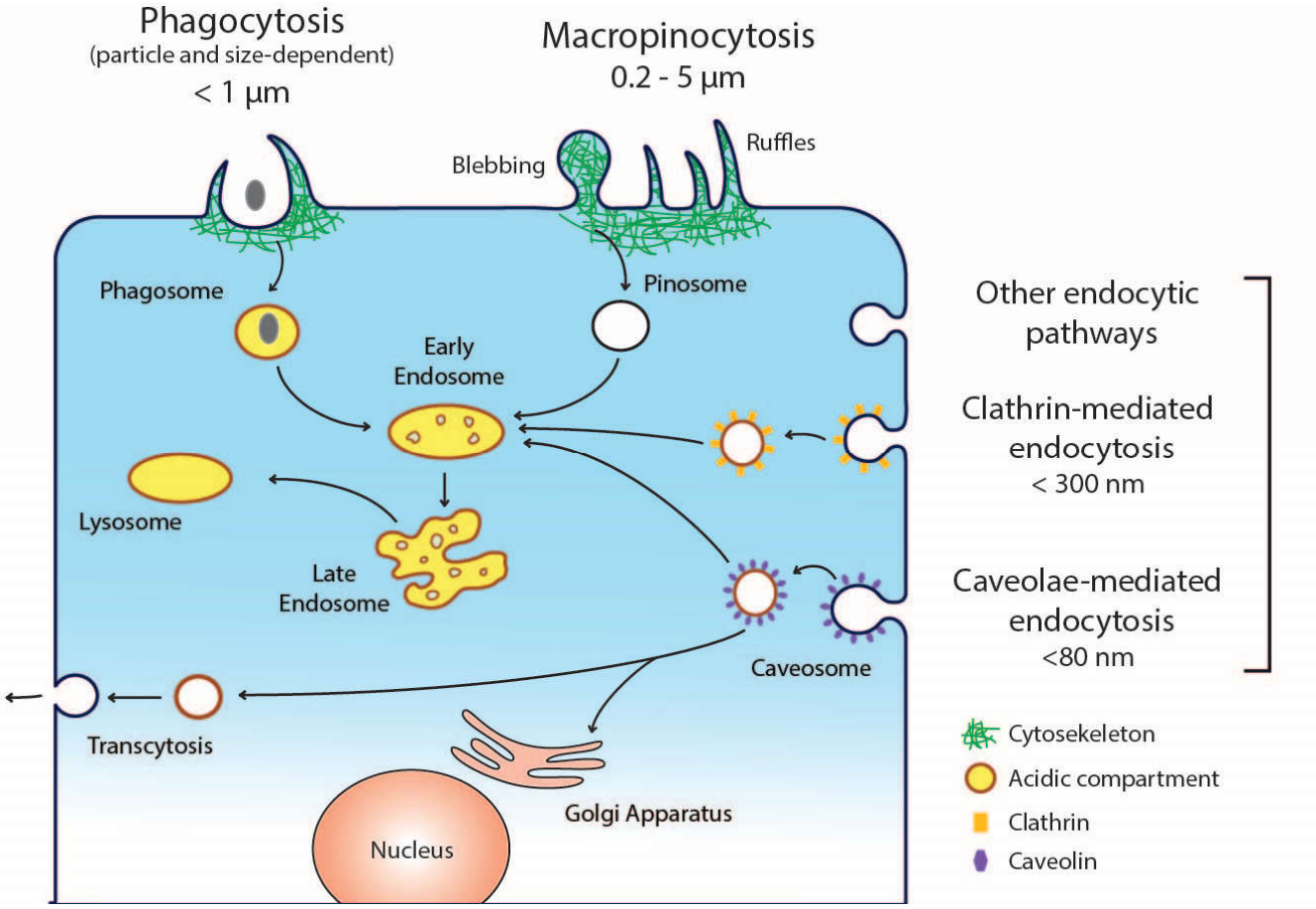

Figure 8: The major active cellular uptake pathways.

Adapted from (Canton and Battaglia 2012).

internalization, and the phagosome formation requires actin polymerization, PtdInsP3K activity, and Rho-family GTPase (Bohdanowicz and Grinstein 2013).

1.4.1.2 Endocytosis

Endocytosis is a vesicle forming process that can be divided into clathrin-mediated endocytosis (CME) and clathrin-independent endocytosis (CIE)

pathways. The latter consists of several pathways, such as caveolae-mediated and flotillin-dependent pathways (Sandvig et al. 2011).

Clathrin-Mediated Endocytosis

Clathrin-mediated endocytosis is the best studied cellular uptake process, in which the budding of clathrin-coated pits forms vesicles, upon the initiation of adaptor proteins and subsequent recruitment of regulatory proteins (such as dynamin and synaptojanin) (Lim and Gleeson 2011). The vesicles then transport cargos into early endosomes and fuse with late endosome and lysosome in less than 30 minutes (Chan et al. 2009; dos Santos et al. 2011).

Since CME is the normal pathway to uptake low density lipoprotein (LDL) and transferrin (Tf) (Kou et al. 2013), LDL and Tf are very often used as the markers for clathrin-mediated endocytosis. Some commonly used inhibitors for it include: hypertonic sucrose, potassium depletion, cytosol acidification, chloropromazine (CPZ), chloroquine, and Dynasore (Dutta and Donaldson 2012).

Clathrin-Independent Endocytosis

CIE pathways is independent of clathrin, adaptor proteins, and dynamin. Caveolae-dependent endocytosis is one of the most well-known CIE, which involves flask-shaped invaginations (~50 - 100 nm) on cell membrane bearing

caveolin-rich microdomains. Caveolin is lipidated in Golgi apparatus before transporting to the plasma membrane, thus like other CIE pathways that depend on lipid rafts oligomerization, caveolae-dependent endocytosis could be inhibited by cholesterol depletion or lipid raft composition alteration, (Sánchez-Wandelmer et al. 2009; Weissig and D'Souza 2010).

It is found that after merging with early endosome, the content of the caveosomes can be transported to trans-Golgi network (TGN) (Canton and Battaglia 2012; Kirkham et al. 2005). Thus, unlike clathrin-mediated endocytosis, cargoes in caveolae-dependent pathway may not go through degradation (Panariti et al. 2012), which is sometimes exploited by pathogens for infection. Caveolae-mediated endocytosis is also a key factor in the trancytosis of epithelial cells, in which vesicles are transported between the apical side and the basolateral side of the polarized cells (McIntosh et al. 2002).

Caveolae-mediated endocytosis is usually labelled by cholera toxin beta subunit or Shiga Toxin (Kou et al. 2013), while CIE can be inhibited by cholesterol depletion (MβCD, filipin, and lovastatin) or inhibition of tyrosine kinase (genistein) (Ivanov 2014).

1.4.1.3 Macropinocytosis

Macropinocytosis is similar to phagocytosis. It involves large scale actin-

remodeling and PtdInsP3K activity for the ruffle of the plasma membrane and ingestion of fluids and solutes in vesicles of 0.2-5 μM (Bohdanowicz and Grinstein 2013). It provides a way to internalize large molecules non-selectively such as viruses and nanoparticles (Iversen et al. 2012). It is a signal-dependent process in response to growth factors and cytokine stimulation, such as EGF. Macropinocytosis is linked to cell motility, antigen presenting and pathogen entry (Lim and Gleeson 2011). Fluid phase markers (such as horseradish peroxidase, Lucifer yellow and dextran) can be used as indicators of macropinocytosis, while ethylisopropylamiloride (EIPA), cytochalasin D (Gold et al. 2010), latrunculin B, rottlerin (Sarkar et al. 2005) and amiloride (Koivusalo et al. 2010) are its known inhibitors.

1.4.1.4 Passive cellular uptake

All of the above-mentioned cellular uptake behaviors are “active” processes. Since they require consumption of ATP (Weissig and D'Souza 2010), they can be inhibited by low temperature or sodium azide, an inhibitor of mitochondrial respiration (Kou et al. 2013; Nhiem and Thomas 2013). It is hypothesized that low temperature could inhibit the motility of cell surface receptors and fusions between vesicles and lysosomes (Dunn et al. 1980; Edelman et al. 1973; Ivanov 2014), thus affecting active endocytosis.

Yet there is another form of cellular uptake process under the energy deprived situation, called “direct translocation”. This energy-independent passive cellular uptake pathway have been reported in recent studies (Treuel et al. 2013).

The passive cellular uptake were found to either affect the integrity of cell membrane, inducing cell toxicity (Treuel et al. 2013), or enhance the flexibility of lipid bilayers without leaving transient membrane disruption (Wang et al. 2012). Determining factors include size, surface charge density (Lin et al. 2010) or surface charge patterns (Verma et al. 2008). Besides, the efficiency of the passive cellular uptake was size-dependent: dos Santos et al. (dos Santos et al. 2011) found that with 30 min preincubation and 2 h incubation at 4°C, larger sized carboxylated-modified polystyrene NP showed higher cellular uptake efficiency.

1.4.2 Factors that affect NP uptake

The uptake of nanoparticles can be affected by many factors, such as size, shape, surface charge, composition and cell types (Li et al. 2015).

Size can not only affect the internalization pathways as mentioned before, it also affects the bio-distribution and elimination of NP *in vivo* (Blanco et al. 2015; Rejman et al. 2004; Shang et al. 2014). NP with size > 5 μm accumulates mostly in the spleen and liver; NP < 5 nm is excreted easily by the renal clearance system.

Besides, NP with size between 100 nm to 200 nm was found to easily accumulate in the tumor tissue due to the EPR effect. In addition, smaller sized NP had the tendency to enter cell nuclei (Huo et al. 2014), which might be attributed to composition of NP (Shang et al. 2014).

Shape could also affect the cellular uptake of NP. Spherical NP was found to enter the cells more easily than rod followed by cube and disk shape (Li et al. 2015). The reason may be the spherical shapes require minimal membrane bending energy barriers (Carnovale et al. ; Li et al. 2015).

Since the cellular membrane is negatively charged, it might have higher affinity towards cationic NP. Thus, it is hypothesized that cationic NP would have better uptake and cytotoxicity than that of neutral or negatively charged NP, (Fröhlich 2012; Yu et al. 2012). However, Treuel et al. (Treuel et al. 2013) reported that ions and proteins in buffer or medium solutions would form a corona around the NP, neutralizing the surface charge and suppress the actual interaction and uptake.

Previous study (dos Santos et al. 2011) found that different cell lines showed different uptake mechanisms, responding differently to the same nanoparticles. Besides, the surface modification has also been reported to affect the composition, charge and topology of NP, thus affecting the internalization and

intracellular trafficking (Kou et al. 2013; Oh and Park 2014).

1.5 Objectives of our research

Pleurotus tuber-regium (Fr.) Singer is a medicinal mushrooms distributed in tropical and subtropical regions like China, Australia and Nigeria (Oso 1977; Wong and Cheung 2009). This basidiomycete is the only *Pleurotus* species that can produce mushroom sclerotium, a compact mass of mycelium with spherical to oval shape around 10-25 cm in diameter (Wong and Cheung 2009).

Our research team has been extensively studying the polysaccharides and polysaccharide-protein complex (PSP) isolated from the sclerotia of *P. tuber-regium*. We recently discovered that its hot water extract PSP, also called PTR, can decorate SeNP and produce highly stable and size controllable PTR-SeNP. PTR-SeNP could be prepared via a simple redox system, in which sodium selenite and ascorbic acid were used as the Se source and reducing agent (Wu et al. 2012).

In previous studies, PTR-SeNP exhibited the highest dose-dependent anti-proliferation effect on MCF-7 human breast cancer cells, among four different cancer cell lines (MCF-7, A549, HepG2 and A375). Its IC_{50} value was 3.7 μM, which was about 40 times lower than that of the normal cell (Hs68 human foreskin fibroblasts; IC_{50} = 127.8 μM). The PSP surface decoration not only stabilized the SeNP, but also significantly enhance their cellular uptake and dose-dependent anti-proliferative effect on MCF-7 cells by inducing apoptosis (Wu et al., 2012).

The study also found that PTR surface decoration significantly enhanced the cellular uptake efficiency of SeNP by the MCF-7 cells (2-4 folds) in both time- and dose-dependent manner, and the PTR-SeNP was mainly localized in lysosomes of MCF-7 cells as early as 10 min (Wu et al. 2012).

As previous reviewed, there is an increasing need for novel therapeutic agents for colorectal cancer treatment. In the meantime, PTR-SeNP was found to be effective anti-cancer agent in multiple cancer cells. The lack of investigation on the anti-cancer mechanism of PTR-SeNP on colorectal cancer poses an interesting knowledge gap to be investigated. We would like to know:

(a) Whether PTR-SeNP has inhibitory effect on CRC cancer cells?

(b) If so, what are the inhibitory mechanisms involved?

(c) Furthermore, does PTR-SeNP have synergistic effect with the widely used CRC drugs, such as 5-FU?

(d) On the other hand, given the selectivity of PTR-SeNP on MCF-7 cancer cells, what are the cellular uptake mechanisms involved in the process, such as passive uptake and endocytosis?

Based on the existing understanding on the anti-cancer mechanisms and cellular uptake pathways, we devised the following research design to address the

questions:

1-1. In terms of anti-cancer mechanisms, the *in vitro* anti-proliferative effect of PTR-SeNP was determined by screening six different human colorectal cancer cell lines.

1-2. Subsequently, cell inhibition mechanisms including apoptosis, cell cycle arrest and autophagy were further investigated in the most susceptible cells (HCT 116).

1-3. Next, the combined effect of PTR-SeNP with existing CRC drug 5-FU, an apoptosis inducer, is investigated to see if synergistic effect exist.

2. In terms of cellular uptake mechanisms, the organelles will be labelled by organelle dyes, and the co-localization of nanoparticles will determine targeted organelles. The use of chemical inhibitors of uptake pathways will help to reveal the cellular uptake mechanisms involved.

A.

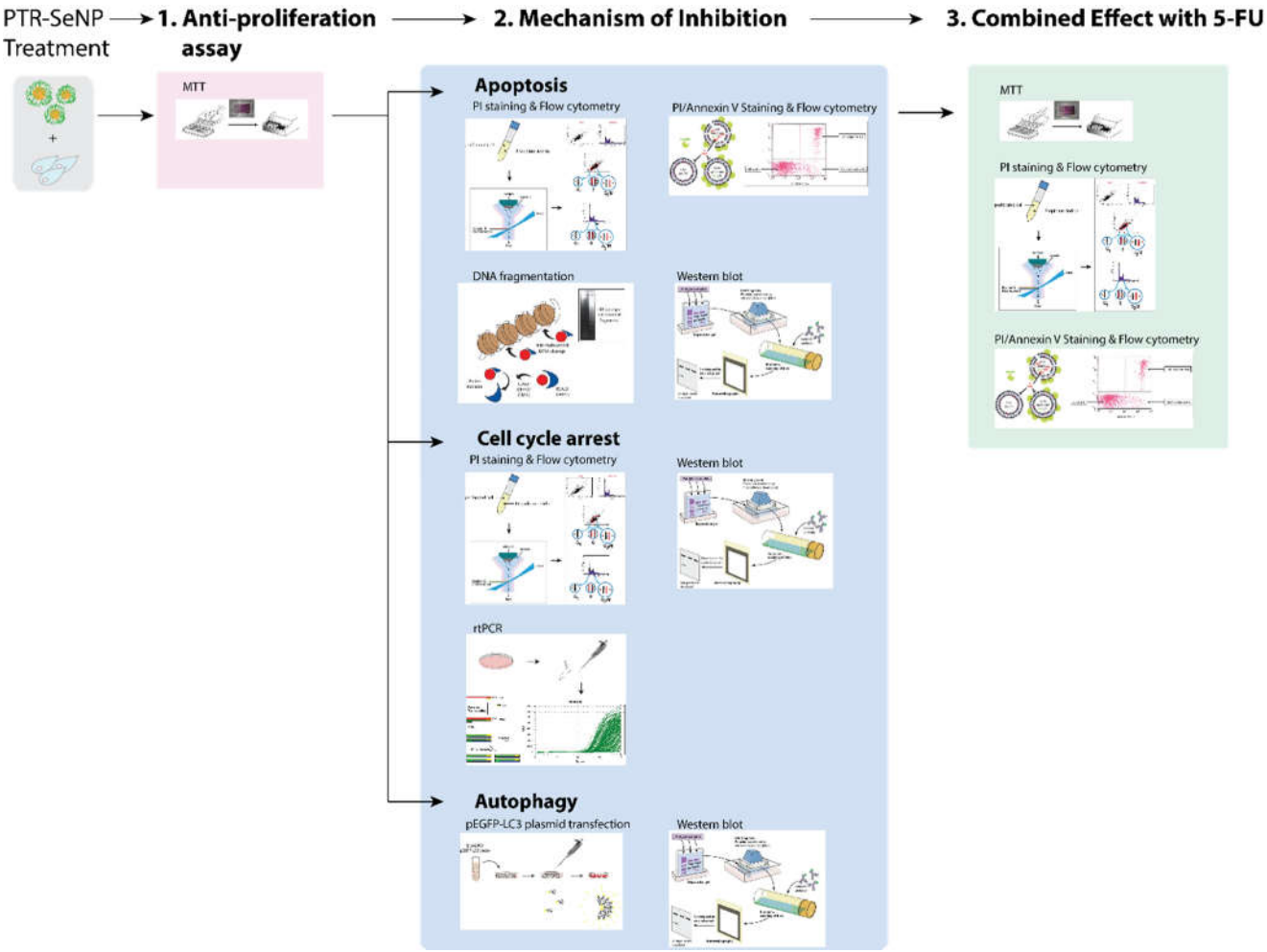
PTR-SeNP Treatment
1. Anti-proliferation assay
MTT
2. Mechanism of Inhibition
Apoptosis
PI staining & Flow cytometry
PI/Annexin V Staining & Flow cytometry
DNA fragmentation
Western blot
Cell cycle arrest
PI staining & Flow cytometry
Western blot
rtPCR
Autophagy
pEGFP-LC3 plasmid transfection
Western blot
3. Combined Effect with 5-FU
MTT
PI staining & Flow cytometry
PI/Annexin V Staining & Flow cytometry

B.

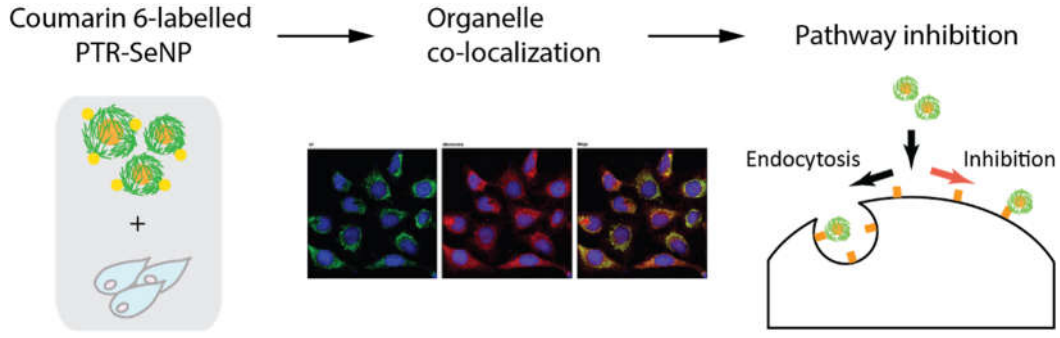
Coumarin 6-labelled PTR-SeNP
Organelle co-localization
Pathway inhibition
Endocytosis
Inhibition

Figure 9. Research design of the study.

(A) Flow chart of the investigation of the proliferation inhibition mechanisms of PTR-SeNP. Various cell lines will be screened to determine the anti-proliferation effect of PTR-SeNP on CRC cancer cells. Next, the mechanisms of inhibition: apoptosis, cell cycle arrest and autophagy will be investigated. Then the combined effect with existing cancer drug 5-FU will be tested.

(B) Flow chart of the investigation on cellular uptake mechanisms. Organelle co-localization and inhibition studies will help to determine the targeted organelles of PTR-SeNP and its pathways of entry.

It is anticipated that findings of this study could provide significant insights on developing the PTR-SeNP into the next generation anti-cancer agent. Our long term goal is to develop an economical, safe and evidence-based anti-cancer agent for our community, hereby alleviating the now spiraling cost of cancer treatments in the local public healthcare system.

Chapter 2 - Materials and Methods

2.1 PTR-SeNP and coumarin-6 labelled PTR-SeNP (C6-PTR-SeNP)

According to the award-winning and patented nanotechnology of our lab, PTR-SeNP (Se concentration: 1.35 ± 0.12μM; particle size: 80.0 ± 12.3 nm) were prepared by standardized procedures using the water-soluble PSPs isolated from the tiger milk mushroom sclerotia cultivated in our own facilities. In brief, aqueous mushroom PTR solution (0.25%) was mixed with sodium selenite solution (25 mM) under magnetic stirring prior to drop-wise addition of freshly prepared ascorbic acid solution (100 mM). After reconstituting to 25 mL with ultrapure water, the mixture was stirred for further 12 h under room temperature followed by dialysis (Mw cutoff = 8,000) until Se content could not be detected by inductively coupled plasma optical emission spectrometry (ICP-OES) analysis in the outer solution. Then the concentration of Se and particle size were determined by ICP-OES as well as Nanosight NS 300, respectively (Wu et al., 2012).

Coumarin-6 labelled PTR-SeNP was synthesized in a similar fashion, with coumarin-6 added to the sodium selenite and PTR solution before adding ascorbic acid for reduction.

2.2 Reagents

Rapamycin (R-5000) was bequeathed by Dr. Wu Xiaoqian and was from LC Laboratories. MTT, propidium iodide were purchased from Invitrogen, Clarity Western ECL Substrates, 30% Acrylamide/Bis solution were acquired from Bio-Rad. Bicinchoninic acid, copper(II) sulfate solution, bovine serum albumin, TEMED, chloroform, ethanol and isopropanol were obtained from Sigma. RIPA buffer were obtained from Cell Signaling.

The following primary antibodies were purchased from Cell Signaling Technology and diluted by 1:1,000 for immunoblotting: Cyclin D1 (#2978), Cyclin D3 (#2936), cdc2/CDK1 (#9116),CDK2 (#2546), CDK4 (#12790), p-p42/44MAPK(T202, Y204) (#4370), Akt(PAN) (#4691), p-Akt(S473) (#4060), Bax (#2772), Bcl-2 (#2870), p-Bcl-2 (T56) (#2875), p-Bcl-2(S70) (#2827), Bcl-xL (#2764), Caspase-3 (#9665). Secondary anti-mouse HRP antibody (#7076P2) and anti-rabbit-HRP antibody (#7074P2) were purchased from Cell Signaling and diluted by 1:10,000 with 5% BSA/TBST for immunoblotting. We thank Dr. Wu Xiaoqian for her generous gift: primary antibody LC3 (#L7543) from Sigma Aldrich, Beclin 1 (#3738) and p62 (#5114) from Cell Signaling.

pEGFP-N3-GFP-LC3 plasmid with kanamycin resistant gene is a generous gift from Dr. Zhao Yanxiang's Lab. Protein kinase K, lysis buffer and

phenol:chloroform:isoamyl alcohol (25:24:1) were generous gift from Dr. Vincent Ken's Lab. Forward and reverse primers for Cyclin D1 and human GAPDH are generous bequeath from Dr. Lo Wai-hung's Lab (Lam et al. 2011).

2.3 Cell culture

HT-29 (ATCC: HTB-38), SW1116 (Dukes' type A, ATCC: CCL-233), HCT-15 (Dukes' type C, ATCC: CCL-225), and COLO 205 (Dukes' type D, ATCC: CCL-222) were obtained from Dr. Lo Wai-Hung's lab; HCT 116 (ATCC: CCL-247) and SW620 (Dukes' type C, ATCC: CCL-227) were obtained from Dr. Ben Ko's lab and Dr. Chen Tianfeng's lab, respectively.

Cells were maintained in modified RPMI-1640 media (SW1116, HCT-15, COLO 205 and SW620) or McCoy's 5a medium (HCT-29 and HCT 116) supplemented with 10% (v/v) fetal bovine serum (FBS), 100 I.U./ml penicillin and 100 μg/ml streptomycin. Cells were incubated at 37 °C and 5% (v/v) CO_2 in a humidified incubator.

2.4 MTT cell viability assay

Cells at exponential phase were seeded into 96-well plates (100 μl/well) at densities of 2.0 – 4.5 x 10^4 cells/ml depending on growth rate. Peripheral wells

were not used and filled with equal amount of PBS. After 24 h for adhesion, 100 µl complete medium containing stock solution of PTR-SeNP, 5-FU or vehicle was added to each well to obtain the desired final concentration. Each concentration was at least triplicated. The plate was then incubated for 72 h before 20 µl of MTT (5 mg/ml in PBS) was added. Plates were further incubated at 37 °C for a further 2 – 4 h until crystallization was observed under microscope. Then the media was carefully removed and 100 µl DMSO was added for the crystals to fully dissolve. Absorbance at 560 nm was measured promptly. The readings were blanked against DMSO and normalized with the control.

2.5 Flow cytometry analysis of cell cycle with PI

Cells at a density of 5 x 10^4 cells/ml were plated in 100 mm dishes and allowed to recover. After treatment for intended periods of time, cells as well as supernatant were harvested by trypsinization, and washed in icy cold PBS and centrifuged at 3,000 rpm for 5 min. The pellet was resuspended in 300 µl of PBS and ice cold ethanol was added dropwise to a final concentration of 70%. Samples were stored at -20 °C overnight for further perforation. Prior to analysis, samples were washed with PBS and incubated with 50 µg/ml of Propidium Iodide (PI) (Sigma) and 50 µg/ml of RNase A (Invitrogen) for 30 min at room temperature.

Since the intercalation between PI and DNA is reversible and dependent on cell density, equal cell density was adjusted for each sample.

Samples were analyzed on a BD FACSVerse analyzer. No less than 10,000 events were recorded per sample. For data analysis, forward/side scatter plot was gated to exclude debris and PI-A/PI-W was gated to exclude doublet cells. A statistical fit and cell cycle analysis was done using Flowjo 7.6 (Tree Star Inc.).

2.6 Flow cytometry analysis of apoptosis with annexin V/PI double stain

Cells were plated in 100 mm dishes at density of 5 x 10^4 cells/ml and allowed to attach before intended treatment. Cells as well as supernatant were harvested and washed with PBS, and ApoDETECT Annexin V-FITC/PI detection kit (Invitrogen) was used.

The double stained cells were analyzed immediately on a BD FACSVerse analyzer. No less than 10,000 events were recorded per sample. Analysis was performed by Flowjo 7.6 software (Tree Star Inc.) for quadruple gating on FITC-A/PI-A plot, based on untreated control sample. An additional gating on FITC-A/FITC-W plot was used to exclude doublets.

2.7 Protein extraction and SDS-PAGE immunoblotting

6 x 10^5 cells were plated in 100 mm dish and allowed to recover before treatments. Then the cells were washed with PBS, lysed on ice in RIPA buffer (CST 9806S) supplemented with PMSF protease inhibitor (1mM) and protease inhibitor cocktail (5.2 mM AEBSF, 4 µM Aprotinin, 200 µM Bestatin, 70 µM E-64, 100 µM Leupeptin, and 75 µM Pepstatin A). Cells were incubated on ice for 20 min, scraped and collected into pre-cooled EP tubes, followed by high speed centrifugation (12,000 x g, 15min, 4 °C) to obtain the total protein in the soluble fraction. Detached cells after long period of treatment were collected into a centrifuge tube with the culture medium, centrifuged, washed with icy cold PBS, lysed, and combined. The samples were stored at -20 °C.

To quantify total amount of protein, bicinchoninic acid (BCA) assay was used with bovine serum albumin (BSA) as standard. The standard curve from the average of duplicates should cover the results measured, and $R^2 > 0.99$ was required. According to the concentration of total protein, lysates were adjusted to the same concentration with 2 x Laemmli sample buffer (Sigma) and Mili-Q water and denatured at 95 °C for 10 min. Samples were stored at -20 °C until further use.

The denatured proteins were resolved by SDS- PAGE gel (15 % separation gel,

6 % stacking gel). The same amount of total protein was loaded onto each lane, and no more than 40 µg loaded per lane. Pre-stained protein ladder was adjusted by 1 x loading buffer to the same volume before loading. The resolved proteins were transferred to PVDF membrane (100 V, 90 min) and blocked by 5% BSA for 1 h before immunoblotting by primary antibody at 4 °C overnight. After sufficient washing with 0.1% TBST, the membrane was incubated with horseradish peroxidase (HRP)-conjugated secondary antibody for 1 h at room temperature. After sufficient washing, substrate for chemiluminescence was added. Image was captured on Azure c500 imager. The acquired digital picture was processed by Image Studio Lite 5.2 (LI-COR Biosciences) for rolling disk background subtraction and intensity quantification.

2.8 pEGFP-LC3 plasmid amplification and purification

pEGFP-N3-GFP-LC3 plasmid carrying kanamycin-resistant gene was amplified by *E. coli* cells and purified by QIAGEN Plasmid Midi Kit.

Frozen competent *E.coli* cells were removed from -80 °C and thawed on ice. 50 µl of competent cells were added slowly to an Eppendorf tube containing 0.5 µl plasmid without further pipetting. The mixture was incubated on ice for 30 min and heat shocked at 42 °C for 90 s, terminated with immediate cool down on the

ice for 2-3 min. 500 µl of LB media without antibiotics was added to the tube, and the mixture was incubated at 37 °C with rigorous shaking at 250 rpm for 1 h. 150 µl of the mixture was spread on an agar plate with kanamycin (50 µg/ml) and incubated overnight at 37 °C.

Single colony from the plate was picked and inoculated into 1 ml LB with kanamycin. After 8 h incubation, turbidity should be observed and 100 µl of the mixture was inoculated into 50 ml LB containing selection marker for incubation overnight. The *E.coli* was lysed and plasmid DNA was purified according to QIAGEN plasmid midi. After the purified plasmid DNA was precipitated by isopropanol, the pellet was washed with 2ml of 70% EtOH and centrifuged at 15,000 x g, 4 °C for 10 min. The pellet DNA was air-dried until it became translucent, prior to redissolving in TE buffer.

The purity and concentration of the plasmid DNA was measured by NanoDrop Lite spectrophotometer. The molecular weight was measured by 1 % agarose gel electrophoresis at 150V for 20 min, with 1Kb Plus DNA Ladder. The plasmid DNA was stored at 4 °C before use.

2.9 Plasmid transfection with lipofactamine 2000

For Lipofactamine 2000 transfection, cells were seeded in 6 well plates in

complete medium without antibiotics. At confluency of ~60 - 70%, the medium was replaced with fresh complete medium without antibiotics. At a ratio of 3 µl Lipo 2000 to 1 ug DNA, DNA and Lipo 2000 were dissolved in 50 µl of Opti-mem medium, respectively. After 5 min, the DNA was added to Lipo 2000 and incubated for 15 min at room temperature. Then the DNA-Lipofactamine 2000 complexes was added directly to cells in culture medium with gentle rocking. The cells were incubated overnight before seeding into confocal dish for further treatment.

2.10 Plasmid transfection by electroporation

Neon transfection system (Invitrogen) was used for plasmid DNA transfection with higher efficiency. Cells in exponential phase was harvested and washed with PBS, and resuspended in PBS at the density of 5 x 10^6 cells/ml. After mixing the cells with plasmid to desired concentrations recommended by protocol (5 x 10^6 cells/ml), the mixture was loaded onto 100 µl electroporation pipette tip (Invitrogen) and pulse was applied according to cell line recommendation (1,530 V, 20 ms, 1 pulse). Then the cells were immediately seeded in pre-incubated medium in confocal dish at desired density (1 x 10^5 cells /ml).

Transfected HCT 116 cells were treated with PTR-SeNP (400 nM) and rapamycin (10 μM) as autophagy inducer, and stained with DAPI (2 μg/ml) for 30 min before visualization under Leica SP8 confocal microscope.

2.11 DNA extraction and agarose gel electrophoresis

HCT 116 cells were seeded and treated in 35 mm dish. Cells were collected via trypsinization into EP tubes. Cells were washed with PBS and lysed by 500 μl lysis buffer and 200 μg/ml protein kinase K. The mixture was incubated at 55 °C overnight with shaking. Undissolved debris were centrifuged at 4 °C, 15,000 rpm for 5min, and liquid phase was transferred to another EP tube. Equal volume of phenol:chloroform:isoamyl alcohol (25:24:1, vol:vol:vol) was added and mixed by inversion. After high speed centrifugation, liquid phase was transferred and DNA was precipitated by adding 0.7 volume of isopropanol. Then DNA was pelleted by high speed centrifugation at 4°C, 15,000 rpm for 10 min and washed with ethanol.

The pellet was air-dried and re-dissolved in TE buffer. The purity and concentration was quantified by NanoVue spectrometer (GE) and equal amount of DNA was loaded to 1.2 % agarose gel with DNA ladder for electrophoresis.

2.12 RNA extraction and real time-PCR analysis

At designated time points (0, 3, 6, 9, 12, 24, 48 and 72 h), total RNA was extracted from cells that were untreated or treated with PTR-SeNP. 1 ml of RNAiso Plus (Takara) was added after the medium was removed, and after shaking for 15 mins, transferred to RNase-free Eppendorf tube. 0.2 volume of chloroform was added and mixed by inversion. After centrifugation at 4 °C, 12,000 rpm for 15 min, the aqueous phase was transferred carefully to another tube, and equal volume of isopropanol was added and mixed by inversion. After centrifugation at 4 °C, 12,000 rpm for 15 min, the precipitate was washed by 70 % ethanol and stored in ethanol at -20 °C.

For cDNA synthesis, total RNA precipitate was air-dried and dissolved in RNAse-free water. Its purity and concentration was measured by NanoVue spectrometer (GE). 2 μg RNA per sample was reversely transcribed to cDNA by High Capacity cDNA Reverse Transcription Kit (Applied Biosystems). The samples were stored at -20 °C.

All RT-PCR were performed on an iQ5 detection system (Bio-Rad). For each reaction, 1 μl of cDNA, 400 nM of forward and reverse primers, and 10 μl of SsoFast EvaGreen Supermix (Bio-Rad) were added. The volume was makeup to 20 μl with water. Serial dilution with standard mixture was used to determine the

efficiency and accuracy of the reaction. Data was analyzed on iQ5 software using the ΔC_T method using GAPDH as reference gene.

The sequence of primers used were: human Cyclin D1 (CCDN1) sense: 5'-GAAGATCGTCGCCACCTG-3', anti-sense: 5'-GACCTCCTCCTCGCACTTCT-3'; human GAPDH sense: 5'-AGCCACATCGCTCAGACA-3', anti-sense: 5'-GCCCAATACGACCAAATCC-3' (Lam et al. 2011).

2.13 Cellular uptake efficiency

HCT 116 cells were plated in 100 mm dishes at density of 6 x 10^4 cells/ml and allowed to recover. After pre-treatment with NaN_3 (10 mM, Sigma Aldrich) for 1 h, chlorpromazine (50 mM, Sigma Aldrich) for 30 min, or incubated at 4 °C for 30 min, coumarin-6 labelled PTR-SeNP was added into the cells followed by incubation at 37 °C/4 °C for 2 hours. Then the HCT 116 cells were washed with PBS, trypsinized and collected in centrifuge tubes. Trypan blue was added, and cells were fixed with 4% paraformaldehyde and stored at 4 °C until further analysis.

2.14 Flow cytometry analysis for cellular uptake

Cellular fluorescence was measured by BD FACSVerse flow cytometric analyzer at excitation and emission wavelength 405 and 488 nm. The threshold

was 10,000 events per sample. Cell debris and doublet cells were excluded from analysis by FSC/SSC and FITC-A/FITC-W gating. The results were plotted as FITC-A histogram, and the average and standard deviation was calculated.

2.15 Lysosomal colocalization analysis by fluorescent microscope

HCT 116 cells were seeded at 1 x 10^5 cells/ml in 35 mm confocal dishes. After cells reached ~70% confluency, cells were incubated with LysoTracker Red (DND-99) (Molecular Probes, Invitrogen) for 1 h at a final concentration of 100 nM, and DAPI at a concentration of 2 μg/ml for 30 min. The medium was replaced with fresh complete medium and visualized on inverted fluorescence microscope (Carl Zeiss Axiovert A1). Coumarin 6 labelled PTR-SeNP was added to the cells at a final concentration of 200 μM. Time lapsed images were then taken.

2.16 Golgi apparatus colocalization analysis by fluorescent microscope

HCT 116 cells were seeded at 1 x 10^5 cells/ml in 35mm confocal dishes. After cells reached ~50% confluency, CellLight Golgi-RFP, BacMan 2.0 (Invitrogen) was added according to cell number at the manufacturer's recommendation. The cells were incubated overnight. DAPI was added to the medium at a concentration of

2 µg/ml and incubated for 30 min. The medium was replaced by fresh complete medium and cells were visualized on inverted fluorescence microscope (Carl Zeiss Axiovert A1). Coumarin 6 labelled PTR-SeNP was added at a final concentration of 200 µM before time lapsed images were taken.

Chapter 3 - Results and Discussion

3.1 *In vitro* anti-tumor efficacy

3.1.1 Anti-proliferative effect of PTR-SeNP on different CRC cell lines

The anti-proliferation effect of PTR-SeNP on six different colorectal cancer cell lines were investigated by MTT assay, in which MTT (3-(4,5-Dimethylthiazol-2-yl)-2,5-diphenyltetrazolium bromide) is reduced to purple formazan by the succinate dehydrogenase in the mitochondria, as an indicator of cellular viability.

As shown in **Figure 10.A**, PTR-SeNP exhibited anti-proliferation effect on all six colorectal cancer cell lines (IC_{50} value ranging from 4 to 40 μM), in which HCT 116 was the most promising one (IC_{50} = 4 μM). Further investigation on cell number and morphology also confirmed that PTR-SeNP significantly inhibited the growth of HCT 116 cells in a dose- and time-dependent manner **(Figure 10. B)**. PTR-SeNP treatment lowered the cell population and induced cell shrinkage and rounding. As a result, HCT 116 was chosen for subsequent cellular and molecular studies.

A.

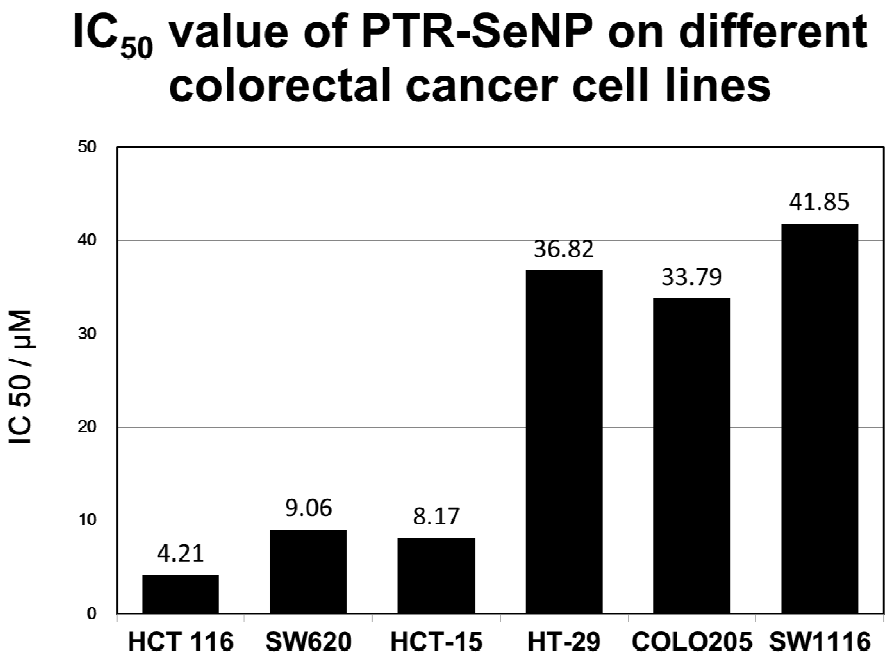
IC50 value of PTR-SeNP on different colorectal cancer cell lines
IC 50 / µM
50
40
30
20
10
0
4.21
9.06
8.17
36.82
33.79
41.85
HCT 116
SW620
HCT-15
HT-29
COLO205
SW1116

B.

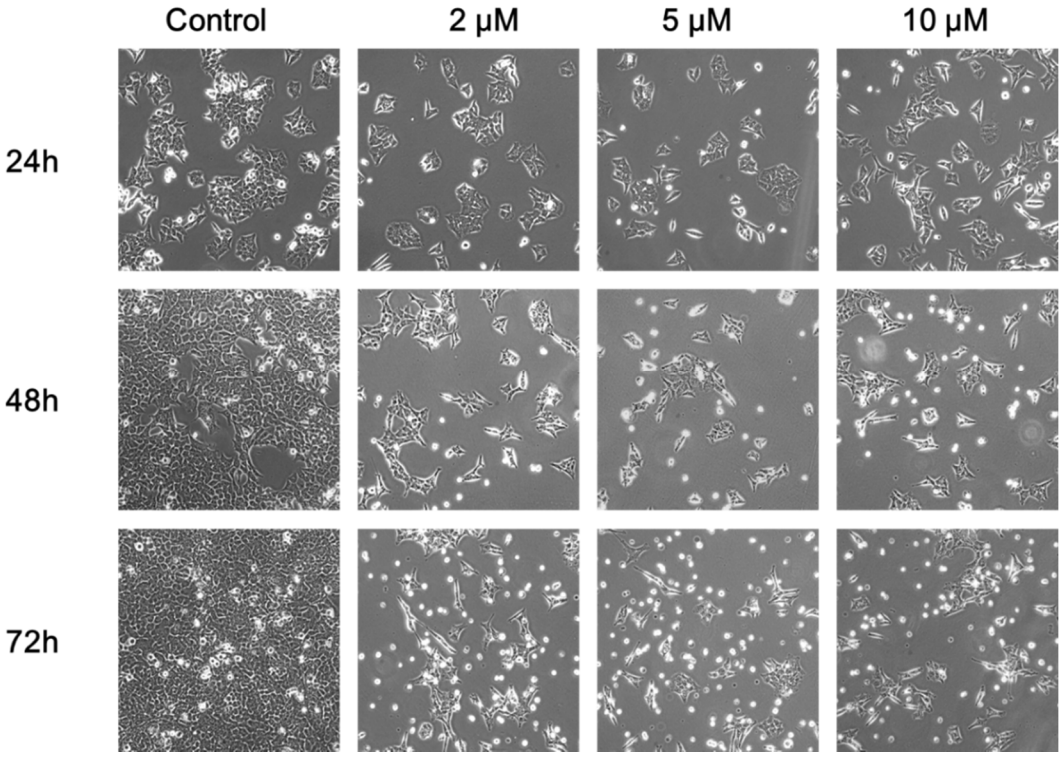
Control
2 µM
5 µM
10 µM
24h
48h
72h

Figure 10: PTR-SeNP exhibits anti-proliferative effect on different colorectal cancer cell lines.

(A) The IC_{50} value of PTR-SeNP on different CRC cell lines were measured by MTT proliferation assay. CRC cells showed different susceptibility, while HCT 116 cells were the most sensitive one towards PTR-SeNP. **(B)** Light microscopic study on growth inhibition of HCT 116 cells pre-treated with PTR-SeNP. The cell morphology and cell density showed dose- and time-dependent effect of PTR-SeNP.

3.1.2 Cell cycle arrest and apoptosis triggered by PTR-SeNP

Propidium Iodide (PI) staining analyzed by flow cytometry is a commonly used method to evaluate cell cycle distribution. Since PI binds to DNA or double strand RNA by intercalating at base pairs, the amount of PI bounded is proportional to the amount of DNA in the cell after degrading RNA with RNase. The fluorescence of PI is proportional to the amount of PI bounded to DNA, and the intensity is detected by laser excitation and emission in flow cytometer when single cell suspension passes through the laser beam.

The DNA content varies in the cell cycle: as cells transition from G1 to S phase, cells start to replicate DNA for later mitosis, and as the synthesis completes in G2 phase, the amount of DNA is twice that of G1 phase. Thus, cells in different phases of cell cycle show different PI intensities. Whereas in apoptotic cells, cells go through DNA fragmentation and secrete DNA fragments in apoptotic bodies, decreasing its total DNA content. Therefore, apoptotic cells contain less amount of DNA, and can be observed on the fluorescence intensity histogram as sub-G1 peak.

As shown in **Figure 11. A**, in the PI study, no significant cell cycle arrest or sub-G1 peak increase was observed in the HCT 116 cells after incubation with different concentrations of PTR-SeNP for 24 h. However, after 48 and 72 h

treatment, HCT 116 cell were found to exhibit dose-dependent increase in both sub-G1 and G2/M phase populations.

However, it would be too early to say that PTR-SeNP induced G2/M phase arrest and apoptosis after 48 h treatment, since another source of sub-G1 peak in PI staining is necrosis. In necrosis, loosely packed DNA can also reduce PI fluorescence intensity, thus FITC conjugated Annexin V/PI double staining was also performed to confirm the presence of apoptosis.

In early apoptosis, phosphatidylserine (PS) on plasma membrane is translocated from the inside to the outer, which can be recognized specifically by Annexin V. PI is non-permeable to live cells and labels necrotic or late apoptotic cells. The double stain method helps to distinguish apoptosis from necrosis, with necrotic cells lacking the sign of early apoptosis as Annexin V+/PI –, and goes directly from Annexin V-/ PI- to Annexin V+/PI+.

In the study, as shown in **Figure 11. B**, the cell population labelled as Annexin V +/PI – elevated before the increase of Annexin V +/ PI + cells after treatment with PTR-SeNP for 48 and 72 h. And the amount of early and late apoptotic population increased was found to be dose-dependent also. Thus, it was confirmed that PTR-SeNP induced apoptosis rather than necrosis in the HCT 116 cells.

Nevertheless, it is worth noting that the amount to apoptotic population detected in HCT 116 cells was about 20% of the total population only, even at dosage as high as 20 μM (about 5 times the IC_{50} concentration). The viable cell counts at this dosage was at around 20% of untreated control in MTT proliferation assay. This ratio is also relatively low comparing to the percentage of apoptosis induced by SeNPs in other studies, which can reach 40 to 50% (Feng et al. 2014; Wu et al. 2012). Thus, it is speculated that apoptosis might not be the major inhibition mechanism induced by PTR-SeNP in the HCT 116 cells, other mechanisms such as autophagy might be involved as well.

In addition to PI staining and Annexin V/PI co-staining, the presence of apoptosis in PTR-SeNP treated HCT 116 cells was further confirmed by DNA electrophoresis, which indicate DNA fragmentation, another hall mark of apoptosis. As shown in **Figure 11.C**, distinctive DNA fragmentation were found in HCT 116 cells pre-treated with PTR-SeNP for 48 and 72 h (lane 3 & 4).

A.

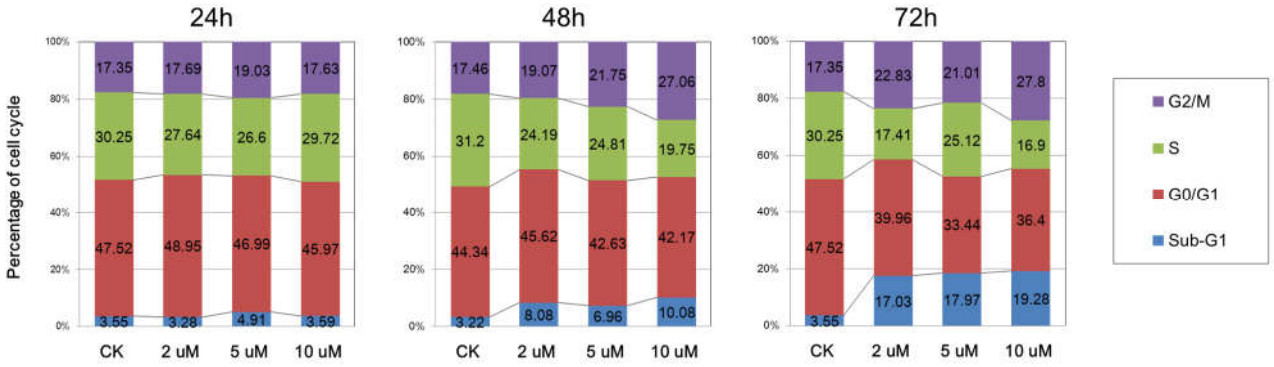
24h
48h
72h
Percentage of cell cycle
100%
80%
60%
40%
20%
0%
17.35
17.69
19.03
17.63
30.25
27.64
26.6
29.72
47.52
48.95
46.99
45.97
3.55
3.28
4.91
3.59
17.46
19.07
21.75
27.06
31.2
24.19
24.81
19.75
44.34
45.62
42.63
42.17
3.22
8.08
6.96
10.08
17.35
22.83
21.01
27.8
30.25
17.41
25.12
16.9
47.52
39.96
33.44
36.4
3.55
17.03
17.97
19.28
CK
2 uM
5 uM
10 uM
G2/M
S
G0/G1
Sub-G1

B.

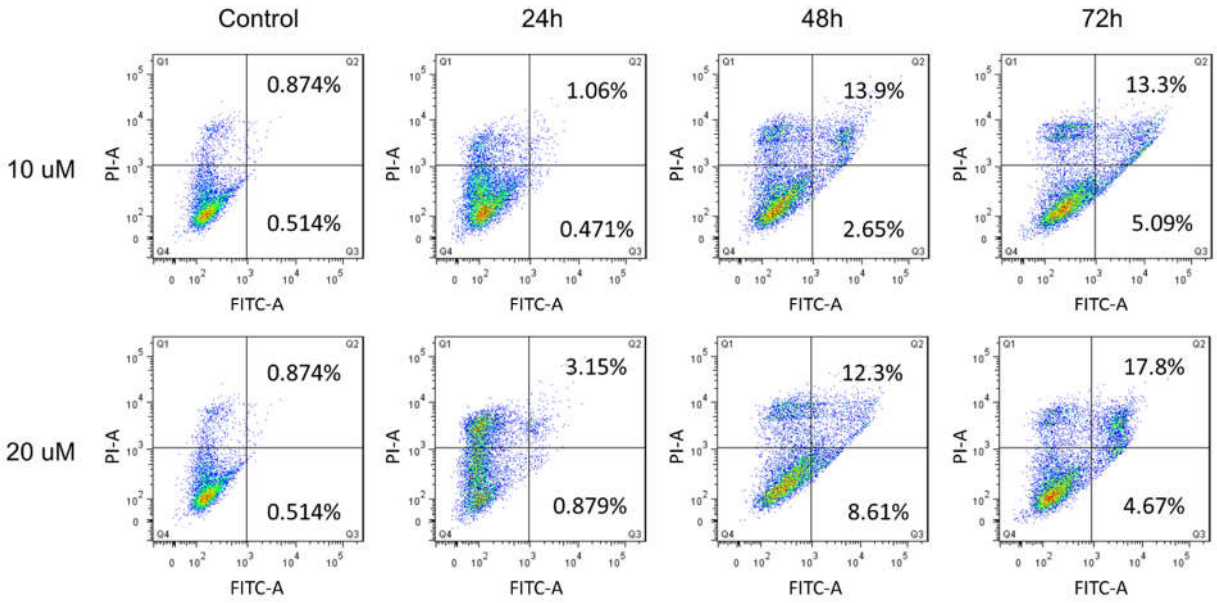
Control
24h
48h
72h
10 uM
20 uM
PI-A
FITC-A
0.874%
0.514%
1.06%
0.471%
13.9%
2.65%
13.3%
5.09%
0.874%
0.514%
3.15%
0.879%
12.3%
8.61%
17.8%
4.67%

C.

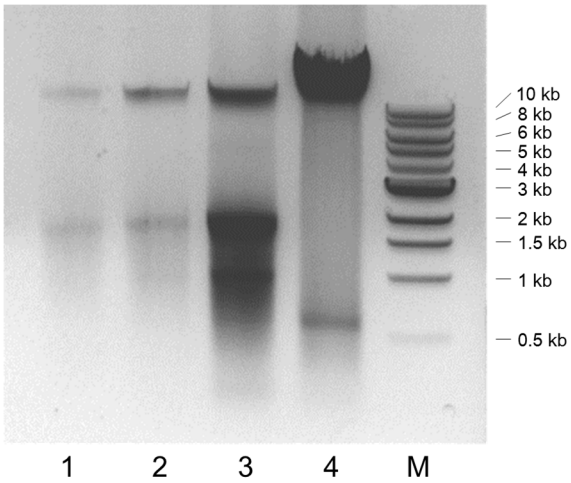
10 kb
8 kb
6 kb
5 kb
4 kb
3 kb
2 kb
1.5 kb
1 kb
0.5 kb
1
2
3
4
M

Figure 11: PTR-SeNP induces dose- and time-dependent G2/M cell cycle arrest and apoptosis in the HCT116 cells.

(A) Flow cytometry analysis of cell cycle distribution and apoptosis in HCT 116 cells pre-treated with different concentration of PTR-SeNP (2- 10 μM) for 24, 48 and 72 h. After PI staining, cellular DNA histogram was analyzed by Flowjo software, and the apoptotic cell death was quantified by measuring the sub-G1 population. **(B)** Flow cytometry analysis of PS translocation and cell membrane permeability in HCT 116 cells after treatment with different concentrations of PTR-SeNP (10 – 20 μM) for 24, 48 and 72 h using Annexin V-FITC and PI staining. **(C)** DNA fragmentation assay. Extracted DNA was electrophoresed by 1.2% agarose gel after pre-treatment with 10 μM of PTR-SeNP for 24, 48 and 72 h. Lane 1: untreated; lane 2: 24 h, lane 3: 48 h, lane 4: 72 h, M: DNA ladder.

3.1.3 Apoptotic signaling pathway triggered by PTR-SeNP

As previously reviewed, various stimulants could trigger the cleavage of caspase -3 in intrinsic and extrinsic pathways of apoptosis, which in turn inhibits DNA repair and promotes DNA fragmentation **(Figure 12. B)**. Intrinsic apoptotic pathway can also be non-caspase dependent, which relies on other factors such as AIF, ENDOG and BNIP3 (Bröker et al. 2005; Cande et al. 2004; Constantinou et al. 2009). In contrast to other studies, we discovered that level of caspase -3 proform remained constant after treatment with PTR-SeNP (10 μM) for 72 h, and the levels of cleaved caspase-3 increased slowly until 12 h before dropping. Besides, Bcl-2 and Bcl-xL, the anti-apoptotic proteins, which are responsible for maintaining the mitochondria membrane potential and caspase sequestration, remained relatively constant throughout the whole process. Pro-apoptotic protein Bax and Bak showed a small increase at 9 and 12 h **(Figure 12. A)**.

These findings suggest that PTR-SeNP might induce apoptosis in HCT 116 cells in a non-caspase-3 dependent manner. One of the possible pathway would be via AIF release from mitochondria. Mitochondria AIF is an apoptosis effector independent of caspases (Liang et al. 2001; Susin et al. 1999). Bax and Bak, whose levels peaked at 12 h, might increase mitochondrial permeability by forming channels on its membrane, and release mitochondrial content such as caspases

and AIF. It is possible that the caspases activated in this process was kept at bay by other processes, while the AIF induced apoptosis continues to initiate DNA fragmentation and cell death.

A.

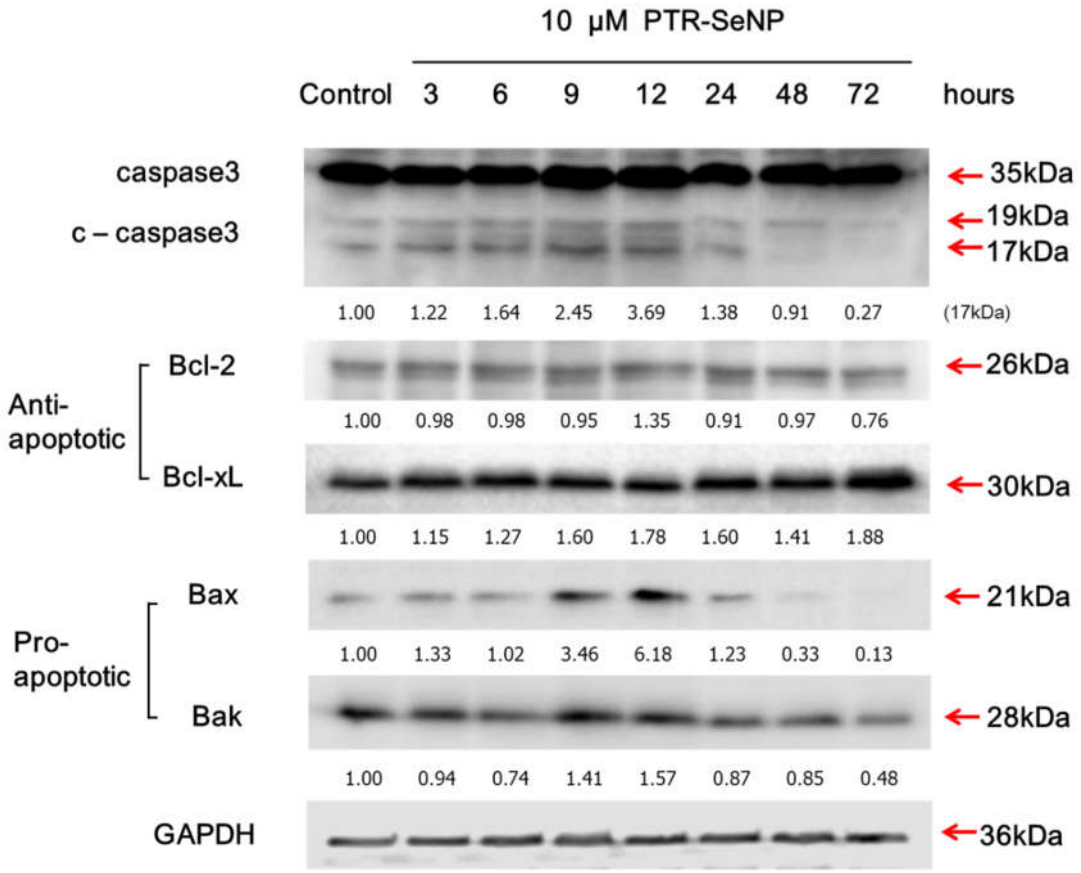
10 μM PTR-SeNP
Control 3 6 9 12 24 48 72 hours
caspase3
c – caspase3
35kDa
19kDa
17kDa
1.00 1.22 1.64 2.45 3.69 1.38 0.91 0.27 (17kDa)
Anti-apoptotic
Bcl-2
26kDa
1.00 0.98 0.98 0.95 1.35 0.91 0.97 0.76
Bcl-xL
30kDa
1.00 1.15 1.27 1.60 1.78 1.60 1.41 1.88
Pro-apoptotic
Bax
21kDa
1.00 1.33 1.02 3.46 6.18 1.23 0.33 0.13
Bak
28kDa
1.00 0.94 0.74 1.41 1.57 0.87 0.85 0.48
GAPDH
36kDa

B.

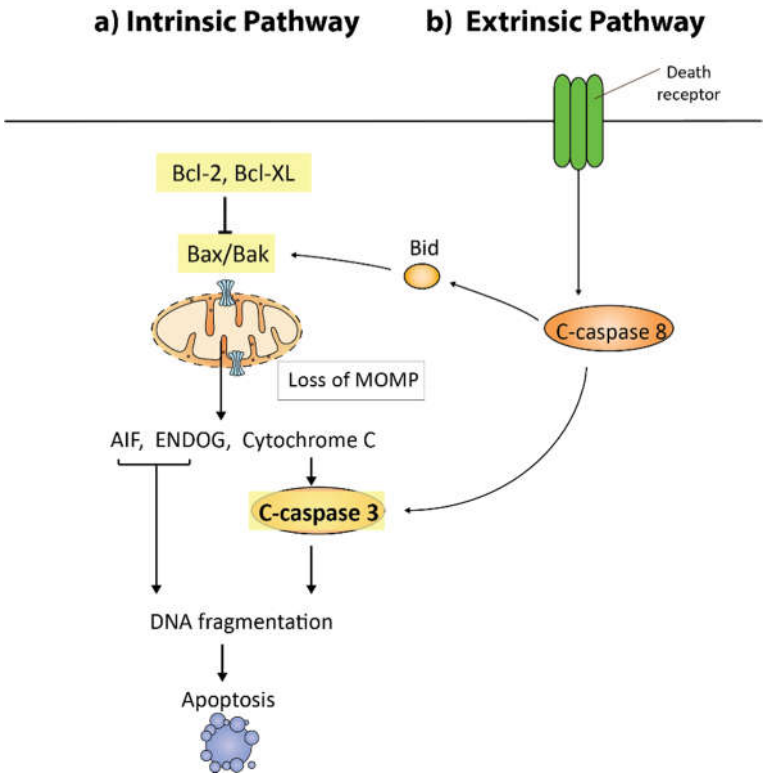
a) Intrinsic Pathway
b) Extrinsic Pathway
Death receptor
Bcl-2, Bcl-XL
Bax/Bak
Bid
C-caspase 8
Loss of MOMP
AIF, ENDOG, Cytochrome C
C-caspase 3
DNA fragmentation
Apoptosis

Figure 12: PTR-SeNP induces apoptosis in HCT 116 via a non-caspase 3-dependent pathway

(A) Western blot analysis of caspase 3 and Bcl-2 family protein expressions in HCT 116 cells induced by PTR-SeNP. Cells were treated with 10 μM PTR-SeNP for different periods of time (0-72h). The quantification is normalized against housekeeping protein GAPDH.

(B) Brief illustration of the intrinsic and extrinsic apoptotic pathways.

3.1.4 Cell cycle arrest triggered by PTR-SeNP

Since PTR-SeNP was found to induce cell cycle arrest at G2/M phase in HCT 116 **(Figure 11. A)**, changes of key regulators in cell cycle over time was further quantified using western blotting. Surprisingly, Cyclin D1 and D3, regulators of G1/S phase entry were down-regulated first at an early time point (12 h). Besides, the Cyclin Ds were down-regulated to a very low level and were not recovered as far as 72 h. Other regulators of G1/S phase entry, such as CDK4/6 was down-regulated at 24 h as well. CDK2 which regulates the checkpoint from G1/S by binding to Cyclin E, and from S/G2 by binding to Cyclin A, was also down-regulated at 24 h, while cdc2/CDK1, regulator of G2/M phase progression was down-regulated at 48 h **(Figure 13. A)**.

Since Cyclin D1 was down-regulated first, and it modulates the transcription of other molecules in proliferation (Musgrove et al. 2011; Roussel 1999) and regulates nuclear hormonal receptors (Fu et al. 2004) **(Figure 13. D)**, we speculate that the downward regulation of Cyclin D1 is one of the early target, which plays an important role. RT-PCR results confirmed that Cyclin D1 was down-regulated at transcriptional level rapidly as early as 3 h, and the inhibition persisted as far as 72 h **(Figure 13. B)**. Worth noting is that, Cyclin Ds over-expression has been

widely reported in multiple cancer cells (Lee and Sicinski 2006; Li et al. 2006). In this study, PTR-SeNP were found to effectively lower their protein expressions as an early event.

However, this early down-regulation of Cyclin Ds, instead of G2/M checkpoint CDK2/cdc1 protein does not fit our expectation according to the classical cell cycle model and previous experimental results. As indicated in **Figure 11.A**, PTR-SeNP were found to induce G2/M arrest, instead of G1 arrest in HCT 116 cells, while Cyclin D1, D3 and CDK 6 were down-regulated as the checkpoint of G1 arrest **(Figure 13.C)**.

This discrepancy between the cell cycle arrest results and the classical cell cycle model has been reported in other studies of SeNPs previously (Feng et al. 2014). One explanation is that the classical model is far from perfect to cover every cell cycle activity. Some studies have indicated that even through some CDKs and Cyclins were knocked out in the mice model, the neo-natal mice were still viable, suggesting that other mechanisms might be able to substitute the function of these proteins (Sherr and Roberts 2004; Xie et al. 2008). Other studies have also found that G2/M arrest may be attributed to defective G1 checkpoint or problematic mitotic structure, instead of G2/M checkpoints (DiPaola 2002).

We hypothesize that HCT 116 cells may be able to bypass G1 arrest in the

absence of Cyclin D1/3, via alternative mechanisms to promote cell cycle. However, after the down-regulation of Cyclin D1 affected the expression of multiple molecules in cell cycle progression, cell cycle was eventually arrested at G2/M phase.

A.

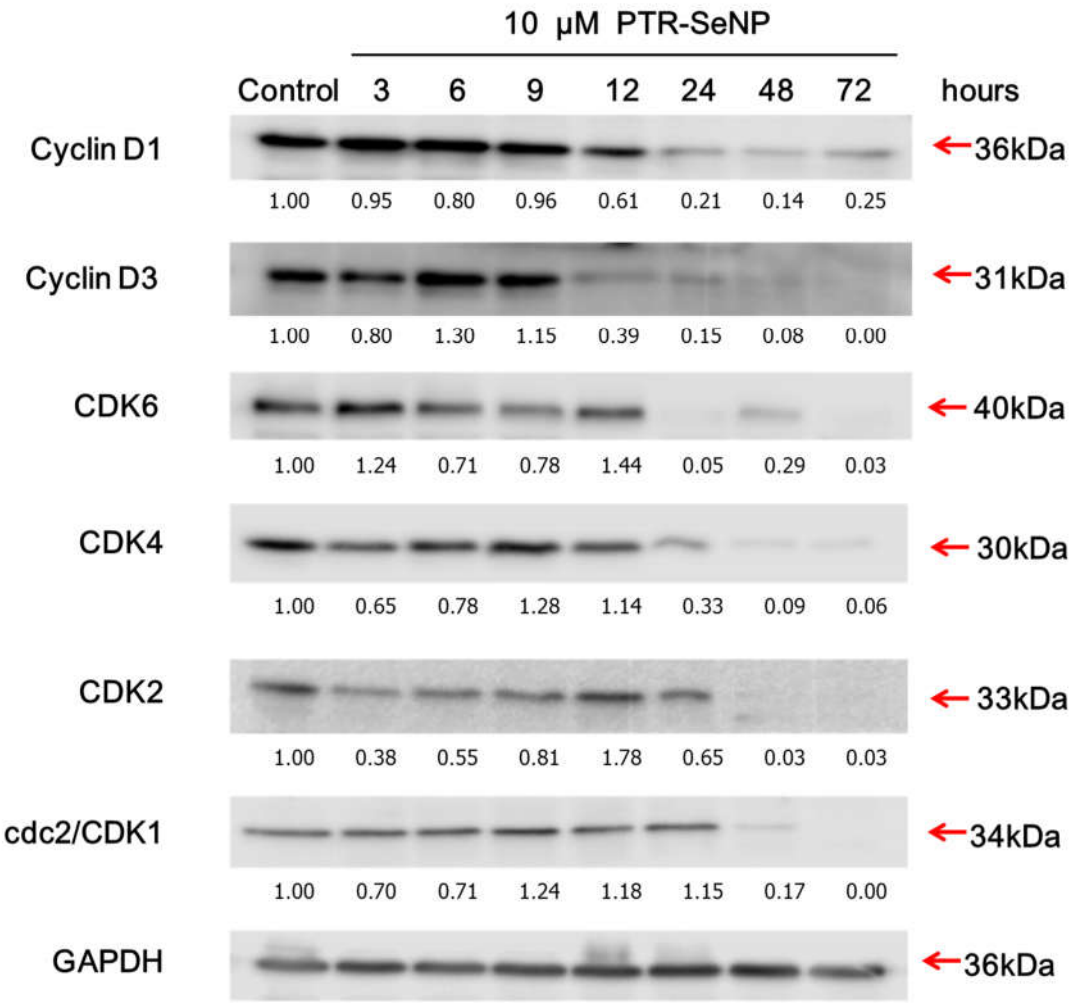
10 μM PTR-SeNP
Control 3 6 9 12 24 48 72 hours
Cyclin D1
1.00 0.95 0.80 0.96 0.61 0.21 0.14 0.25
36kDa
Cyclin D3
1.00 0.80 1.30 1.15 0.39 0.15 0.08 0.00
31kDa
CDK6
1.00 1.24 0.71 0.78 1.44 0.05 0.29 0.03
40kDa
CDK4
1.00 0.65 0.78 1.28 1.14 0.33 0.09 0.06
30kDa
CDK2
1.00 0.38 0.55 0.81 1.78 0.65 0.03 0.03
33kDa
cdc2/CDK1
1.00 0.70 0.71 1.24 1.18 1.15 0.17 0.00
34kDa
GAPDH
36kDa

B.

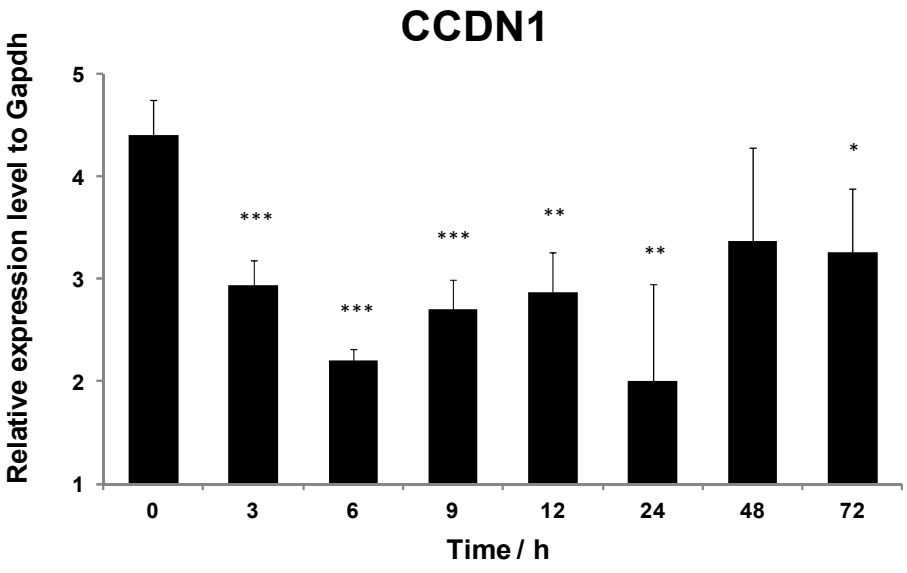
CCDN1
Relative expression level to Gapdh
5
4
3
2
1
***
***
***
**
**
*
0 3 6 9 12 24 48 72
Time / h

C.

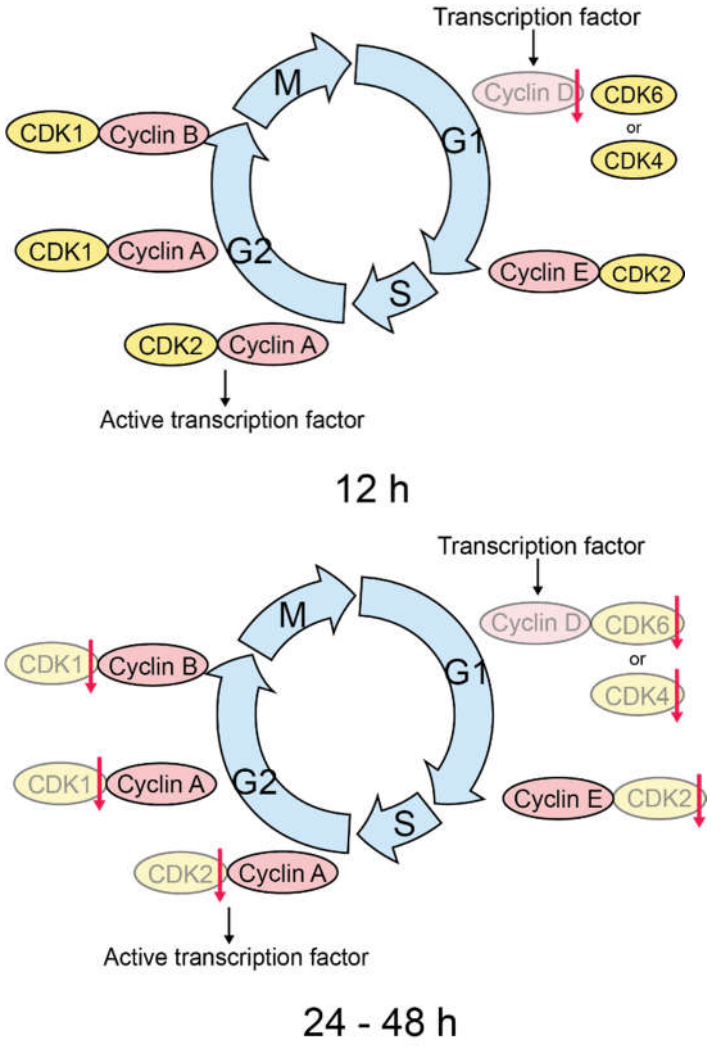
Transcription factor
M
G1
S
G2
Cyclin D
CDK6
or
CDK4
CDK1
Cyclin B
CDK1
Cyclin A
Cyclin E
CDK2
CDK2
Cyclin A
Active transcription factor
12 h
Transcription factor
M
G1
S
G2
Cyclin D
CDK6
or
CDK4
CDK1
Cyclin B
CDK1
Cyclin A
Cyclin E
CDK2
CDK2
Cyclin A
Active transcription factor
24 - 48 h

D.

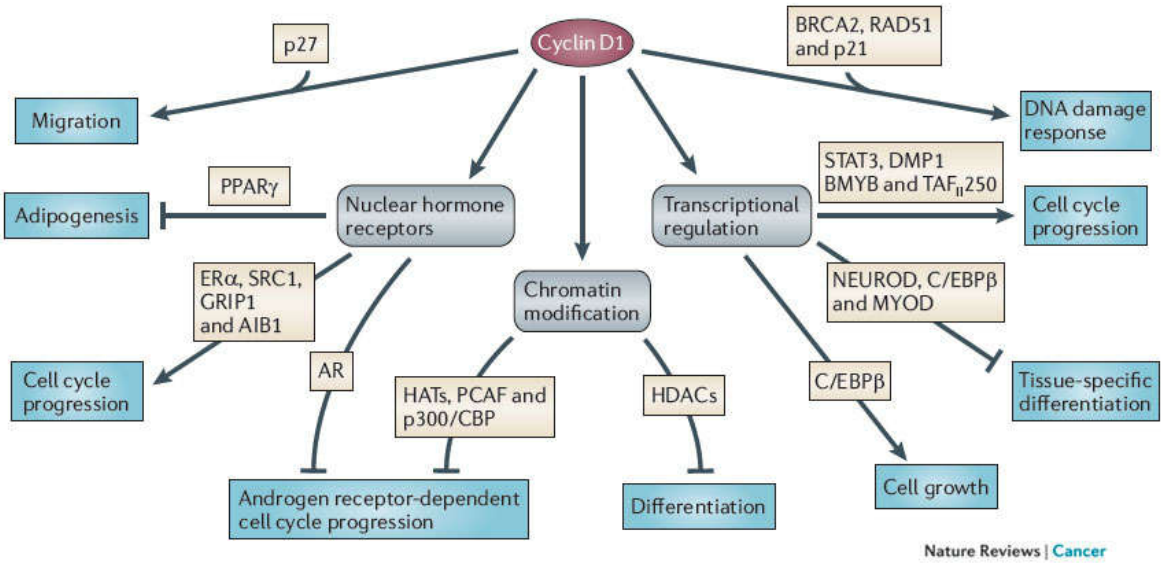
Cyclin D1
p27
BRCA2, RAD51 and p21
Migration
DNA damage response
PPARγ
Adipogenesis
Nuclear hormone receptors
Transcriptional regulation
STAT3, DMP1 BMYB and TAFII250
Cell cycle progression
ERα, SRC1, GRIP1 and AIB1
Chromatin modification
NEUROD, C/EBPβ and MYOD
Cell cycle progression
AR
HATs, PCAF and p300/CBP
HDACs
C/EBPβ
Tissue-specific differentiation
Androgen receptor-dependent cell cycle progression
Differentiation
Cell growth
Nature Reviews | Cancer

Figure 13: PTR-SeNP induce down-regulation of Cyclin D1/3, CDK1, CDK2, CDK4 and CDK6.

(A) Western blot analysis of Cyclin D1, Cyclin D3, cdc2/CDK1, CDK2, CDK4 and CDK6 protein expressions in HCT 116 cells induced by PTR-SeNP. Cells were treated with 10 µM PTR-SeNP. The quantification is normalized against housekeeping GAPDH. **(B)** Real time-PCR analysis of the mRNA level of Cyclin D1 gene CCDN1 in HCT 116 after treatment with 10 µM PTR-SeNP.for different period of time (0-72 h). (* $p<0.05$, ** $p< 0.01$, ***$p<0.001$). **(C)** Schematic of the changes of protein expressions relevant to cell cycle regulation. **(D)** CDK-independent functions of Cyclin D: cyclin D1 modulate functions in cell migration, DNA damage response, cell proliferation, growth and differentiation, via interacting with CKIs and transcription factors (Musgrove et al. 2011).

3.1.5. Autophagy in HCT 116 cells triggered by PTR-SeNP

Autophagy is the type II programmed cell death, as prolonged autophagy could trigger autosis. Autophagy has many interactions with apoptosis and other cell death pathways. Many nanoparticles and quantum dots were reported to induce autophagy (Ma et al. 2011; Stern et al. 2012), while there were no previous reports on SeNP's ability to induce autophagy. It is possible that PTR-SeNP may induce autophagy at certain stage, which could either counteracts the apoptotic cell death pathways as a pro-survival mechanism, or independently induces cell death in HCT 116 cells. It is worthwhile to investigate whether autophagy is involved.

We transfected HCT 116 cells with EGFP-LC3 plasmid, which has a size of ~ 5 kb **(Figure 14. A)**. When cells go through autophagy, LC3 will be cleaved at the C-terminus and lipidated to form LC3-II, which is then recruited to the phagophore as a crucial step in autophagosome formation. The EGFP is tagged at the N terminus in the EGFP-LC3 plasmid used, thus remains intact in this truncation and lipidation process. As the autophagosome is formed, the green fluorescence of EGFP indicates the position of accumulated LC3-II **(Figure 14. C).**

As shown in **Figure 14. B**, treatment by rapamycin, an autophagy inducer promoted autophagy and autophagosome formation, with EGFP-LC3 II punta was

observed at 6 h. EGFP-LC3 punta were formed in PTR-SeNP treated cells as well after 17 h of PTR-SeNP treatment. Due to the low efficiency of transfection, only the existence of autophagy in PTR-SeNP treated cells could be confirmed, without being able to quantify the percentage of cells going through autophagy.

Further study by Western immunoblotting assays demonstrated that HCT 116 cells went through autophagy under PTR-SeNP treatment. Beclin 1 is the mammalian homologue of yeast Atg6, which interacts with other Atg proteins and enhances the catalytic ability of PI3-Kinase (III) to form phagophore. LC3 is cleaved and lipidated to form LC3-II, which is recruited to phagophore and took part in membrane elongation. P62/SQSTM1 is an adaptor molecule that sequester the cargo proteins and serves as a substrate of autophagic degradation, which also affects the levels of LC3-II (Bjørkøy et al. 2005; Watanabe and Tanaka 2011). These three molecules can be used as a rudimental indicator to assess autophagic flux, the process of autophagosomes maturation by fusing with lysosome and consequent protein degradation over time.

As shown in **Figure 14. D**, Beclin 1 increased 1.78 folds at 12 h, before declining significantly. The uncleaved form of LC3 was found to remain stable throughout, while cleaved LC3-II increased significantly after 12 h, reaching 5.23 folds at 24 h and remained at 3.51 folds of normal level at 72 h. Similarly, the level

of autophagic substrate, p62/SQSTM1 maximized at 12 h at 1.96 folds, and dropped below normal level at 72 h. Thus, from 12 h to 24h, the level of LC3-II accumulated, corresponding with the increase of Beclin 1 and decrease of p62 levels. These findings also indicated the formation of autophagosome and completion of autophagic flux, which were consistent with the previous observation of EGFP-LC3 punta formation after 17 h treatment in plasmid transfection experiment.

Since PTR-SeNP were found to induce time- and dose-dependent apoptosis at 48 h and 72 h, the autophagy induced by PTR-SeNP must have subsided at certain point within 72 h, or transitioned to induce cell death. But how PTR-SeNP induced autophagy transitioned to cell death required further investigation, and there are two possible hypothesis:

Bcl-2 has been found to interact with Beclin 1 and suppress its interaction with Vsp34 in the formation of autophagy inducing complex, while Bcl-2 phosphorylation at T56 and S70 position were found to reduce its binding with Beclin 1, releasing Beclin 1 for autophagy pathway (Kang et al. 2011; Pattingre et al. 2005). As shown in **Figure 14.E**, Beclin 1 level dropped below normal after 48 h, indicating a possible inhibition of autophagy. Nevertheless, the level of total Bcl-2 remained relatively stable throughout, the levels of phosphorylated Bcl-2 at

T56 and S70 diverged, making it hard to decide the effect of Bcl-2 on Beclin 1, and its consequent effect on autophagy induction **(Figure 14. E)**.

However, this hypothesis is supported by the drop of p-ERK levels at 48 h. Phosphorylated ERK is downstream molecule in MAPK pathway and is found to regulate autophagy via Beclin 1 modulation (Wang et al. 2009). Thus, as p-ERK level increases until 24 h and dropped later on **(Fig 14. E),** it is likely that the depletion of phosphorylated ERK inhibited Beclin 1 activity and autophagy.

Another hypothesis is that, prolonged autophagy leads to the depletion of cytoplasmic membrane and a novel type of autophagic cell death, autosis. Despite Beclin 1 level was found to decrease after 24 h, the level of LC3-II remained 3.5 folds higher than normal at 72 h. Since the substrate p62/SQSTM1 decreased steadily **(Figure 14. E)**, this ruled out the possibility that LC3-II accumulation was due to the blockage in maturation process of autophagosomes. To confirm this hypothesis, further cellular and molecular experiments are required to determine whether autosis features could be observed in the HCT 116 cells, and the transcriptional levels of LC3, P62/SQSTM1 and Beclin 1.

A.

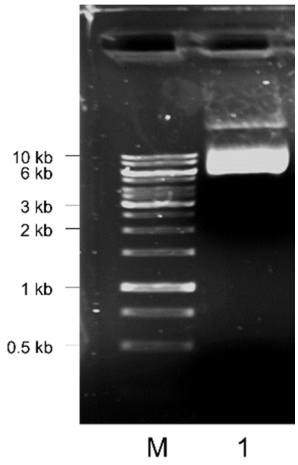
10 kb
6 kb
3 kb
2 kb
1 kb
0.5 kb
M
1

B..

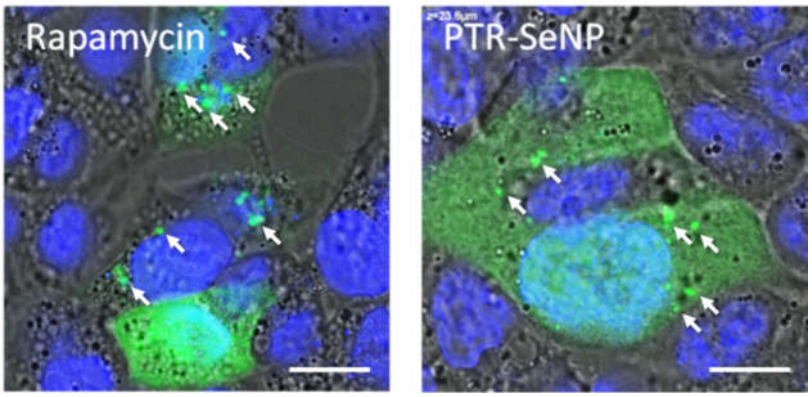
Rapamycin
PTR-SeNP

C.

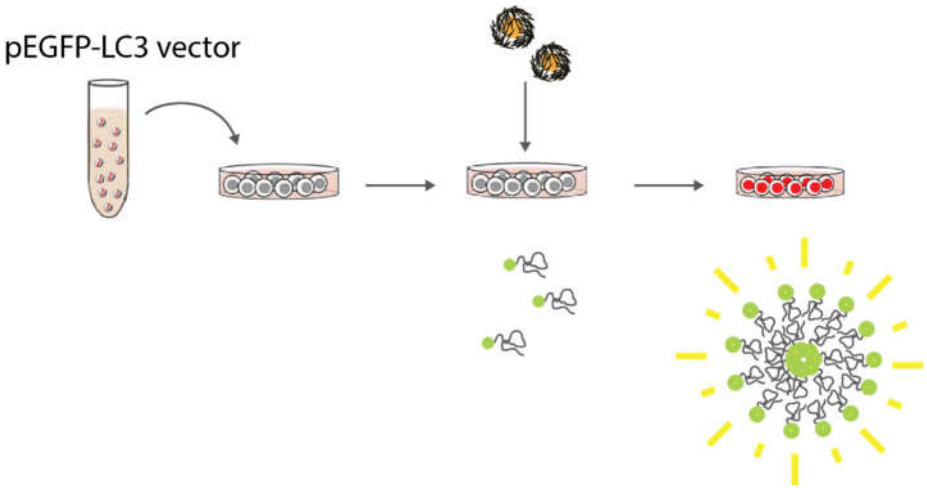
pEGFP-LC3 vector

D.

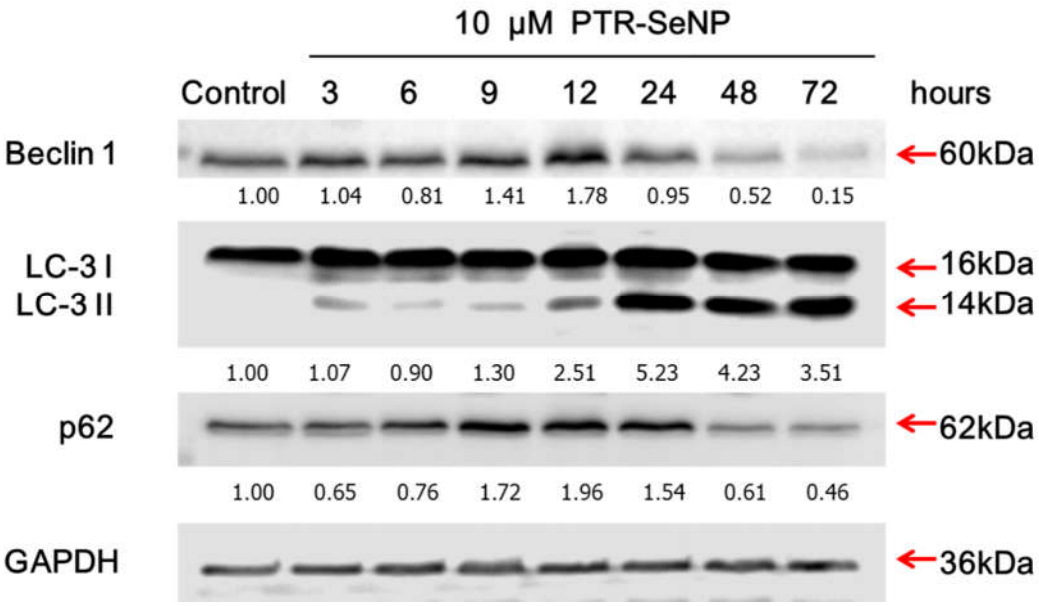
10 μM PTR-SeNP
Control 3 6 9 12 24 48 72 hours
Beclin 1
60kDa
1.00 1.04 0.81 1.41 1.78 0.95 0.52 0.15
LC-3 I
LC-3 II
16kDa
14kDa
1.00 1.07 0.90 1.30 2.51 5.23 4.23 3.51
p62
62kDa
1.00 0.65 0.76 1.72 1.96 1.54 0.61 0.46
GAPDH
36kDa

E.

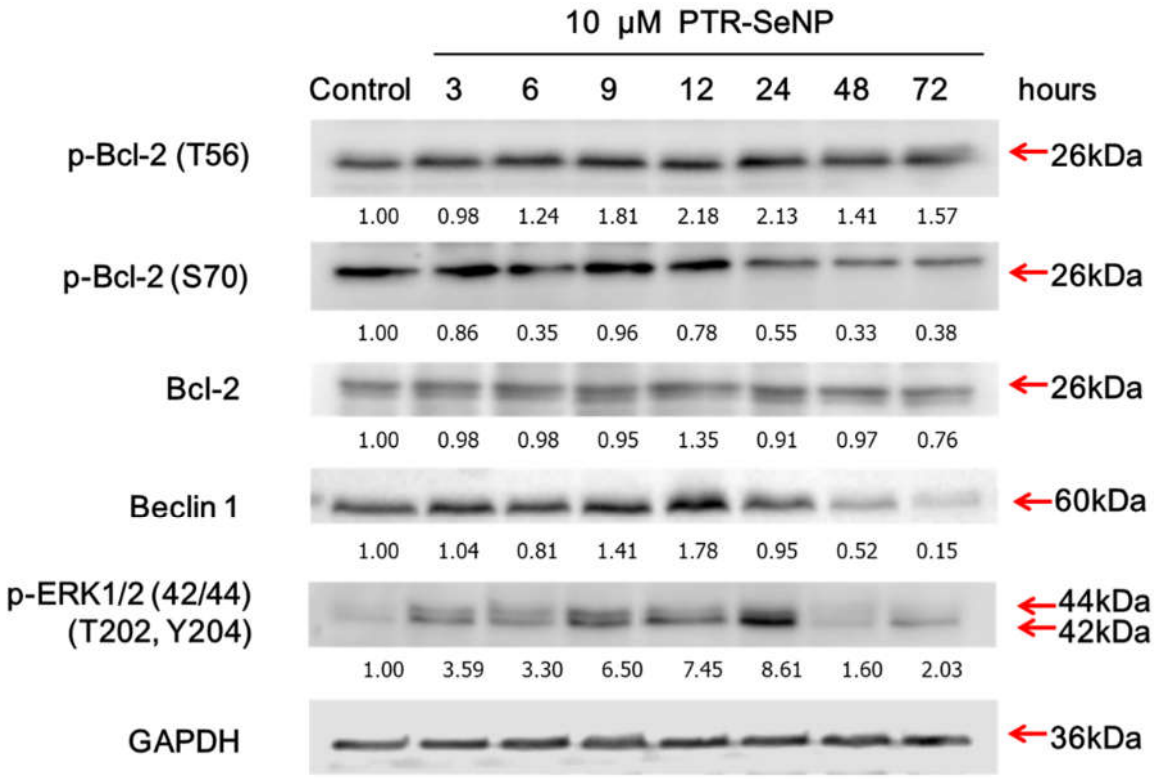

Figure 14: PTR-SeNP induces autophagy in HCT-116.

(A) 1% agarose gel electrophoresis of purified EGFP-LC3 plasmid (lane 1). M: DNA marker. **(B)** HCT 116 cells transfected with EGFP-LC3 plasmid was treated with autophagy inducer rapamycin (400 nM) for 6 h (left) and PTR-SeNP (10 μM) for 17 h (right). Bar: 15 μm. Autophagosome punta (arrows) were seen in the cytosol. **(C)** Illustration of the mechanism of pEGFP-LC3 plasmid transfection **(D), (E)** Western blot analysis of the autophagic protein levels in HCT 116 treated with 10 μM PTR-SeNP. The quantification is normalized against housekeeping GAPDH.

3.1.6 Combined effect of PTR-SeNP and 5-FU

A synergistic effect of SeNP and 5-fluorouracil (5-FU), a widely used anti-cancer drug which causes DNA damage and induces apoptosis has been reported previously (Liu et al. 2012). 5-FU is also a classical cancer drug for colorectal cancer treatment. In order to find out whether PTR-SeNP and 5-FU has synergestic effect, MTT proliferation assay and cell cycle analysis were conducted to determine the efficacy of 5-FU and PTR-SeNP alone, and their combination regime at different ratios. Since 5-FU is unstable in aqueous solution, all parallel assays were performed simultaneously.

As shown in **Figure 15. A**, the IC_{50} values of 5-FU and PTR-SeNP for HCT 116 cells were 27.23 μM (x-axis) and 4.21 μM (y-axis), respectively. Interestingly, we discovered that PTR-SeNP/5-FU combination regime at ratio of 1:10, 1:5 and 1:3 exhibited antagonistic effect. This finding suggested that PTR-SeNP and 5-FU induced apoptosis via different cell inhibition mechanisms.

Flow cytometry confirmed that both PTR-SeNP and 5-FU could individually induce apoptosis in HCT 116 cells. Nevertheless, at IC_{50} concentration, 5-FU was able to induce apoptosis in around 40% of all populations, with no G2/M phase arrest observed. Instead, PTR-SeNP only induced 17.1% apoptosis and G2/M arrest **(Figure 15. B)**.

This finding was further validated by the Annexin V/PI analysis. As shown in **Figure 15. C,** after 72 h treatment, reducing the PTR-SeNP concentration in combination regime from 10 μM: 10 μM (PTR/5-FU) to 2 μM : 10 μM significantly increased the late apoptotic population from 23.7% to 31.5%, while reducing 5-FU concentration in combination regime 10 μM : 2 μM would further decrease the late apoptotic population to 11.3%. It is postulated that even though both 5-FU and PTR-SeNP could induce apoptosis, their different cell inhibition pathways might be antagonistic to each other. This postulation was further supported by our previous result that PTR-SeNP could induce autophagy, while 5-FU was found to have synergistic effect with autophagy inhibitor, such as 3-MA (Li et al. 2010a; Li et al. 2008),

A.

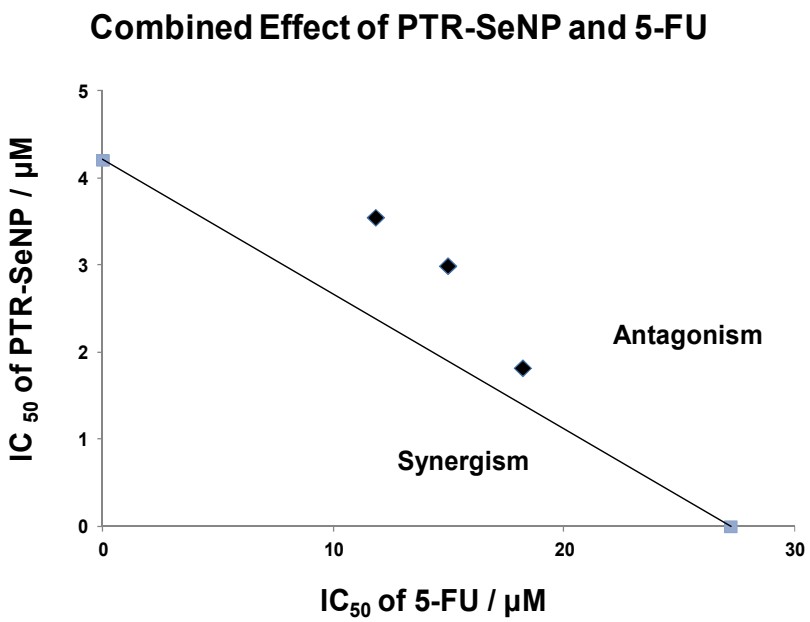
Combined Effect of PTR-SeNP and 5-FU
IC 50 of PTR-SeNP / µM
IC50 of 5-FU / µM
Antagonism
Synergism
0
1
2
3
4
5
0
10
20
30

B.

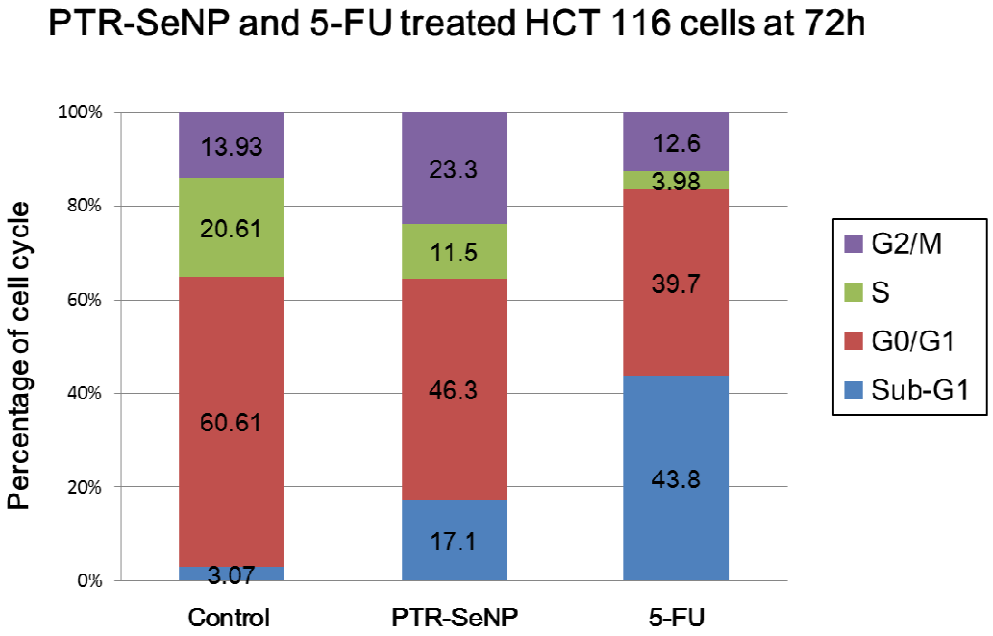
PTR-SeNP and 5-FU treated HCT 116 cells at 72h
Percentage of cell cycle
100%
80%
60%
40%
20%
0%
13.93
20.61
60.61
3.07
23.3
11.5
46.3
17.1
12.6
3.98
39.7
43.8
Control
PTR-SeNP
5-FU
G2/M
S
G0/G1
Sub-G1

C.

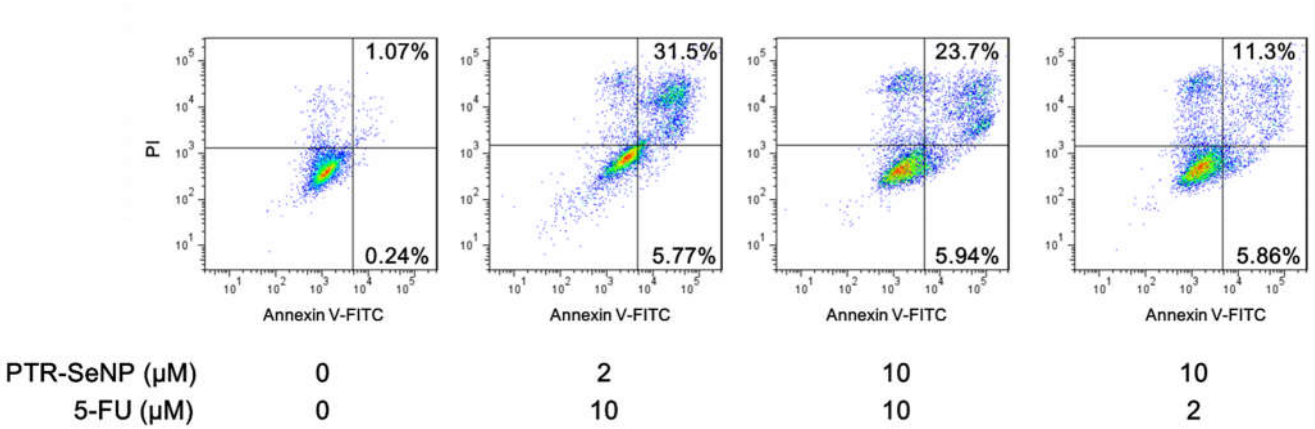

Figure 15: PTR-SeNP plays antagonistic effect on 5-FU induced apoptosis.

(A) The IC_{50} of 5-FU and PTR-SeNP alone, and different combinations of PTR-SeNP/5-FU regime (1:10, 1:5 and 1:3) were determined by MTT cell proliferation assay. The effect of combined regime at different ratio falls within the antagonism area. In other words, the combined effect was less potent than using single drugs alone. **(B)** Flow cytometric analysis of the cell cycle distribution in HCT 116 cells pre-treated with PTR-SeNP and 5-FU at their IC_{50} concentration. 5-FU treated cells showed higher population of apoptosis, while PTR-SeNP treated cells showed higher G2/M phase arrest **(C)** Annexin V-FITC/PI double staining assay of HCT 116 cells pre-treated with different PTR-SeNP/5-FU combinations at different ratios for 72 h. Early apoptosis (Annexin V +/ PI -) is the population in the fourth quadrant (lower right), while late apoptosis (Annexin V +/PI+) is the population in the first quadrant (upper right). Under the same concentration of 5-FU, reduced amount of PTR-SeNP induced higher total apoptotic population and shift from early apoptosis to late apoptosis (5.77 % early apoptosis and 31.5 % late apoptosis, compared with 5.94 % early apoptosis and 23.7% late apoptosis.).

3.2 Cellular uptake behavior induced by PTR-SeNP

3.2.1 C6-PTR-SeNP internalization and colocalization

Endocytosis has been widely reported as the major cellular uptake mechanism for nanoparticles (Ekkapongpisit et al. 2012). Fung et al. has reported that modified by different amino acids, SeNPs exhibited different cellular uptake behavior, which may be due to different hydrophobicity, surface charge and even particle size by different modification (Feng et al. 2014). There were no previous study on the organelle target and internalization pathways of PTR coated SeNP before, which could help to reveal the interaction between PTR-SeNP and the cells.

Coumarin -6 (C6) is a hydrophobic fluorescent probe widely used for labelling drug. It can form host-guest inclusion complex with other macromolecules, such as cyclodextrins (Wagner 2009) and cucurbit[n]uril (Miao et al. 2015) by enclosure of its hydrophobic benzopyrone portion. By using coumarin-6 loaded PTR-SeNP (C6-PTR-SeNP), our previous study found that PTR surface decoration significantly enhanced the cellular uptake efficiency of SeNP by the MCF-7 cells (2-4 folds) in both time- (0.5, 1 and 2 h) and dose-dependent (30, 60 and 120 μM) manners (Wu et al. 2012). The exact reason of why PTR modification enhance the cellular uptake is still under investigation, but possible reasons include a) modified surface charge of the nanoparticle could increase nanoparticle solubility and proximity

with cell surface, b) the interaction of PTR motifs with cell surface receptors could increase the interaction between PTR-SeNP and cell surface, and c) the surface modification reduced the nanoparticle size significantly (from around 200 – 600 nm to around 50 – 100 nm) (Wu et al. 2012), which may promote the utilization of extra cellular uptake pathways for finer particles. In addition, PTR-SeNP was found to mainly localize in lysosomes of MCF-7 cells as early as 10 min after cellular internalization.

In this study, the cellular uptake pathways involved in the uptake of coumarin 6 decorated PTR-SeNP by HCT116 cells and its initial intracellular co-localization with organelles were investigated.

As shown in **Figure 16. A**, the cellular uptake of C6-PTR-SeNP (5 and 20 μM) by the HCT116 cells peaked at 2 h and then dropped at 4 h, followed by a slight increase till 24 h. This decrease of cellular uptake of PTR-SeNP might be attributed to (a) exocytosis of C-6 along with SeNP (Yu et al. 2013), or (b) the protonation to C-6 structure causing its fluorescent band shift/oxidation (Barooah et al. 2012).

In the first hypothesis, the drop of fluorescent signal at 4 h is due to exocytosis, the transportation of caveolae (and the encapsulated C6-PTR-SeNP) out of the basolateral side of the epithelial cells, right after its cellular uptake at the apical side. The hypothesis is supported by the epithelial origin of HCT 116

cells and the observation that exocytosis peaked at 1-2 h in polarized epithelial cells by nanoparticles around 80 nm (Oh and Park 2014). However, cellular uptake normally reaches a plateaued saturation curve when exocytosis is underway (Lu et al. 2012), while in our experiment, the fluorescent signal decreased drastically at 2 to 4 h (∽60%) before recovering steadily.

Thus, the second hypothesis is more likely, in which the conformational change of Coumarin-6 in the acidic environment of organelles contribute to the rapid shift of fluorescence intensity. After entering the cells, the C6-PTR-SeNP connection might break down and the release of C-6 to the acidic environment may accelerate a shift in emission spectrum.

As shown in **Figure 16. B and .C**, C6-PTR-SeNP was found to colocalize with both lysosomes and Golgi apparatus in the HCT 116 cells as early as 5 and 2 min, respectively after cellular internalization. This indicated that the cellular uptake of PTR-SeNP by HCT 116 cells was very fast. Unlike the lysosomes, it is the first study of its kind to report the intracellular colocalization of SeNPs with Golgi apparatus. This finding suggests that caveolae-dependent pathways are likely involved in the endocytosis of PTR-SeNP by HCT 116 cells, since caveolae-mediated endocytosis is the only known cellular uptake route to transport the cargo along trans-Golgi network.

A.

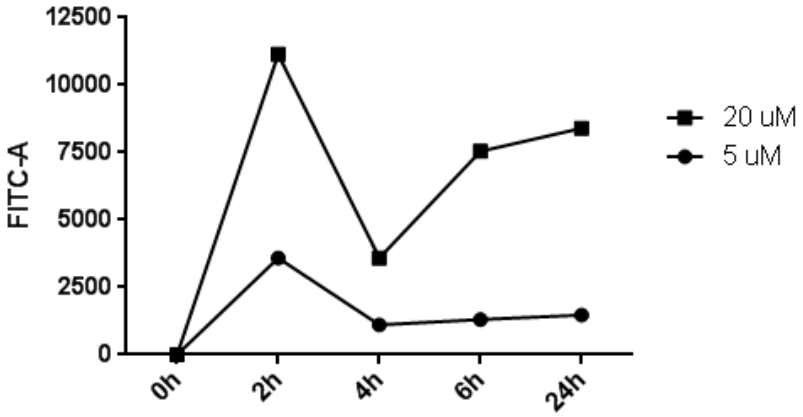
12500
10000
7500
5000
2500
0
FITC-A
0h
2h
4h
6h
24h
20 uM
5 uM

B.

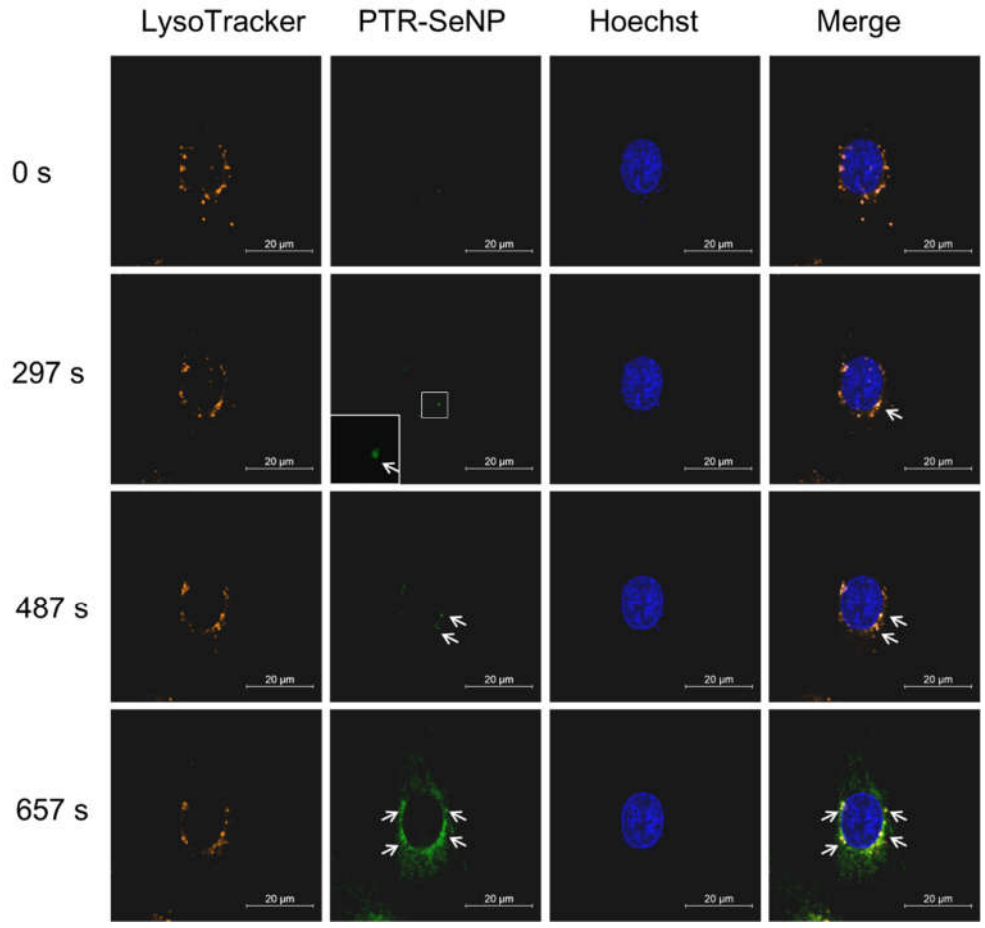
LysoTracker
PTR-SeNP
Hoechst
Merge
0 s
297 s
487 s
657 s
20 μm

C.

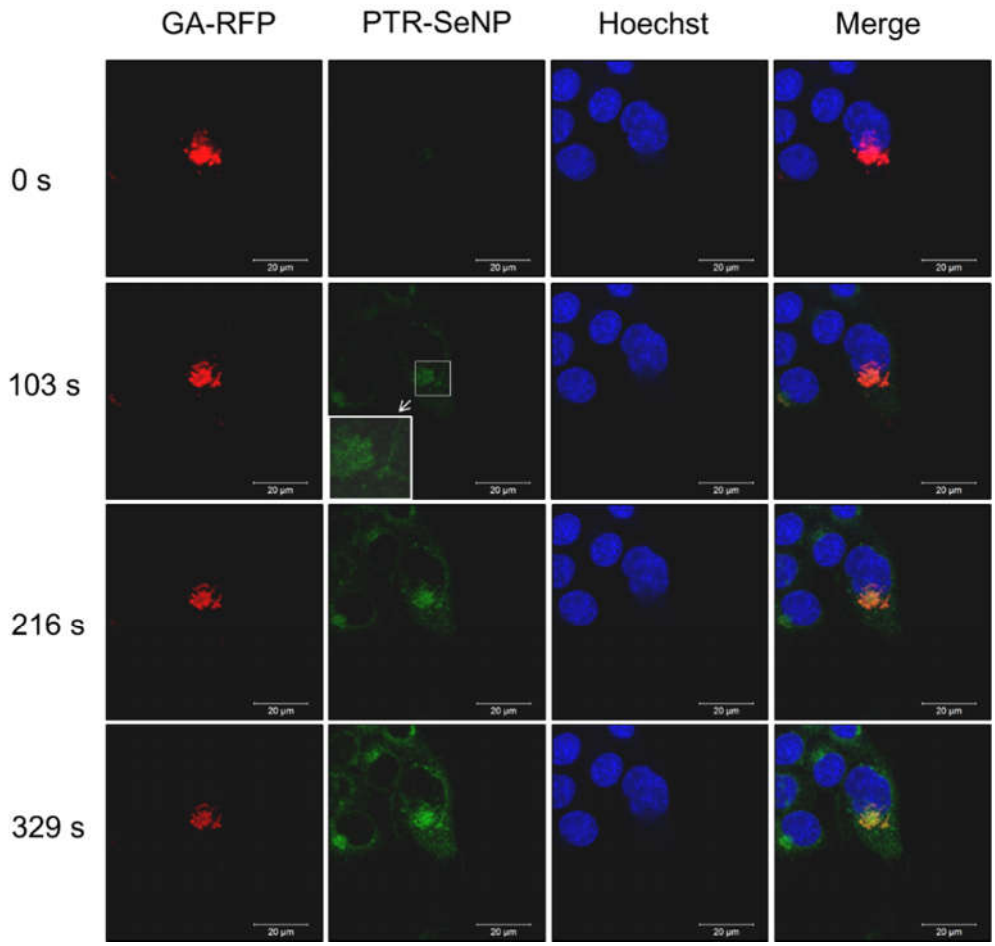

Figure 16: Cellular uptake and colocalization of coumarin-6 labeled PTR-SeNP (C6-PTR-SeNP) in HCT 116 cells.

(A) Flow cytometry analysis of cellular uptake behavior of C6-PTR-SeNP by the HCT 116 cells, after treatment for 2, 4, 6 and 24 h. **(B) and (C)** Cellular uptake and intracellular colocalization of PTR-SeNP by the HCT 116 cells. Cells were exposed to LysoTracker Red DND 99 (lysosomes; red fluorescence) **(B)** or CellLight Golgi-RFP (Golgi-apparatus; red fluorescence) **(C)**, and Hoechst 33365 (nucleus; blue fluorescence) at 37 °C prior to exposure to coumarin -6 loaded PTR-SeNP (225 µM, green fluorescence) and visualization by confocal microscope at different time intervals. Bar, 20 µm.

3.2.2 Effect of different inhibitors on internalization of C6-PTR-SeNP by the HCT 116 cells

In order to find out the specific endocytic pathways triggered by PTR-SeNP for entering HCT 116 cells, further investigation of the cellular uptake behavior using different chemical inhibitors was performed. Since the size of the PTR-SeNP being studied is around 100 nm (99.5 ± 4.73 nm), various cellular uptake pathways could be exploited by nanoparticles in this range **(Figure 8)**(Canton and Battaglia 2012).

As the cellular fluorescence peaked at 2 h in the previous study **(Figure 15.A)**, and that the chemical inhibitors impair the cell functions after 1.5 -2 h (Kuhn et al. 2014), the post-incubation time was limited to 2 h, after a pre-incubation of 30 min with the inhibitors. The concentrations of inhibitors were set where no cytotoxicity was observed.

As shown in **Figure 17**, under the energy deprived conditions (such as 4 °C and 4 °C together with sodium azide), the cellular uptake of C6-PTR-SeNP by HCT 116 cells was significantly inhibited (75.9% - 81.1%, **Table 1**). As previously reported in numerous studies, the low temperature and inactivation of mitochondria by NaN_3 would inhibit the surface receptor motility (Dunn et al. 1980; Edelman et al. 1973; Ivanov 2014) and block all active endocytosis that requires energy and receptors. Thus, instead of endosomal membrane

destabilization and nanoparticle escape after internalization, the partially diffusive cellular uptake behavior (Verma et al. 2008) in HCT 116 after long time PTR-SeNP exposure might be caused by direct passive translocation (Adjei et al. 2014).

Similarly, by using chlorpromazine (CPZ), an inhibitor of clathrin-mediated endocytosis, the cellular uptake of C6-PTR-SeNP by HCT 116 cells decreased significantly by around 50%, suggesting that clathrin-mediated endocytosis (CME) would likely be the major endocytotic pathway involved. The remaining 20% of the internalization might be attributed to CIE and micropinocytosis processes, since epithelial cells were reported to take several hours in phagocytosis (Kuhn et al. 2014).

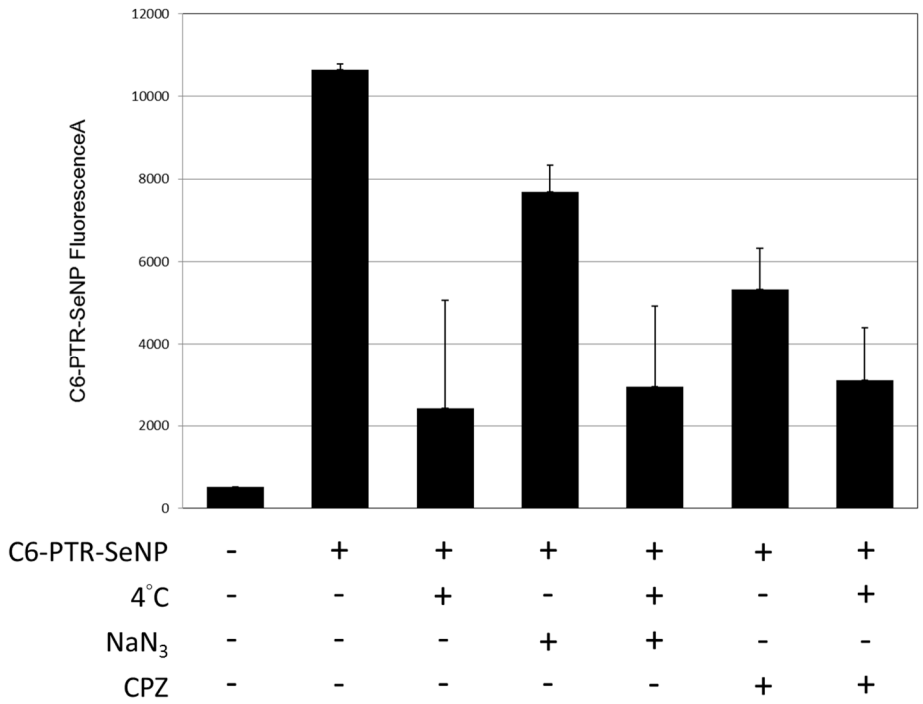

Figure 17: Cellular uptake of C6-PTR-SeNP by HCT 116 cells is inhibited by low temperature, sodium azide and chlorpromazine. Flow cytometry analysis of cellular uptake behavior of C6-PTR-SeNP (20 μM) by the HCT 116 cells after treatment with different inhibitors for 2 hours. NaN3: sodium azide, CPZ: chlorpromazine.

	4°C	NaN_3	4°C + NaN3	CPZ	4°C + CPZ
% of cellular uptake inhibition	81.1	29.2	75.9	52.5	74.4

Table 1: Percentage of inhibition on cellular uptake of C6-PTR-SeNP by HCT 116 cells induced by different inhibitors. The fluorescent intensity was normalized against negative control (normal HCT 116 cells) and positive control (normal HCT 116 exposed to C6-PTR-SeNP) to calculate the percentage of cellular uptake inhibited by each inhibitor.

Chapter 4 - Conclusions and Future Perspectives

4.1 Summary

Anti-cancer efficacy of PTR-SeNP

Among the panel of six different human colorectal cancer cell lines, the cell lines have different susceptibility towards PTR-SeNP treatment. The reason behind the difference is complex, which may be attributed to their different genetic phenotypes, such as TP53 status and microsatellite stability (MSS) status. Among the six cell lines, HCT 116 cells exhibited the highest dose- and time-dependent anti-proliferation effect by PTR-SeNP, with an IC_{50} value of 4.0 μM, and the cell line was thus chosen for our further studies in anti-cancer mechanisms and cellular uptake pathways involved.

Further investigation on the mechanisms of PTR-SeNP's proliferation inhibition showed that at least cell cycle arrest, autophagy and apoptosis were involved **(Figure 18. B)**. The change in cell cycle signal were found to be the earliest event triggered by PTR-SeNP. The protein levels of Cyclin D1/D3 dropped by 12 h, and the levels of CDK1, CDK2, CDK4 and CDK6 were down-regulated within 24-48 h. All the protein levels were not recovered by 72 h, leading to dose- and time-dependent G2/M phase arrest after 48 h **(Figure 18. A. I)**. Even earlier

than that, Cyclin D1 were down-regulated rapidly at transcriptional levels within 3 h of treatment, and its protein levels dropped as early as 12 h. Given Cyclin D1's role as regulator of downstream cell cycle molecular transcription, it may suggest that Cyclin D1 and its relevant upstream pathways, such as EGFR pathway, were involved as early target of PTR-SeNP's anti-cancer function.

The early downward regulation of Cyclin D1 may also help to explain the discrepancy, that most cancer cell lines exhibit G1 phase cell cycle arrest towards SeNP treatment, as opposed to the G2/M phase arrest in HCT 116 cells among some other cells. As studies have found, actual cell cycle does not always follow the classical model of Cyclin-CDK complex regulation and CKI inhibitions, but may have alternative substitutes to promotion cell cycle progression and bypass the check point regulations. Due to Cyclin D1's role in regulating other cell functions and some other cell cycle proteins, it is likely that HCT 116 cells possess some of the routes to bypass G1 phase cell cycle check points induced by Cyclin D1 degradation, but underwent cell cycle arrest in G2/M phase in response to the down-regulation of cell cycle molecules down stream of Cyclin D1.

A.

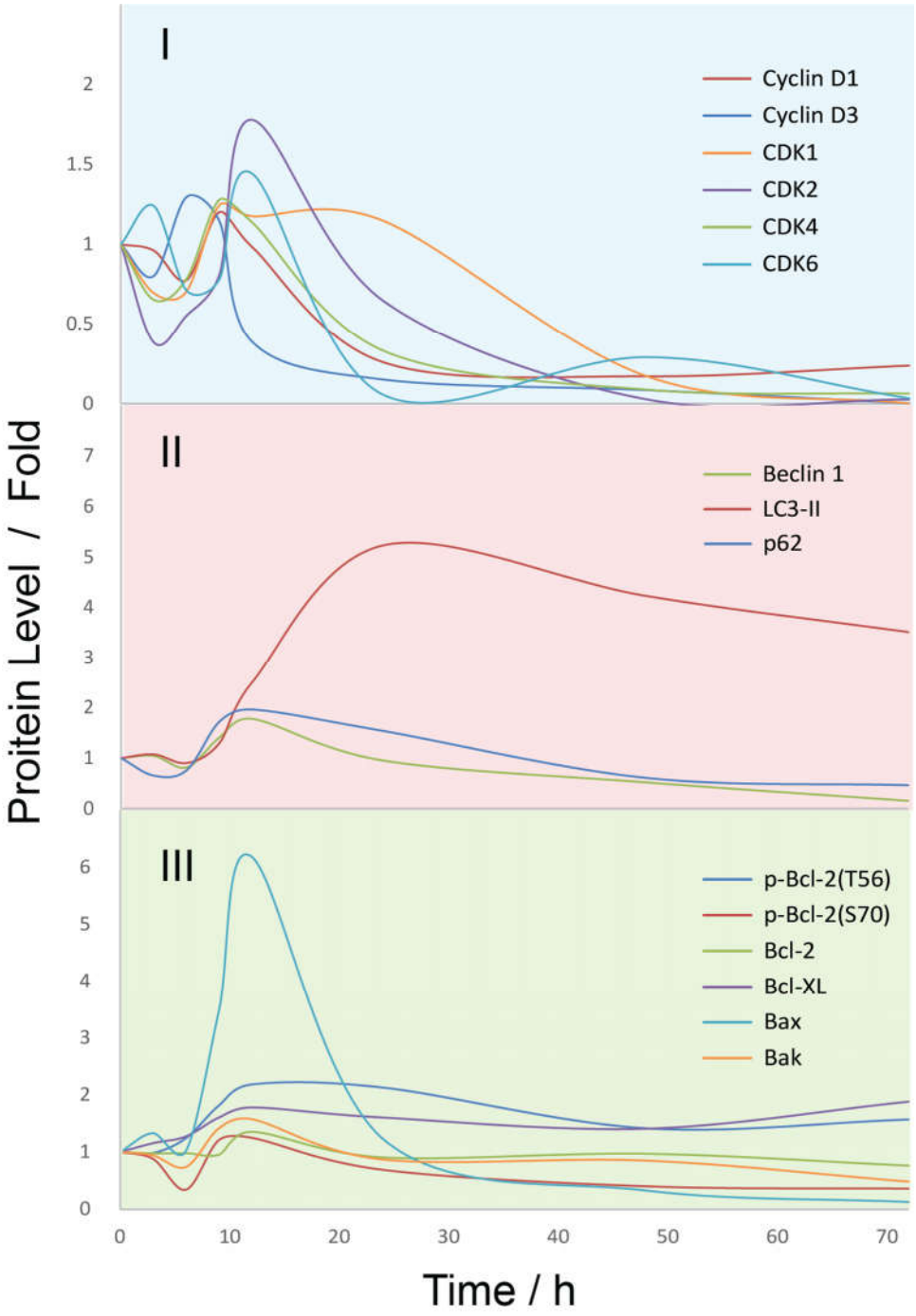
I
Cyclin D1
Cyclin D3
CDK1
CDK2
CDK4
CDK6
II
Beclin 1
LC3-II
p62
III
p-Bcl-2(T56)
p-Bcl-2(S70)
Bcl-2
Bcl-XL
Bax
Bak
Proitein Level / Fold
Time / h
0
10
20
30
40
50
60
70

B.

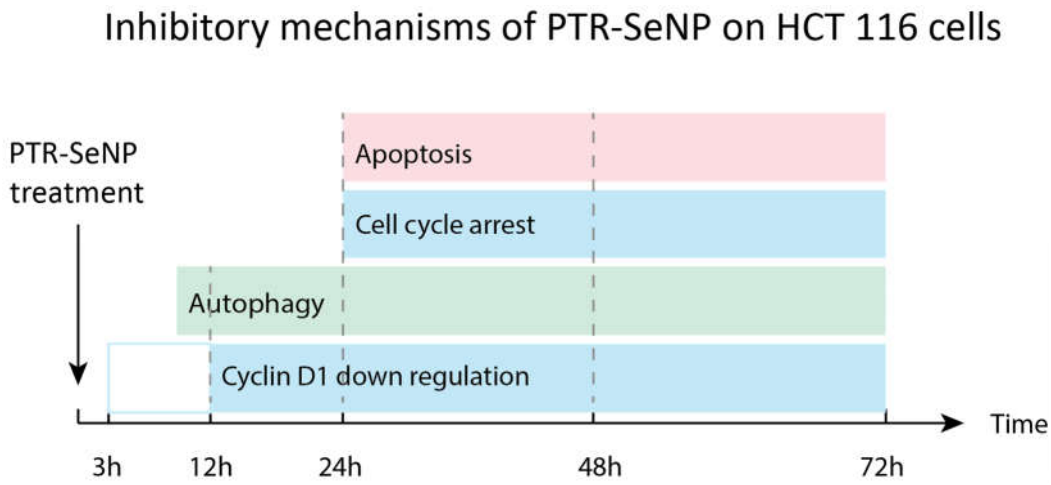

Figure 18: Multiple proliferation inhibition mechanisms involved in the process of the anti-cancer effect of PTR-SeNP on HCT 116 cells

(A) The change of protein levels of (I) cell cycle, (II) autophagy and (III) apoptosis over time in HCT 116 cells under PTR-SeNP treatment. **(B)** The time line of different mechanisms in HCT 116 cells.

On the other hand, within the first 24 h, PTR-SeNP treated HCT 116 cells showed clear sign of autophagy induction, which was unreported in selenium nanoparticles before. Autophagy initiator Beclin 1 was up-regulated and LC3-II level increased as p62/SQSTM1 decreased in the first 24h, indicating the initiation of autophagy as autophagosome formation (Beclin 1, LC3-II) and the completion of autophagic flux with degradation of substrate (p62). Formation of autophgosome was also confirmed by confocal microscopy. Subsequently, after 48 h autophagy was hypothesized to be suppressed, as the levels of Beclin 1 dropped below normal level, with a steady decrease of p62 and LC3-II levels **(Figure 18. A. II)**. This change in LC3-II levels indicate that the majority of LC3-II has shifted from being a component of autophagosome to the substrate of autophagy **(Figure 19)**.

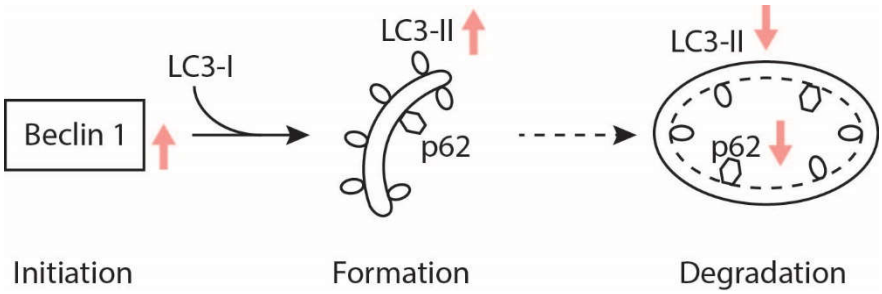

Figure 19: The changes of Beclin 1, LC3-II and p62 in different stages of autophagy.

The initiation of autophagy may have antagonized apoptosis in the first 24 h, since no major increase in sub-G1 peak or Annexin V +/ PI + population were observed in the PI staining and Annexin V/ PI double staining at 24 h. After that, cell death might either be induced by pro-survival autophagy transitioning to autophagic cell death (autosis), or pro-survival autophagy shifting to apoptotic cell death. Our current evidence is that in later stages, p62 levels decrease steadily after 48 h, while the level of Beclin 1 and LC3-II has a slight return **(Figure 14. B)**. Since the dynamic levels of autophagic proteins doesn't necessarily correlate with the level of autophagic flux, further investigation is needed to determine the function and level of completion of autophagy in later stage of PTR-SeNP inhibition.

The activation of autophagy may also be attributed to the cell cycle arrest, as Cyclin D1 suppression was reported to induce autophagy (Brown et al. 2012), and happens around the same time as Beclin 1 increase at 12 h **(Figure 19)**. The initiation and inhibition of autophagy may also be contributed to MAPK/ERK pathway. Phosphorylated ERK is downstream molecule in MAPK pathway and is found to regulate autophagy via Beclin 1 modulation (Wang et al. 2009). The phosphorylated ERK level was found to increase until 24 h and dropped after, corresponding to the activity of autophagic molecules.

After 24 h, PTR-SeNP induced apoptosis was found to be significant, although caspase -3 cleavage and activation was not observed. Thus the apoptotic cell death was non-caspase-3 dependent, and may be mediated via other apoptotic molecules such as AIF and ENDOG. Anti-apoptotic Bcl-2 and Bcl-xL levels remained constant, while pro-apoptotic protein Bax had a sudden increase at 12 h **(Figure 18. A. III)**. Despite of this, no apparent apoptosis was observed at 24 h, which may be inhibited by autophagy. Therefore, the anti-proliferative effect of PTR-SeNP on HCT 116 cells would likely be a result of complicated interplay between several cell inhibitory mechanisms: after PTR-SeNP treatment, the HCT 116 cells went through autophagy in the first 24 h and may have transitioned to apoptosis over long term exposure. Cell cycle arrest was initiated very early and persisted throughout the whole process. However, the interaction between autophagy and apoptosis needs further study.

Cellular uptake behavior of PTR-SeNP

By using Coumarin-6 fluorescent dye for tracking, the cellular uptake of PTR-SeNP by the HCT 116 cells was found to reach maximum level at 2 h followed by a rapid drop at 4 h and steady increase until 24 h. This sudden drop of coumarin-6 signals at 4 h may be due to the conformational changes of coumarin-6 in lower pH. Thus, 2 – 4 h will be the best time to observe cellular uptake of C6-PTR-SeNP.

In the study with multiple cellular uptake inhibitors, clathrin-mediated endocytosis were found to be a major contributor to PTR-SeNP internalization, accounting for around 50% of all internalized nanoparticles. Interestingly, passive translocation, the non-energy dependent pathway of internalization was present in HCT 116 cells, as evidenced by the remaining 30% of PTR-SeNP cellular uptake after active uptake was inhibited by low temperature (4 °C) and/or sodium azide. The mechanisms behind the remaining 20% NP uptake by HCT 116 may be accounted by caveolae-mediated endocytosis, since in addition to targeting lysosomes, C6-PTR-SeNP was found to co-localize rapidly with Golgi apparatus. This was an indication of the involvement of caveolae-mediated endocytosis, since it was the only reported pathway so far that could transport cargoes to trans-Golgi network in addition to lysosomes. This possible utilization of caveolae-

mediated endocytosis by SeNP was not reported previously. Since size is a determinant factor for cellular uptake pathways, these observations basically fit our expectations based on the size of PTR-SeNP.

In conclusion, the major highlights of this study include:

(1) PTR-SeNP, has anti-cancer efficacies in six CRC cell lines, among which HCT 116 cells were the most sensitive;

(2) SeNP could induce autophagy in CRC cells, which was unreported;

(3) PTR-SeNP triggered complicated cell inhibition mechanisms in the CRC, including non-caspase-3 dependent apoptosis pathways, G2/M cell cycle arrest, and autophagy;

(4) PTR-SeNP's inhibitory effect was found to be antagonistic with apoptosis inducer 5-FU, which may be attributed to its ability to induce autophagy;

(5) PTR-SeNP induced cellular internalization not only via clathrin-depedent endocytosis, but also via passive translocation and possibly caveolae-dependent endocytosis.

4.2 Disadvantage and future perspectives

Like every single study, this project was limited by the shortcomings of available techniques, for example, autophagy is a process of consecutive events, and it is only complete autophagic flux, in which autophagosomes fuse with lysosome to form autolysosomes, and the proton pump on the membrane lower the pH to activate hydrolytic enzymes to degrade the cargo. Since the dynamic levels of LC3-II and p62/SQSTM1 could be affected by multiple factors in the "inflow" and "outflow", measuring certain marker proteins at certain time points has a risk of mis-interpretation. For example, upregulation of LC3-I level could increase the protein level and lower LC3-I/LC3-II ratio, even though autophagic flux level remain unchanged; on the other hand, inhibition in the lysosome fusion or proton pump functions could block LC3-II degradation, making the level increase while autophagy flux is blocked. Thus, it would be preferential to conduct gene knockout or knockdown technique targeting autophagy related genes (such as Atg5/7) and/or apoptosis related genes (such as Bcl-2, Bax or Bak) to determine the functions of autophagy, apoptosis and their interactions in the process. In addition, TEM technique could help to verify the morphological structures of autophagosome at different time points, in order to monitor and confirm the progression and completion of autophagic flux.

In addition, in terms of experimental design, the study could have used autophagic and apoptosis inhibitors as negative controls. The exploration on cellular uptake mechanism is also more or less tentative, without a systematic design to encompass all possible pathways into exploration. These would all require further studies to fully confirm and explore the research results.

The next step of this series of study would point to further study on the function and mechanism of autophagy in the inhibition of HCT 116, and its interactions with apoptosis, using techniques such as gene knock down or silencing and TEM structural microscopy. Also the functions of Cyclin D1 and the interaction of PTR-SeNP with its upstream pathways and receptors (such as EGF receptor pathways), which might also provide important insights into the PTR-SeNP triggered cell cycle arrest. On the *in vivo* level, it is worthwhile to investigate the practical effect of PTR-SeNP in CRC prevention and treatment in animal models, which involves model development and drug delivery in its original form to lower GI tract as major questions. Our long term goal is to develop economical, safe and evidence-based anti-tumor agent for our community, hereby alleviating the now spiraling cost of cancer treatments in the local public healthcare system.

Chapter 5 - References

Abraham R.T. 2001. Cell cycle checkpoint signaling through the ATM and ATR kinases. Genes & Development 15:2177-2196.

Adjei I.M., Sharma B., Labhasetwar V. 2014. Nanoparticles: Cellular Uptake and Cytotoxicity. In: Capco G.D., Chen Y., editors. Nanomaterial: Impacts on Cell Biology and Medicine. Dordrecht: Springer Netherlands. p. 73-91.

American Joint Committee on Cancer [Internet]. 2013. Colon and Rectum Cancer Staging. American Joint Committee on Cancer. Available from: http://cancerstaging.org/references-tools/quickreferences/documents/colonmedium.pdf

Aune D., Chan D.S.M., Lau R., Vieira R., Greenwood D.C., Kampman E., Norat T. 2011. Dietary fibre, whole grains, and risk of colorectal cancer: Systematic review and dose-response meta-analysis of prospective studies. The BMJ 343:d6617.

Bao P., Chen Z., Tai R.Z., Shen H.M., Martin F.L., Zhu Y.G. 2015. Selenite-Induced Toxicity in Cancer Cells Is Mediated by Metabolic Generation of Endogenous Selenium Nanoparticles. Journal of Proteome Research 14:1127-1136.

Barooah N., Mohanty J., Pal H., Bhasikuttan A.C. 2012. Stimulus-responsive supramolecular pKa tuning of cucurbit[7]uril encapsulated coumarin 6 dye. The Journal of Physical Chemistry B 116:3683-3689.

Bellinger F.P., Raman A.V., Reeves M.A., Berry M.J. 2009. Regulation and function of selenoproteins in human disease. Biochemical Journal 422:11-22.

Berger A.C., Sigurdson E.R., LeVoyer T., Hanlon A., Mayer R.J., Macdonald J.S., Catalano P.J., Haller D.G. 2005. Colon cancer survival is associated with decreasing ratio of metastatic to examined lymph nodes. Journal of Clinical Oncology 23:8706-8712.

Berglund P. 2008. Cell cycle perspective on breast cancer cell behavior. Lund University, Sweden. p. 59.

Bermano G., Pagmantidis V., Holloway N., Kadri S., Mowat N.A.G., Shiel R.S., Arthur J.R., Mathers J.C., Daly A.K., Broom J. *et al.* . 2007. Evidence that a polymorphism within the 3′UTR of glutathione peroxidase 4 is functional and is associated with susceptibility to colorectal cancer. Genes & Nutrition 2:225-232.

Berry M.J., Tujebajeva R.M., Copeland P.R., Xu X.M., Carlson B.A., Martin G.W., Low S.C., Mansell J.B., Grundner-Culemann E., Harney J.W. *et al.* . 2001. Selenocysteine incorporation directed from the 3′UTR: Characterization of eukaryotic EFsec and mechanistic implications. BioFactors 14:17-24.

Bertrand N., Wu J., Xu X., Kamaly N., Farokhzad O.C. 2014. Cancer nanotechnology: The impact of passive and active targeting in the era of modern cancer biology. Advanced Drug Delivery Reviews 66:2-25.

Bjelakovic G., Nikolova D., Simonetti R.G., Gluud C. 2004. Antioxidant supplements for prevention of gastrointestinal cancers: A systematic review and meta-analysis. The Lancet 364:1219-1228.

Bjørkøy G., Lamark T., Brech A., Outzen H., Perander M., Øvervatn A., Stenmark H., Johansen T. 2005. p62/SQSTM1 forms protein aggregates degraded by autophagy and has a protective effect on huntingtin-induced cell death. The Journal of Cell Biology 171:603-614.

Blanco E., Shen H., Ferrari M. 2015. Principles of nanoparticle design for overcoming biological barriers to drug delivery. Nature Biotechnology 33:941-951.

Bohdanowicz M., Grinstein S. 2013. Role of Phospholipids in Endocytosis, Phagocytosis, and Macropinocytosis. Physiological Reviews 93:69-106.

Boyle T., Keegel T., Bull F., Heyworth J., Fritschi L. 2012. Physical activity and risks of proximal and distal colon cancers: A systematic review and meta-analysis. Journal of the National Cancer Institute 104:1548-1561.

Bröker L.E., Kruyt F.A.E., Giaccone G. 2005. Cell death independent of caspases: A review. Clinical Cancer Research 11:3155-3162.

Broome C.S., McArdle F., Kyle J.A., Andrews F., Lowe N.M., Hart C.A., Arthur J.R., Jackson M.J. 2004. An increase in selenium intake improves immune function and poliovirus handling in adults with marginal selenium status. The American Journal of Clinical Nutrition 80:154-162.

Brown K., Arthur J. 2001. Selenium, selenoproteins and human health: A review. Public Health Nutrition 4:593-599.

Brown N.E., Jeselsohn R., Bihani T., Hu M.G., Foltopoulou P., Kuperwasser C., Hinds P.W. 2012. Cyclin D1 activity regulates autophagy and senescence in the mammary epithelium. Cancer research 72:6477-6489.

Burk R.F., Hill K.E. 2009. Selenoprotein P—Expression, functions, and roles in mammals. Biochimica et Biophysica Acta (BBA) - General Subjects 1790:1441-1447.

Burk R.F., Hill K.E. 2015. Regulation of selenium metabolism and transport. In: Bowman B.A., Stover P.J., editors. Annual Review of Nutrition, Vol 35. Palo Alto: Annual Reviews. p. 109-134.

Cande C., Vahsen N., Garrido C., Kroemer G. 2004. Apoptosis-inducing factor (AIF): Caspase-independent after all. Cell Death & Differentiation 11:591-595.

Canton I., Battaglia G. 2012. Endocytosis at the nanoscale. Chemical Society Reviews 41:2718-2739.

Carnovale C., Bryant G., Shukla R., Bansal V. 2016. Size, shape and surface chemistry of nano-gold dictate its cellular interactions, uptake and toxicity. Progress in Materials Science 83:152-190.

Carrato A. 2008. Adjuvant Treatment of Colorectal Cancer. Gastrointestinal Cancer Research : GCR 2:S42-S46.

Castro-Obregon S. 2010. The discovery of lysosomes and autophagy. Nature Education 3:49.

Chan A.T., Giovannucci E.L. 2010. Primary prevention of colorectal cancer. Gastroenterology 138:2029-2043.e2010.

Chan G.C.F., Chan W.K., Sze D.M.Y. 2009. The effects of β-glucan on human immune and cancer cells. Journal of Hematology & Oncology 2:1-11.

Chaudhary S., Mehta S. 2014. Selenium nanomaterials: Applications in electronics, catalysis and sensors. Journal of Nanoscience and Nanotechnology 14:1658-1674.

Chee C.E., Sinicrope F.A. 2010. Targeted therapeutic agents for colorectal cancer. Gastroenterology Clinics of North America 39:601-613.

Chen W., Zheng R., Baade P.D., Zhang S., Zeng H., Bray F., Jemal A., Yu X.Q., He J. 2016. Cancer statistics in China, 2015. CA: A Cancer Journal for Clinicians 66:115-132.

Chipuk J.E., Green D.R. 2005. Do inducers of apoptosis trigger caspase-independent cell death? Nature Reviews Molecular Cell Biology 6:268-275.

Chudobova D., Cihalova K., Dostalova S., Ruttkay-Nedecky B., Merlos Rodrigo M.A., Tmejova K., Kopel P., Nejdl L., Kudr J., Gumulec J. *et al.* . 2014. Comparison of the effects of silver phosphate and selenium nanoparticles on *Staphylococcus aureus* growth reveals potential for selenium particles to prevent infection. FEMS Microbiology Letters 351:195-201.

Clark L.C., Hixson L.J., Combs G.F., Reid M.E., Turnbull B.W., Sampliner R.E. 1993. Plasma selenium concentration predicts the prevalence of colorectal adenomatous polyps. Cancer Epidemiology Biomarkers & Prevention 2:41-46.

Clarke P.G.H. 1990. Developmental cell death: Morphological diversity and multiple mechanisms. Anatomy and Embryology 181:195-213.

Compton C.C., Greene F.L. 2004. The staging of colorectal cancer: 2004 and beyond. CA: A Cancer Journal for Clinicians 54:295-308.

Connelly-Frost A., Poole C., Satia J.A., Kupper L.L., Millikan R.C., Sandler R.S. 2009.

Selenium, folate, and colon cancer. Nutrition and Cancer 61:165-178.

Constantinou C., Papas K.A., Constantinou A.I. 2009. Caspase-independent pathways of programmed cell death: The unraveling of new targets of cancer therapy? Current Cancer Drug Targets 9:717-728.

Corpet D.E., Tache S. 2002. Most effective colon cancer chemopreventive agents in rats: A systematic review of aberrant crypt foci and tumor data, ranked by potency. Nutrition and Cancer 43:1-21.

Cregan S.P., Fortin A., MacLaurin J.G., Callaghan S.M., Cecconi F., Yu S.-W., Dawson T.M., Dawson V.L., Park D.S., Kroemer G. *et al.* . 2002. Apoptosis-inducing factor is involved in the regulation of caspase-independent neuronal cell death. The Journal of Cell Biology 158:507-517.

Cuervo A.M., Wong E. 2014. Chaperone-mediated autophagy: Roles in disease and aging. Cell Research 24:92-104.

Damania D., Roy H.K., Subramanian H., Weinberg D.S., Rex D.K., Goldberg M.J., Muldoon J., Cherkezyan L., Zhu Y., Bianchi L.K. *et al.* . 2012. Nanocytology of rectal colonocytes to assess risk of colon cancer based on field cancerization. Cancer Research 72:2720-2727.

Davies J.M., Goldberg R.M. 2011. Treatment of metastatic colorectal cancer. Seminars in Oncology 38:552-560.

Dennert G., Zwahlen M., Brinkman M., Vinceti M., Zeegers M.P.A., Horneber M. 2011. Selenium for preventing cancer. Cochrane database of systematic reviews (Online):CD005195.

Descloux C., Ginet V., Clarke P.G.H., Puyal J., Truttmann A.C. 2015. Neuronal death after perinatal cerebral hypoxia-ischemia: Focus on autophagy-mediated cell death. International Journal of Developmental Neuroscience 45:75-85.

DiPaola R.S. 2002. To arrest or not to G2-M cell-cycle arrest. Clinical Cancer Research 8:3311-3314.

Djavaheri-Mergny M., Maiuri M.C., Kroemer G. 2010. Cross talk between apoptosis

and autophagy by caspase-mediated cleavage of Beclin 1. Oncogene 29:1717-1719.

dos Santos T., Varela J., Lynch I., Salvati A., Dawson K.A. 2011. Effects of transport inhibitors on the cellular uptake of carboxylated polystyrene nanoparticles in different cell lines. PLoS ONE 6:e24438.

Duffield-Lillico A.J., Reid M.E., Turnbull B.W., Combs G.F., Slate E.H., Fischbach L.A., Marshall J.R., Clark L.C. 2002. Baseline characteristics and the effect of selenium supplementation on cancer incidence in a randomized clinical trial: A summary report of the nutritional prevention of cancer trial. Cancer Epidemiology Biomarkers & Prevention 11:630-639.

Dunn W.A., Hubbard A.L., Aronson N.N. 1980. Low temperature selectively inhibits fusion between pinocytic vesicles and lysosomes during heterophagy of 125I-asialofetuin by the perfused rat liver. Journal of Biological Chemistry 255:5971-5978.

Dutta D., Donaldson J.G. 2012. Search for inhibitors of endocytosis. Cellular Logistics 2:203-208.

Edelman G.M., Yahara I., Wang J.L. 1973. Receptor mobility and receptor-cytoplasmic interactions in lymphocytes. Proceedings of the National Academy of Sciences of the United States of America 70:1442-1446.

Ekkapongpisit M., Giovia A., Follo C., Caputo G., Isidoro C. 2012. Biocompatibility, endocytosis, and intracellular trafficking of mesoporous silica and polystyrene nanoparticles in ovarian cancer cells: Effects of size and surface charge groups. International Journal of Nanomedicine 7:4147-4158.

Essner E., Novikoff A.B. 1961. Localization of acid phosphatase activity in hepatic lysosomes by means of electron microscopy. The Journal of Biophysical and Biochemical Cytology 9:773-784.

Fang W., Han A., Bi X., Xiong B., Yang W. 2010. Tumor inhibition by sodium selenite is associated with activation of c-Jun NH2-terminal kinase 1 and suppression of β-catenin signaling. International Journal of Cancer 127:32-42.

Feng Y., Su J., Zhao Z., Zheng W., Wu H., Zhang Y., Chen T. 2014. Differential effects of amino acid surface decoration on the anticancer efficacy of selenium nanoparticles. Dalton Transactions 43:1854-1861.

Fernandez-Banares F., Cabre E., Esteve M., Mingorance M.D., Abad-Lacruz A., Lachica M., Gil A., Gassull M.A. 2002. Serum selenium and risk of large size colorectal adenomas in a geographical area with a low selenium status. The American Journal of Gastroenterology 97:2103-2108.

Ferrari P., Jenab M., Norat T., Moskal A., Slimani N., Olsen A., Tjønneland A., Overvad K., Jensen M.K., Boutron-Ruault M.-C. *et al.* . 2007. Lifetime and baseline alcohol intake and risk of colon and rectal cancers in the European prospective investigation into cancer and nutrition (EPIC). International Journal of Cancer 121:2065-2072.

Fleming M., Ravula S., Tatishchev S.F., Wang H.L. 2012. Colorectal carcinoma: Pathologic aspects. Journal of Gastrointestinal Oncology 3:153-173.

Fröhlich E. 2012. The role of surface charge in cellular uptake and cytotoxicity of medical nanoparticles. International Journal of Nanomedicine 7:5577-5591.

Fu L.-l., Cheng Y., Liu B. 2013. Beclin-1: Autophagic regulator and therapeutic target in cancer. The International Journal of Biochemistry & Cell Biology 45:921-924.

Fu M., Wang C., Li Z., Sakamaki T., Pestell R.G. 2004. Minireview: Cyclin D1: Normal and abnormal functions. Endocrinology 145:5439-5447.

Galluzzi L., Vitale I., Abrams J.M., Alnemri E.S., Baehrecke E.H., Blagosklonny M.V., Dawson T.M., Dawson V.L., El-Deiry W.S., Fulda S. *et al.* . 2012. Molecular definitions of cell death subroutines: Recommendations of the Nomenclature Committee on Cell Death 2012. Cell Death & Differentiation 19:107-120.

Glade M.J. 1999. Food, nutrition, and the prevention of cancer: A global perspective. . Nutrition 15:523-526.

Glick D., Barth S., Macleod K.F. 2010. Autophagy: Cellular and molecular mechanisms. The Journal of Pathology 221:3-12.

Gold S., Monaghan P., Mertens P., Jackson T. 2010. A clathrin independent macropinocytosis-like entry mechanism used by bluetongue virus-1 during infection of BHK cells. PLoS ONE 5:e11360.

Gottlieb R.A., Andres A.M., Sin J., Taylor D.P.J. 2015. Untangling autophagy measurements: All fluxed up. Circulation Research 116:504-514.

Hong Kong Cancer Registry [Internet]. 2015. Overview of 2013 HK Cancer Statistics. Hong Kong Hospital Authority. Available from: http://www3.ha.org.hk/cancereg/Summary%20of%20CanStat%202013.pdf

Hong Kong Department of Health [Internet]. 2015a. Centre for Health Protection- Life Expectancy at Birth (Male and Female), 1971 - 2015: . Available from: http://www.chp.gov.hk/en/data/4/10/27/111.html

Hong Kong Department of Health [Internet]. 2015b. HealthyHK - Public Health Information and Statistics of Hong Kong - Colorectal Cancer. Hong Kong Department of Health. Available from: http://www.healthyhk.gov.hk/phisweb/en/healthy_facts/disease_burden/major_causes_death/cancers/colorectal_cancer/

Hou N., Huo D., Dignam J.J. 2013. Prevention of colorectal cancer and dietary management. Chinese Clinical Oncology 2.

Hou W., Han J., Lu C., Goldstein L.A., Rabinowich H. 2010. Autophagic degradation of active caspase-8: A crosstalk mechanism between autophagy and apoptosis. Autophagy 6:891-900.

Howe G.R., Benito E., Castelleto R., Cornée J., Estève J., Gallagher R.P., Iscovich J.M., Deng-ao J., Kaaks R., Kune G.A. *et al.* . 1992. Dietary intake of fiber and decreased risk of cancers of the colon and rectum: Evidence from the combined analysis of 13 case-control studies. Journal of the National Cancer Institute 84:1887-1896.

Hu Y., McIntosh G.H., Le Leu R.K., Woodman R., Young G.P. 2008. Suppression of colorectal oncogenesis by selenium-enriched milk proteins: Apoptosis and K-ras mutations. Cancer Research 68:4936-4944.

Huang Z., Rose A.H., Hoffmann P.R. 2012. The role of selenium in inflammation and immunity: from molecular mechanisms to therapeutic opportunities. Antioxidants & Redox Signaling 16:705-743.

Huo S., Jin S., Ma X., Xue X., Yang K., Kumar A., Wang P.C., Zhang J., Hu Z., Liang X.-J. 2014. Ultrasmall gold nanoparticles as carriers for nucleus-based gene therapy due to size-dependent nuclear entry. ACS Nano 8:5852-5862.

Iacopetta B. 2002. Are there two sides to colorectal cancer? International Journal of Cancer 101:403-408.

Irons R., Carlson B.A., Hatfield D.L., Davis C.D. 2006. Both selenoproteins and low molecular weight selenocompounds reduce colon cancer risk in mice with genetically impaired selenoprotein expression. The Journal of Nutrition 136:1311-1317.

Ivanov A.I. 2014. Pharmacological Inhibitors of Exocytosis and Endocytosis: Novel Bullets for Old Targets. In: Ivanov A.I., editor. Exocytosis and Endocytosis 2ed. NY: Springer. p. 3-18.

Iversen T.G., Frerker N., Sandvig K. 2012. Uptake of ricinB-quantum dot nanoparticles by a macropinocytosis-like mechanism. Journal of Nanobiotechnology 10:1-11.

Jacobs E.T., Jiang R., Alberts D.S., Greenberg E.R., Gunter E.W., Karagas M.R., Lanza E., Ratnasinghe L., Reid M.E., Schatzkin A. *et al.* . 2004. Selenium and colorectal adenoma: Results of a pooled analysis. Journal of the National Cancer Institute 96:1669-1675.

Jemal A., Siegel R., Ward E., Hao Y., Xu J., Murray T., Thun M.J. 2008. Cancer Statistics, 2008. CA: A Cancer Journal for Clinicians 58:71-96.

Jirawatnotai S., Hu Y., Michowski W., Elias J.E., Becks L., Bienvenu F., Zagozdzon A., Goswami T., Wang Y.E., Clark A.B. *et al.* . 2011. A function for cyclin D1 in

DNA repair uncovered by interactome analyses in human cancers. Nature 474:230-234.

Kang R., Zeh H.J., Lotze M.T., Tang D. 2011. The Beclin 1 network regulates autophagy and apoptosis. Cell Death and Differentiation 18:571-580.

Kelekar A., Thompson C.B. 1998. Bcl-2-family proteins: The role of the BH3 domain in apoptosis. Trends in Cell Biology 8:324-330.

Kheradmand E., Rafii F., Yazdi M.H., Sepahi A.A., Shahverdi A.R., Oveisi M.R. 2014. The antimicrobial effects of selenium nanoparticle-enriched probiotics and their fermented broth against *Candida albicans*. DARU Journal of Pharmaceutical Sciences 22:1-6.

Khiralla G.M., El-Deeb B.A. 2015. Antimicrobial and antibiofilm effects of selenium nanoparticles on some foodborne pathogens. LWT - Food Science and Technology 63:1001-1007.

Kirkham M., Fujita A., Chadda R., Nixon S.J., Kurzchalia T.V., Sharma D.K., Pagano R.E., Hancock J.F., Mayor S., Parton R.G. 2005. Ultrastructural identification of uncoated caveolin-independent early endocytic vehicles. The Journal of Cell Biology 168:465-476.

Kirkin V., McEwan D.G., Novak I., Dikic I. 2009. A role for ubiquitin in selective autophagy. Molecular Cell 34:259-269.

Klionsky D.J., Abdalla F.C., Abeliovich H., Abraham R.T., Acevedo-Arozena A., Adeli K., Agholme L., Agnello M., Agostinis P., Aguirre-Ghiso J.A. *et al.* . 2012. Guidelines for the use and interpretation of assays for monitoring autophagy. Autophagy 8:445-544.

Klionsky D.J., Eskelinen E.-L., Deretic V. 2014. Autophagosomes, phagosomes, autolysosomes, phagolysosomes, autophagolysosomes… Wait, I'm confused. Autophagy 10:549-551.

Koivusalo M., Welch C., Hayashi H., Scott C.C., Kim M., Alexander T., Touret N., Hahn K.M., Grinstein S. 2010. Amiloride inhibits macropinocytosis by lowering submembranous pH and preventing Rac1 and Cdc42 signaling. The Journal

of Cell Biology 188:547-563.

Kong L., Yuan Q., Zhu H., Li Y., Guo Q., Wang Q., Bi X., Gao X. 2011. The suppression of prostate LNCaP cancer cells growth by Selenium nanoparticles through Akt/Mdm2/AR controlled apoptosis. Biomaterials 32:6515-6522.

Kou L., Sun J., Zhai Y., He Z. 2013. The endocytosis and intracellular fate of nanomedicines: Implication for rational design. Asian Journal of Pharmaceutical Sciences 8:1-10.

Kuhn D.A., Vanhecke D., Michen B., Blank F., Gehr P., Petri-Fink A., Rothen-Rutishauser B. 2014. Different endocytotic uptake mechanisms for nanoparticles in epithelial cells and macrophages. Beilstein Journal of Nanotechnology 5:1625-1636.

Kuma A., Hatano M., Matsui M., Yamamoto A., Nakaya H., Yoshimori T., Ohsumi Y., Tokuhisa T., Mizushima N. 2004. The role of autophagy during the early neonatal starvation period. Nature 432:1032-1036.

Kuma A., Mizushima N. 2010. Physiological role of autophagy as an intracellular recycling system: With an emphasis on nutrient metabolism. Seminars in Cell & Developmental Biology 21:683-690.

Kuppusamy P., Yusoff M.M., Maniam G.P., Ichwan S.J.A., Soundharrajan I., Govindan N. 2014. Nutraceuticals as potential therapeutic agents for colon cancer: A review. Acta Pharmaceutica Sinica B 4:173-181.

Lam T.L., Wong G.K.Y., Chow H.Y., Chong H.C., Chow T.L., Kwok S.Y., Cheng P.N.M., Wheatley D.N., Lo W.H., Leung Y.C. 2011. Recombinant human arginase inhibits the *in vitro* and *in vivo* proliferation of human melanoma by inducing cell cycle arrest and apoptosis. Pigment Cell & Melanoma Research 24:366-376.

Larsson S.C., Wolk A. 2007. Obesity and colon and rectal cancer risk: A meta-analysis of prospective studies. The American Journal of Clinical Nutrition 86:556-565.

Lee Y.M., Sicinski P. 2006. Targeting cyclins and cyclin-dependent kinases in cancer:

Lessons from mice, hopes for therapeutic applications in humans. Cell Cycle 5:2110-2114.

Levin B., Lieberman D.A., McFarland B., Smith R.A., Brooks D., Andrews K.S., Dash C., Giardiello F.M., Glick S., Levin T.R. *et al.* . 2008. Screening and surveillance for the early detection of colorectal cancer and adenomatous polyps, 2008: A joint guideline from the American Cancer Society, the US Multi-Society Task Force on Colorectal Cancer, and the American College of Radiology. CA: A Cancer Journal for Clinicians 58:130-160.

Li F., Lutz P.B., Pepelyayeva Y., Arnér E.S.J., Bayse C.A., Rozovsky S. 2014. Redox active motifs in selenoproteins. Proceedings of the National Academy of Sciences of the United States of America 111:6976-6981.

Li H., Zhu H., Xu C.J., Yuan J. 1998. Cleavage of BID by caspase 8 mediates the mitochondrial Damage in the Fas pathway of apoptosis. Cell 94:491-501.

Li J., Hou N., Faried A., Tsutsumi S., Kuwano H. 2010a. Inhibition of autophagy augments 5-fluorouracil chemotherapy in human colon cancer *in vitro* and *in vivo* model. European Journal of Cancer 46:1900-1909.

Li J., Hou N., Faried A., Tsutsumi S., Takeuchi T., Kuwano H. 2008. Inhibition of autophagy by 3-MA enhances the effect of 5-FU-induced apoptosis in colon cancer cells. Annals of Surgical Oncology 16:761-771.

Li W.W., Li J., Bao J.K. 2011. Microautophagy: Lesser-known self-eating. Cellular and Molecular Life Sciences 69:1125-1136.

Li Y., Kroger M., Liu W.K. 2015. Shape effect in cellular uptake of PEGylated nanoparticles: Comparison between sphere, rod, cube and disk. Nanoscale 7:16631-16646.

Li Z., Jiao X., Wang C., Shirley L.A., Elsaleh H., Dahl O., Wang M., Soutoglou E., Knudsen E.S., Pestell R.G. 2010b. Alternative Cyclin D1 splice forms differentially regulate the DNA damage response. Cancer research 70:8802-8811.

Li Z., Wang C., Jiao X., Lu Y., Fu M., Quong A.A., Dye C., Yang J., Dai M., Ju X. *et al.* .

2006. Cyclin D1 regulates cellular migration through the inhibition of Thrombospondin 1 and ROCK signaling. Molecular and Cellular Biology 26:4240-4256.

Liang Y., Yan C., Schor N.F. 2001. Apoptosis in the absence of caspase 3. Oncogene 20:6570-6578.

Lim J.P., Gleeson P.A. 2011. Macropinocytosis: An endocytic pathway for internalising large gulps. Immunology & Cell Biology 89:836-843.

Lim S.H., Kaldis P. 2013. Cdks, cyclins and CKIs: Roles beyond cell cycle regulation. Development 140:3079-3093.

Lin J., Zhang H., Chen Z., Zheng Y. 2010. Penetration of lipid membranes by gold nanoparticles: Insights into cellular uptake, cytotoxicity, and their relationship. ACS Nano 4:5421-5429.

Lin J.H., Giovannucci E. 2010. Sex hormones and colorectal cancer: What have we learned so far? Journal of the National Cancer Institute 102:1746-1747.

Lindqvist L.M., Simon A.K., Baehrecke E.H. 2015. Current questions and possible controversies in autophagy. Cell Death Discovery 1:15036.

Linton P.J., Gurney M., Sengstock D., Mentzer Jr R.M., Gottlieb R.A. 2015. This old heart: Cardiac aging and autophagy. Journal of Molecular and Cellular Cardiology 83:44-54.

Liu W., Li X., Wong Y.S., Zheng W., Zhang Y., Cao W., Chen T. 2012. Selenium nanoparticles as a carrier of 5-fluorouracil to achieve anticancer synergism. ACS Nano 6:6578-6591.

Liu Y., Levine B. 2015. Autosis and autophagic cell death: The dark side of autophagy. Cell Death and Differentiation 22:367-376.

Longley D.B., Harkin D.P., Johnston P.G. 2003. 5-Fluorouracil: Mechanisms of action and clinical strategies. Nature Reviews Cancer 3:330-338.

Los M., Mozoluk M., Ferrari D., Stepczynska A., Stroh C., Renz A., Herceg Z., Wang

Z.-Q., Schulze-Osthoff K. 2002. Activation and caspase-mediated inhibition of PARP: A molecular switch between fibroblast necrosis and apoptosis in death receptor signaling. Molecular Biology of the Cell 13:978-988.

Lu W., Xiong C., Zhang R., Shi L., Huang M., Zhang G., Song S., Huang Q., Liu G.-y., Li C. 2012. Receptor-mediated transcytosis: A mechanism for active extravascular transport of nanoparticles in solid tumors. Journal of Controlled Release 161:959-966.

Lynch-Day M.A., Klionsky D.J. 2010. The Cvt pathway as a model for selective autophagy. FEBS Letters 584:1359-1366.

Lynch H., de la Chapelle A. 1999. Genetic susceptibility to non-polyposis colorectal cancer. Journal of Medical Genetics 36:801-818.

Lynch H.T., de la Chapelle A. 2003. Hereditary colorectal cancer. New England Journal of Medicine 348:919-932.

Ma X., Wu Y., Jin S., Tian Y., Zhang X., Zhao Y., Yu L., Liang X.i. 2011. Gold nanoparticles induce autophagosome accumulation through size-dependent nanoparticle uptake and lysosome impairment. ACS Nano 5:8629-8639.

Ma Y., Yang H., Pitt J.M., Kroemer G., Zitvogel L. 2016. Therapy-induced microenvironmental changes in cancer. Journal of Molecular Medicine:497-508.

Malumbres M., Barbacid M. 2009. Cell cycle, CDKs and cancer: A changing paradigm. Nature Reviews Cancer 9:153-166.

Martin D.D.O., Ladha S., Ehrnhoefer D.E., Hayden M.R. 2015. Autophagy in Huntington disease and huntingtin in autophagy. Trends in Neurosciences 38:26-35.

Mary T.A., Shanthi K., Vimala K., Soundarapandian K. 2016. PEG functionalized selenium nanoparticles as a carrier of crocin to achieve anticancer synergism. RSC Advances 6:22936-22949.

Matanoski G., Tao X.G., Almon L., Adade A.A., Davies-Cole J.O. 2006. Demographics and tumor characteristics of colorectal cancers in the United States, 1998-2001. Cancer 107:1112-1120.

Mauvezin C., Nagy P., Juhasz G., Neufeld T.P. 2015. Autophagosome-lysosome fusion is independent of V-ATPase-mediated acidification. Nature Communications 6.

McIntosh D.P., Tan X.-Y., Oh P., Schnitzer J.E. 2002. Targeting endothelium and its dynamic caveolae for tissue-specific transcytosis in vivo: A pathway to overcome cell barriers to drug and gene delivery. Proceedings of the National Academy of Sciences of the United States of America 99:1996-2001.

Méplan C., Hesketh J. 2012. The influence of selenium and selenoprotein gene variants on colorectal cancer risk. Mutagenesis 27:177-186.

Méplan C., Hughes D.J., Pardini B., Naccarati A., Soucek P., Vodickova L., Hlavatá I., Vrána D., Vodicka P., Hesketh J.E. 2010. Genetic variants in selenoprotein genes increase risk of colorectal cancer. Carcinogenesis 31:1074-1079.

Miao X., Li Y., Wyman I., Lee S.M.Y., Macartney D.H., Zheng Y., Wang R. 2015. Enhanced *in vitro* and *in vivo* uptake of a hydrophobic model drug coumarin-6 in the presence of cucurbit[7]uril. MedChemComm 6:1370-1374.

Michalak E.M., Villunger A., Adams J.M., Strasser A. 2008. In several cell types tumour suppressor p53 induces apoptosis largely via Puma but Noxa can contribute. Cell Death & Differentiation 15:1019-1029.

Moscat J., Diaz-Meco M.T. 2009. p62 at the crossroads of autophagy, apoptosis, and cancer. Cell 137:1001-1004.

Murff H.J., Greevy R.A., Syngal S. 2007. The comprehensiveness of family cancer history assessments in primary care. Public Health Genomics 10:174-180.

Musgrove E.A., Caldon C.E., Barraclough J., Stone A., Sutherland R.L. 2011. Cyclin D as a therapeutic target in cancer. Nat Rev Cancer 11:558-572.

National Registry of Disease Office (NRDO) [Internet]. 2014. Singapore Cancer Registry Annual Registry Report: Trends in Cancer Incidence in Singapore 2009-2013. National Registry of Disease Office (NRDO). Available from: https://www.nrdo.gov.sg/docs/librariesprovider3/Publications-Cancer/cancer-trends-report-2009-2013.pdf?sfvrsn=0&AspxAutoDetectCookieSupport=1

Navarro-Alarcon M., Cabrera-Vique C. 2008. Selenium in food and the human body: A review. Science of The Total Environment 400:115-141.

Nawa T., Kato J., Kawamoto H., Okada H., Yamamoto H., Kohno H., Endo H., Shiratori Y. 2008. Differences between right- and left-sided colon cancer in patient characteristics, cancer morphology and histology. Journal of Gastroenterology and Hepatology 23:418-423.

Nelson R.L., Davis F.G., Sutter E., Kikendall J.W., Sobin L.H., Milner J.A., Bowen P.E. 1995. Serum selenium and colonic neoplastic risk. Diseases of the Colon & Rectum 38:1306-1310.

Neugut A.I., Lebwohl B. 2009. Screening for colorectal cancer: The glass is half full. American Journal of Public Health 99:592-594.

Nhiem T., Thomas J.W. 2013. Understanding magnetic nanoparticle osteoblast receptor-mediated endocytosis using experiments and modeling. Nanotechnology 24:185102.

Nikoletopoulou V., Markaki M., Palikaras K., Tavernarakis N. 2013. Crosstalk between apoptosis, necrosis and autophagy. Biochimica et Biophysica Acta (BBA) - Molecular Cell Research 1833:3448-3459.

Norat T., Bingham S., Ferrari P., Slimani N., Jenab M., Mazuir M., Overvad K., Olsen A., Tjønneland A., Clavel F. *et al.* . 2005. Meat, fish, and colorectal cancer risk: The European prospective investigation into cancer and nutrition. Journal of the National Cancer Institute 97:906-916.

O'Connell J.B., Maggard M.A., Ko C.Y. 2004. Colon cancer survival rates with the new American Joint Committee on Cancer sixth edition staging. Journal of the National Cancer Institute 96:1420-1425.

Oh N., Park J.-H. 2014. Endocytosis and exocytosis of nanoparticles in mammalian cells. International Journal of Nanomedicine 9:51-63.

Ohsumi Y. 2014. Historical landmarks of autophagy research. Cell Research 24:9-23.

Oso B.A. 1977. *Pleurotus tuber-regium* from Nigeria. Mycologia 69:271-279.

Panariti A., Miserocchi G., Rivolta I. 2012. The effect of nanoparticle uptake on cellular behavior: Disrupting or enabling functions? Journal of Nanotechnology, Science and Applications 5:87-100.

Pankiv S., Clausen T.H., Lamark T., Brech A., Bruun J.-A., Outzen H., Øvervatn A., Bjørkøy G., Johansen T. 2007. p62/SQSTM1 binds directly to Atg8/LC3 to facilitate degradation of ubiquitinated protein aggregates by autophagy. Journal of Biological Chemistry 282:24131-24145.

Pattingre S., Tassa A., Qu X., Garuti R., Liang X.H., Mizushima N., Packer M., Schneider M.D., Levine B. 2005. Bcl-2 antiapoptotic proteins inhibit Beclin 1-dependent autophagy. Cell 122:927-939.

Perfettini J.-L., Reed J.C., Israël N., Martinou J.-C., Dautry-Varsat A., Ojcius D.M. 2002. Role of Bcl-2 family members in caspase-independent apoptosis during Chlamydia infection. Infection and Immunity 70:55-61.

Peters U., Chatterjee N., Church T.R., Mayo C., Sturup S., Foster C.B., Schatzkin A., Hayes R.B. 2006. High serum selenium and reduced risk of advanced colorectal adenoma in a colorectal cancer early detection program. Cancer Epidemiology Biomarkers & Prevention 15:315-320.

Polajnar M., Žerovnik E. 2014. Impaired autophagy: A link between neurodegenerative and neuropsychiatric diseases. Journal of Cellular and Molecular Medicine 18:1705-1711.

Puissant A., Fenouille N., Auberger P. 2012. When autophagy meets cancer through p62/SQSTM1. American Journal of Cancer Research 2:397-413.

Pyo J.O., Yoo S.M., Ahn H.H., Nah J., Hong S.H., Kam T.I., Jung S., Jung Y.K. 2013.

Overexpression of Atg5 in mice activates autophagy and extends lifespan. Nature Communications 4.

Rahmanto A.S., Davies M.J. 2012. Selenium-containing amino acids as direct and indirect antioxidants. IUBMB Life 64:863-871.

Rajamanickam S., Agarwal R. 2008. Natural products and colon cancer: Current status and future prospects. Drug Development Research 69:460-471.

Ramos J.F., Tran P.A., Webster T.J. Selenium nanoparticles for the prevention of PVC-related medical infections. 2012 38th Annual Northeast Bioengineering Conference (NEBEC); 16-18 March 2012 2012. p. 185-186.

Reid M.E., Duffield-Lillico A.J., Sunga A., Fakih M., Alberts D.S., Marshall J.R. 2006. Selenium supplementation and colorectal adenomas: An analysis of the nutritional prevention of cancer trial. International Journal of Cancer 118:1777-1781.

Rejman J., Oberle V., Zuhorn I.S., Hoekstra D. 2004. Size-dependent internalization of particles via the pathways of clathrin- and caveolae-mediated endocytosis. Biochemical Journal 377:159-169.

Rello-Varona S., Herrero-Martín D., López-Alemany R., Muñoz-Pinedo C., Tirado O.M. 2015. "(Not) All (dead) things share the same breath": Identification of cell death mechanisms in anticancer therapy. Cancer Research 75:913-917.

Rothwell P.M., Wilson M., Elwin C.-E., Norrving B., Algra A., Warlow C.P., Meade T.W. 2010. Long-term effect of aspirin on colorectal cancer incidence and mortality: 20-year follow-up of five randomised trials. The Lancet 376:1741-1750.

Roussel M.F. 1999. The INK4 family of cell cycle inhibitors in cancer. Oncogene 18:5311-5317.

Russo M.W., Murray S.C., Wurzelmann J.I., Woosley J.T., Sandler R.S. 1997. Plasma selenium levels and the risk of colorectal adenomas. . Nutrition and Cancer 28:125-129.

Sánchez-Wandelmer J., Dávalos A., Herrera E., Giera M., Cano S., de la Peña G., Lasunción M.A., Busto R. 2009. Inhibition of cholesterol biosynthesis disrupts lipid raft/caveolae and affects insulin receptor activation in 3T3-L1 preadipocytes. Biochimica et Biophysica Acta (BBA) - Biomembranes 1788:1731-1739.

Sandvig K., Pust S., Skotland T., van Deurs B. 2011. Clathrin-independent endocytosis: Mechanisms and function. Current Opinion in Cell Biology 23:413-420.

Sanmartín C., Plano D., Sharma A.K., Palop J.A. 2012. Selenium compounds, apoptosis and other types of cell death: An overview for cancer therapy. International Journal of Molecular Sciences 13:9649-9672.

Sarkar K., Kruhlak M.J., Erlandsen S.L., Shaw S. 2005. Selective inhibition by rottlerin of macropinocytosis in monocyte-derived dendritic cells. Immunology 116:513-524.

Scaltriti M., Baselga J. 2006. The epidermal growth factor receptor pathway: A model for targeted therapy. Clinical Cancer Research 12:5268-5272.

Schrauzer G.N. 2000. Selenomethionine: A review of its nutritional significance, metabolism and toxicity. The Journal of Nutrition 130:1653-1656.

Schuler M., Maurer U., Goldstein J.C., Breitenbucher F., Hoffarth S., Waterhouse N.J., Green D.R. 2003. p53 triggers apoptosis in oncogene-expressing fibroblasts by the induction of Noxa and mitochondrial Bax translocation. Cell Death and Differentiation 10:451-460.

Secretan B., Straif K., Baan R., Grosse Y., El Ghissassi F., Bouvard V., Benbrahim-Tallaa L., Guha N., Freeman C., Galichet L. *et al.* . 2009. A review of human carcinogens 2014;Part E: tobacco, areca nut, alcohol, coal smoke, and salted fish. The Lancet Oncology 10:1033-1034.

Selznick L.A., Zheng T.S., Flavell R.A., Rakic P., Roth K.A. 2000. Amyloid beta-induced neuronal eeath is Bax-dependent but caspase-independent. Journal of Neuropathology & Experimental Neurology 59:271-279.

Shakibaie M., Salari Mohazab N., Ayatollahi Mousavi S.A. 2015. Antifungal activity of selenium nanoparticles synthesized by Bacillus species Msh-1 against *Aspergillus fumigatus* and *Candida albicans*. Jundishapur Journal of Microbiology 8:e26381.

Shang L., Nienhaus K., Nienhaus G.U. 2014. Engineered nanoparticles interacting with cells: Size matters. Journal of Nanobiotechnology 12:1-11.

Sherr C.J., Roberts J.M. 2004. Living with or without cyclins and cyclin-dependent kinases. Genes & Development 18:2699-2711.

Shin A., Kim K.-Z., Jung K.-W., Park S., Won Y.-J., Kim J., Kim D.Y., Oh J.H. 2012. Increasing trend of colorectal cancer incidence in Korea, 1999-2009. Cancer Research and Treatment : Official Journal of Korean Cancer Association 44:219-226.

Siegel R., Jemal A. Colorectal Cancer Facts & Figures 2014 - 2016 [Internet]. American Cancer Society; 2014. Available from: http://www.cancer.org/acs/groups/content/documents/document/acspc-042280.pdf

Siegel R.L., Miller K.D., Jemal A. 2016. Cancer statistics, 2016. CA: A Cancer Journal for Clinicians 66:7-30.

Stern S.T., Adiseshaiah P.P., Crist R.M. 2012. Autophagy and lysosomal dysfunction as emerging mechanisms of nanomaterial toxicity. Particle and Fibre Toxicology 9:1-17.

Su M., Mei Y., Sinha S. 2013. Role of the crosstalk between autophagy and apoptosis in cancer. Journal of Oncology 2013:14 pages.

Su S.Y., Huang J.Y., Jian Z.H., Ho C.C., Lung C.C., Liaw Y.P. 2012. Mortality of colorectal cancer in Taiwan, 1971–2010: Temporal changes and age-period-cohort analysis. International Journal of Colorectal Disease 27:1665-1672.

Sun Y., Liu J.h., Jin L., Lin S.M., Yang Y., Sui Y.x., Shi H. 2010. Over-expression of the Beclin1 gene upregulates chemosensitivity to anti-cancer drugs by enhancing therapy-induced apoptosis in cervix squamous carcinoma CaSki

cells. Cancer Letters 294:204-210.

Susin S.A., Lorenzo H.K., Zamzami N., Marzo I., Snow B.E., Brothers G.M., Mangion J., Jacotot E., Costantini P., Loeffler M. *et al.* . 1999. Molecular characterization of mitochondrial apoptosis-inducing factor. Nature 397:441-446.

Tait S.W.G., Green D.R. 2010. Mitochondria and cell death: Outer membrane permeabilization and beyond. Nature Reviews Molecular Cell Biology 11:621-632.

Thomson C.D. 2004. Assessment of requirements for selenium and adequacy of selenium status: A review. European Journal of Clinical Nutrition 58:391-402.

Touvier M., Chan D.S.M., Lau R., Aune D., Vieira R., Greenwood D.C., Kampman E., Riboli E., Hercberg S., Norat T. 2011. Meta-analyses of vitamin D intake, 25-hydroxyvitamin D status, vitamin D receptor polymorphisms, and colorectal cancer risk. Cancer Epidemiology Biomarkers & Prevention 20:1003-1016.

Treuel L., Jiang X., Nienhaus G.U. 2013. New views on cellular uptake and trafficking of manufactured nanoparticles. Journal of the Royal Society Interface 10:20120939.

Tsuji P.A., Carlson B.A., Yoo M.-H., Naranjo-Suarez S., Xu X.-M., He Y., Asaki E., Seifried H.E., Reinhold W.C., Davis C.D. *et al.* . 2015. The 15kDa selenoprotein and Thioredoxin Reductase 1 promote colon cancer by different pathways. PLoS ONE 10:e0124487.

Tsujimoto Y., Shimizu S. 2005. Another way to die: Autophagic programmed cell death. Cell Death & Differentiation 12:1528-1534.

van Houdt W.J., Hoogwater F.J.H., de Bruijn M.T., Emmink B.L., Nijkamp M.W., Raats D.A.E., van der Groep P., van Diest P., Borel Rinkes I.H.M., Kranenburg O. 2010. Oncogenic KRAS desensitizes colorectal tumor cells to epidermal growth factor receptor inhibition and activation. Neoplasia 12:443-452.

Vekariya K.K., Kaur J., Tikoo K. 2012. ERα signaling imparts chemotherapeutic

selectivity to selenium nanoparticles in breast cancer. Nanomedicine: Nanotechnology, Biology and Medicine 8:1125-1132.

Verma A., Uzun O., Hu Y., Hu Y., Han H.-S., Watson N., Chen S., Irvine D.J., Stellacci F. 2008. Surface-structure-regulated cell-membrane penetration by monolayer-protected nanoparticles. Nature Materials 7:588-595.

Wagner D.B. 2009. The use of coumarins as environmentally-sensitive fluorescent probes of heterogeneous inclusion systems. Molecules 14:210-237.

Wallace K., Byers T., Morris J.S., Cole B.F., Greenberg E.R., Baron J.A., Gudino A., Spate V., Karagas M.R. 2003. Prediagnostic serum selenium concentration and the risk of recurrent colorectal adenoma: A nested case-control study. Cancer Epidemiology Biomarkers & Prevention 12:464-467.

Wanebo H.J., LeGolvan M., Paty P.B., Saha S., Zuber M., D'Angelica M.I., Kemeny N.E. 2012. Meeting the biologic challenge of colorectal metastases. Clinical & Experimental Metastasis 29:821-839.

Wang J., Whiteman M.W., Lian H., Wang G., Singh A., Huang D., Denmark T. 2009. A non-canonical MEK/ERK signaling pathway regulates autophagy via regulating Beclin 1. The Journal of Biological Chemistry 284:21412-21424.

Wang Q., Mejía Jaramillo A., Pavon J.J., Webster T.J. 2015. Red selenium nanoparticles and gray selenium nanorods as antibacterial coatings for PEEK medical devices [Internet]. Journal of Biomedical Materials Research Part B: Applied Biomaterials. Available from: http://dx.doi.org/10.1002/jbm.b.33479
http://onlinelibrary.wiley.com/store/10.1002/jbm.b.33479/asset/jbmb33479.pdf?v=1&t=ink1323e&s=87e3e2f0d819d2a9f2b645288bdff29bdbda9668

Wang T., Bai J., Jiang X., Nienhaus G.U. 2012. Cellular uptake of nanoparticles by membrane penetration: A study combining confocal microscopy with FTIR spectroelectrochemistry. ACS Nano 6:1251-1259.

Watanabe Y., Tanaka M. 2011. p62/SQSTM1 in autophagic clearance of a non-ubiquitylated substrate. Journal of Cell Science 124:2692-2701.

Wei Y., Pattingre S., Sinha S., Bassik M., Levine B. 2008. JNK1-mediated phosphorylation of Bcl-2 regulates starvation-induced autophagy. Molecular Cell 30:678-688.

Weissig V., D'Souza G.G. 2010. Organelle-Specific Pharmaceutical Nanotechnology. September 2010 ed.: John Wiley & Sons. p. 622.

Wolf B.B., Schuler M., Echeverri F., Green D.R. 1999. Caspase-3 is the primary activator of apoptotic DNA fragmentation via DNA fragmentation factor-45/inhibitor of caspase-activated DNase inactivation. Journal of Biological Chemistry 274:30651-30656.

Wolfe D.M., Lee J.-h., Kumar A., Lee S., Orenstein S.J., Nixon R.A. 2013. Autophagy failure in Alzheimer's disease and the role of defective lysosomal acidification. The European journal of neuroscience 37:1949-1961.

Wolpin B.M., Mayer R.J. 2008. Systemic treatment of colorectal cancer. Gastroenterology 134:1296-1310.

Wong K.H., Cheung P.C.K. 2009. Sclerotia: Emerging functional food derived from mushrooms. Mushrooms as Functional Foods. John Wiley & Sons, Inc. p. 111-146.

Wong R.S.Y. 2011. Apoptosis in cancer: From pathogenesis to treatment. Journal of Experimental & Clinical Cancer Research : CR 30:87-87.

World Health Organization. 2014. World Cancer Report 2014: Lyon, France : International Agency for Research on Cancer, Geneva, Switzerland : WHO Press, World Health Organization 2014.

Wu H., Li X., Liu W., Chen T., Li Y., Zheng W., Man C.W.Y., Wong M.K., Wong K.H. 2012. Surface decoration of selenium nanoparticles by mushroom polysaccharides-protein complexes to achieve enhanced cellular uptake and antiproliferative activity. Journal of Materials Chemistry 22:9602-9610.

Xia Y., You P., Xu F., Liu J., Xing F. 2015. Novel functionalized Selenium nanoparticles for enhanced anti-hepatocarcinoma activity *in vitro*. Nanoscale Research Letters 10:349.

Xiao Y., Ma C., Yi J., Wu S., Luo G., Xu X., Lin P.H., Sun J., Zhou J. 2015. Suppressed autophagy flux in skeletal muscle of an amyotrophic lateral sclerosis mouse model during disease progression. Physiological Reports 3:e12271.

Xie D.X., Yao J., Zhang P., Li X.L., Feng Y.D., Wu J.H., Tao D.D., Hu J.B., Gong J.P. 2008. Are progenitor cells pre-programmed for sequential cell cycles not requiring cyclins D and E and activation of Cdk2? Cell Proliferation 41:265-278.

Xie Z., Klionsky D.J. 2007. Autophagosome formation: Core machinery and adaptations. Nature Cell Biology 9:1102-1109.

Yang F., Tang Q., Zhong X., Bai Y., Chen T., Zhang Y., Li Y., Zheng W. 2012. Surface decoration by Spirulina polysaccharide enhances the cellular uptake and anticancer efficacy of selenium nanoparticles. International Journal of Nanomedicine 7:835-844.

Yang Y., Luo H.U.I., Hui K., Ci Y., Shi K., Chen G.E., Shi L.E.I., Xu C. 2016. Selenite-induced autophagy antagonizes apoptosis in colorectal cancer cells *in vitro* and *in vivo*. Oncology Reports 35:1255-1264.

Yang Z., Klionsky D.J. 2010. Eaten alive: A history of macroautophagy. Nature Cell Biology 12:814-822.

Yu B., Zhang Y., Zheng W., Fan C., Chen T. 2012. Positive surface charge enhances selective cellular uptake and anticancer efficacy of selenium nanoparticles. Inorganic Chemistry 51:8956-8963.

Yu C., He B., Xiong M.H., Zhang H., Yuan L., Ma L., Dai W.B., Wang J., Wang X.L., Wang X.Q. *et al.* . 2013. The effect of hydrophilic and hydrophobic structure of amphiphilic polymeric micelles on their transport in epithelial MDCK cells. Biomaterials 34:6284-6298.

Zeng H., Yan L., Cheng W.H., Uthus E.O. 2011. Dietary selenomethionine increases exon-specific DNA methylation of the p53 gene in rat liver and colon mucosa. The Journal of Nutrition 141:1464-1468.

Zhang S.Y., Zhang J., Wang H.Y., Chen H.Y. 2004. Synthesis of selenium nanoparticles

in the presence of polysaccharides. Materials Letters 58:2590-2594.

Zhang Y., Li X., Huang Z., Zheng W., Fan C., Chen T. 2013. Enhancement of cell permeabilization apoptosis-inducing activity of selenium nanoparticles by ATP surface decoration. Nanomedicine: Nanotechnology, Biology and Medicine 9:74-84.

Zhang Y., Wang J., Zhang L. 2010. Creation of highly stable selenium nanoparticles capped with hyperbranched polysaccharide in water. Langmuir 26:17617-17623.

Zhou Y., Sun K., Ma Y., Yang H., Zhang Y., Kong X., Wei L. 2014. Autophagy inhibits chemotherapy-induced apoptosis through downregulating Bad and Bim in hepatocellular carcinoma cells. Scientific Reports 4:5382.

Zisman A.L., Nickolov A., Brand R.E., Gorchow A., Roy H.K. 2006. Associations between the age at diagnosis and location of colorectal cancer and the use of alcohol and tobacco: Implications for screening. Archives of Internal Medicine 166:629-634.